

DEVELOPMENT OF AN ANALYTICAL MODEL OF RIVER RESPONSE

By

ROBERT GARY MILLAR

B.Sc. (Hons) Geol., University of Queensland, Brisbane, Australia, 1984

**A THESIS SUBMITTED IN PARTIAL FULFILLMENT OF
THE REQUIREMENTS FOR THE DEGREE OF
MASTER OF APPLIED SCIENCE**

in

**THE FACULTY OF GRADUATE STUDIES
CIVIL ENGINEERING**

We accept this thesis as conforming
to the required standard

THE UNIVERSITY OF BRITISH COLUMBIA

August 1991

© ROBERT GARY MILLAR, 1991

In presenting this thesis in partial fulfilment of the requirements for an advanced degree at the University of British Columbia, I agree that the Library shall make it freely available for reference and study. I further agree that permission for extensive copying of this thesis for scholarly purposes may be granted by the head of my department or by his or her representatives. It is understood that copying or publication of this thesis for financial gain shall not be allowed without my written permission.

Department of Civil Engineering

The University of British Columbia
Vancouver, Canada

Date August 13, 1991

Abstract

A physically based, analytical model of river response is developed. RIVERMOD was designed to aid in the prediction of gravel-bed river channel response to variations in the water and sediment regime.

RIVERMOD is a procedure which iteratively solves the governing equations which describe the movement of water and sediment through a channel, calculate the distribution of the boundary shear stresses, and assesses the bank stability. To arrive at a unique solution an additional closure hypothesis is required. The hypothesis of maximum sediment transport potential (MSTP) is proposed which states that a channel will develop a cross sectional geometry such that the potential for sediment transport is a maximum. The MSTP hypothesis is shown to be generally equivalent to the concept maximum transport capacity suggested by White *et al* (1982), and the minimum stream power theories of Chang (1979) and Yang (1976).

RIVERMOD is used to demonstrate the response of the channel geometry to variations in the bankfull discharge, sediment load, and the properties of the bank sediment.

Preliminary verification and testing indicate that RIVERMOD models the geometry of existing gravel rivers reasonably well. The river channel responses predicted by RIVERMOD are shown to agree with qualitative observations and empirical regime equations. The analysis in this study indicates that the bank stability exerts a strong control on the geometry of alluvial channels.

Further development of RIVERMOD is suggested.

Table of Contents

Abstract	ii
Table of Contents	vii
List of Tables	viii
List of Tables	viii
List of Figures	ix
List of Figures	x
List of Symbols	xi
Acknowledgements	xiv
1 INTRODUCTION	1
1.1 ADJUSTMENT OF THE HYDRAULIC GEOMETRY	1
1.1.1 Runoff	3
1.1.2 Sediment Yield	4
1.2 THESIS PROPOSAL	5
2 MODEL TYPES	7
2.1 INTRODUCTION	7
2.2 QUALITATIVE MODELS	7
2.2.1 Lane's Model	7

2.2.2	Schumm's Model	8
2.2.3	Discussion of the Qualitative Models	8
2.3	REGIME MODELS	9
2.3.1	Width	10
2.3.2	Depth	10
2.3.3	Slope	11
2.3.4	Effect of Slope on Channel Width	11
2.3.5	Analysis of the Data of Wolman and Brush	12
2.3.6	Discussion of Regime Equations	13
2.4	ANALYTICAL MODELS	15
2.4.1	Stable Channel Models	15
2.4.2	Mobile-Bed Models	16
2.5	CONCLUSIONS	17
3	THEORETICAL BACKGROUND	19
3.1	INTRODUCTION	19
3.2	DOMINANT DISCHARGE	19
3.2.1	Bankfull Discharge	19
3.2.2	Frequency of Bankfull Discharge	20
3.2.3	Bankfull Flow and Sediment Transport	20
3.2.4	Discussion	21
3.3	FLOW RESISTANCE	21
3.3.1	Logarithmic Flow Resistance Equations	22
3.3.2	Power-Law Flow Resistance Equations	23
3.3.3	Discussion	25
3.4	THRESHOLD OF MOVEMENT	25

3.4.1	Dimensionless Shear Stress Approach	27
3.4.2	Excess Stream Power Approach	28
3.4.3	Threshold of Movement from Field Studies	28
3.4.4	Discussion	30
3.4.5	Conclusions	31
3.5	BANK STABILITY	32
3.5.1	USBR Method for Non-Cohesive Banks	33
3.5.2	Modification of ϕ	34
3.5.3	Vegetation	35
3.6	DISTRIBUTION OF THE BOUNDARY SHEAR STRESS	35
3.7	SEDIMENT TRANSPORT	37
3.8	EXTREMAL HYPOTHESES	42
3.8.1	Minimization Hypotheses	42
3.8.2	Maximum Transport Capacity	42
3.8.3	Discussion	43
3.9	Conclusions	43
4	DEVELOPMENT OF RIVERMOD	45
4.1	INTRODUCTION	45
4.2	SIMPLIFYING ASSUMPTIONS	45
4.3	MODEL THEORY	46
4.3.1	Flow Resistance	46
4.3.2	Continuity	47
4.3.3	Distribution of the Boundary Shear Stress	48
4.3.4	Bank Stability	48
4.3.5	Sediment Transport	49

4.3.6	Extremal Hypothesis	50
4.4	RIVERMOD	56
4.4.1	STABLECHANNEL	56
4.4.2	RIVERMOD	60
4.5	CONCLUSIONS	62
5	VERIFICATION OF RIVERMOD	64
5.1	INTRODUCTION	64
5.2	MODELLING EXISTING RIVERS	64
5.2.1	Discussion	65
5.3	RESIDUAL ERRORS	70
5.3.1	Comparison Between The Output from RIVERMOD and the Regime Equations	73
5.3.2	Systematic Variation of the Residuals	75
5.4	PREDICTIONS OF CHANNEL ADJUSTMENTS	84
5.4.1	Bank Sediment Size	85
5.4.2	Angle of Repose	85
5.4.3	Discharge	92
5.4.4	Sediment Load	96
5.5	COMPARISON WITH REGIME EQUATIONS	100
5.6	CONCLUSIONS	101
6	CONCLUSIONS	103
6.1	SUMMARY	103
6.2	APPLICATION TO THE CARMANAH VALLEY	106
6.3	FUTURE WORK	107

REFERENCES	109
APPENDICES	117
A DATA FROM WOLMAN AND BRUSH (1961)	117
B RIFFLE DATA FROM HEY (1979)	118
C DERIVATION OF EQUATION 3.12	119
D DERIVATION OF EQUATION 4.7	120
E HYDRAULIC GEOMETRY OF SELECTED GRAVEL RIVERS	122
F DERIVATION OF EQUATION 3.32	125
G ARTIFICIAL DATA SET	127
H RIVERMOD PROGRAM	130

List of Tables

5.1	RIVERMOD Residual Errors	71
5.2	Regime Residual Errors	72
A.1	Experimental Data of Wolman and Brush (1961)	117
B.1	Riffle Data from Hey (1979)	118
E.1	Observed Hydraulic Geometry of Selected Gravel Rivers	123
E.2	Modelled Hydraulic Geometry of Selected Gravel Rivers	124
G.1	Artificial Data Set	128
G.2	Artificial Data Set Ctd.	129

List of Figures

1.1	Location of the Carmanah Valley	2
2.1	Effect of Slope on Channel Width	14
3.1	Flow Resistance Equations	24
3.2	Semi-log plots of the Functions $y = \log x$, $y = x^{1/6}$, and $y = x^{1/4}$	26
3.3	% <i>SF</i> Carried By the Banks	38
3.4	$\bar{\tau}_{bank}$ as a Function of P_{bed}/P_{bank}	39
3.5	$\bar{\tau}_{bed}$ as a Function of P_{bed}/P_{bank}	40
4.1	Bed-Load Transport Capacity for A Stable Channel as a Function of Bed Width	51
4.2	Einstein Bed Load Function	53
4.3	Comparison of MSTP and MTC	54
4.4	Flow Chart of RIVERMOD	57
4.5	Flow Chart of Subfunction STABLECHANNEL	58
4.6	Definition Sketch for RIVERMOD	59
4.7	Possible Channel Configurations	61
5.1	Modelled and Observed Channel Widths	66
5.2	Modelled and Observed Channel Depths	67
5.3	Modelled and Observed Channel Slopes	68
5.4	Modelled and Observed Channel Areas	69
5.5	Channel Width Residual Errors as a Function of Width	76

5.6	Channel Width Residual Errors as a Function of Slope	77
5.7	Channel Width Residual Errors as a Function of Discharge	78
5.8	Channel Width Residual Errors as a Function of Unit Sediment Load . .	79
5.9	Channel Width Residual Errors as a Function of $\tau_{D_{50}}^*$	80
5.10	Average Channel Depth Residual Errors as a Function of $\tau_{D_{50}}^*$	81
5.11	Channel Slope Residual Errors as a Function of $\tau_{D_{50}}^*$	82
5.12	Channel Area Residual Errors as a Function of $\tau_{D_{50}}^*$	83
5.13	Effect of Bank Sediment Size on the Channel Surface Width	86
5.14	Effect of Bank Sediment Size on the Average Channel Depth	87
5.15	Effect of Bank Sediment Size on the Channel Slope	88
5.16	Effect of the Angle of Repose of the Bank Sediment on the Channel Surface Width	89
5.17	Effect of the Angle of Repose of the Bank Sediment on the Channel Av- erage Depth	90
5.18	Effect of the Angle of Repose of the Bank Sediment on the Channel Slope	91
5.19	Effect of Discharge on the Channel Surface Width	93
5.20	Effect of Discharge on the Average Channel Depth	94
5.21	Effect of Discharge on the Channel Slope	95
5.22	Effect of Sediment Load on the Channel Surface Width	97
5.23	Effect of Sediment Load on the Average Channel Depth	98
5.24	Effect of Sediment Load on the Channel Slope	99

List of Symbols

a	Empirical Coefficient
a, b	Empirical Exponents
b	Empirical Coefficient
D	Grain Diameter (metres)
D_{50}	Median Grain Diameter (metres)
D_{84}	84% Finer Grain Size (metres)
d_i	i^{th} Size Fraction of the Subpavement (metres)
d_{50}	Median Subpavement Grain Diameter (metres)
$D_{50_{bank}}$	Mean Bank Grain Diameter (metres)
f	Darcy-Weisbach Friction Factor
G_b	Dry Bedload Transport Rate (kg/sec)
g_b	Dry Bedload Transport Rate per metre width (kg/sec/m)
G'_b	Sediment Transport Capacity (kg/sec)
g	Gravitational Acceleration (m/sec ²)
i_b	Immersed Bedload Transport Rate per metre width (kg/sec/m)
k	Empirical Coefficient
k_s	Effective Boundary Roughness (metres)
K	Bank Stability Factor
L	Meander Wavelength
M	Index of Sediment Transport Potential (Eqn. 4.7)
o	Subscript to Denote the Observed Value
m	Subscript to Denote the Modelled Value

P	Channel Perimeter (metres)
P_{bed}	Bed Perimeter or Width (metres)
P_{bank}	Bank Perimeter (metres)
q_s^*	Einstein Dimensionless Bedload Parameter
q_s	Volumetric Bedload Per Unit Bed Width (m^2/sec)
Q	Discharge (m^3/sec)
Q'	Discharge Capacity from Eqn. 4.4 (m^3/sec)
q	Discharge per metre width. (m^2/sec)
R	Hydraulic Radius (metres)
S	Channel or Water Surface Slope
S_v	Valley Slope
S_s	Specific Gravity of Sediment (Assumed = 2.65)
SF	Shear Force = τP (N)
$\%SF_{bank}$	Percentage of the Shear Force Acting on Banks
v	Mean Channel Velocity (m/sec)
v^*	Shear Velocity (m/sec)
W^*	Total Dimensionless Bedload
W	Channel Surface Width (metres)
X	Variable Considered in Residual Error Analysis
Y	Average Channel Depth (metres)
Y_o	Maximum Channel Depth (metres)
Z	Sinuosity
α	Empirical Coefficient
γ	Unit Weight of Water ($9810 N/m^3$)
ϵ_x	Residual Error as a Percentage

ω	Stream Power Per Unit Bed Area (kg/sec)
ρ	Density of Water (Assumed 1000 kg/m ³)
ϕ_{50}	Bed Mobility Number from Parker <i>et al</i> (1982)
τ	Mean Boundary Shear Stress (N/m ²)
τ_o	Mean Bed Shear Stress = $\gamma Y_o S$ (N/m ²)
τ^*	Dimensionless (Shields) Shear Stress
τ_c^*	Critical Dimensionless Shear Stress
τ_{ci}^*	Critical Dimensionless Shear Stress for the i^{th} Size Fraction
τ_{cd50}^*	Critical Dimensionless Shear Stress for the Median Subpavement Grain Diameter
τ_{cD50}^*	Critical Dimensionless Shear Stress for the Median Pavement Grain Diameter
$\bar{\tau}_{bed}$	Mean Bed Shear Stress (N/m ²)
$\bar{\tau}_{bank}$	Mean Bank Shear Stress (N/m ²)
ϕ	Angle of Repose of the Bank Sediment (degrees)
ϕ'	Effective Angle of Repose (degrees)
θ	Bank Angle (degrees)
ν	Kinematic Viscosity (m ² /sec)

Acknowledgements

The author is very grateful to Professor M.C. Quick for his encouragement and financial support during this project.

And to my wife Karen who remained supportive despite my preoccupations.

Chapter 1

INTRODUCTION

The Carmanah Valley contains exceptional stands of Sitka Spruce including the 94 metre Carmanah Giant, the tallest tree in Canada and possibly the world's tallest Sitka Spruce. The majority of the trees colonize the alluvial floodplain along the central valley Carmanah Pacific Provincial Park.

Considerable controversy surrounds proposed logging within the upper Carmanah Creek and August Creek valleys. Opponents of the logging state that logging will result in increased flooding and erosion which will damage the riparian habitat of the central valley, and have a negative impact on the Spruce stands. This land use conflict stimulated this initial interest in the subject of this thesis.

In this Chapter the impact of timber harvesting and road construction on watershed hydrology and sediment production will be reviewed to determine the focus, or indeed the need, for this study. A thesis proposal will be presented in Section 1.2.

1.1 ADJUSTMENT OF THE HYDRAULIC GEOMETRY

The geometry of alluvial channels such as the Carmanah Creek are described as self formed. These rivers flow through their own sediment. The width (W), depth (Y), and channel gradient (S), of these channels develops as a function of the independent variables discharge (Q), sediment load (G_b), sediment size (d), and valley slope (S_v). The value of the independent variables is determined by the physiography, geology, vegetation, climate and land use patterns within the watershed.

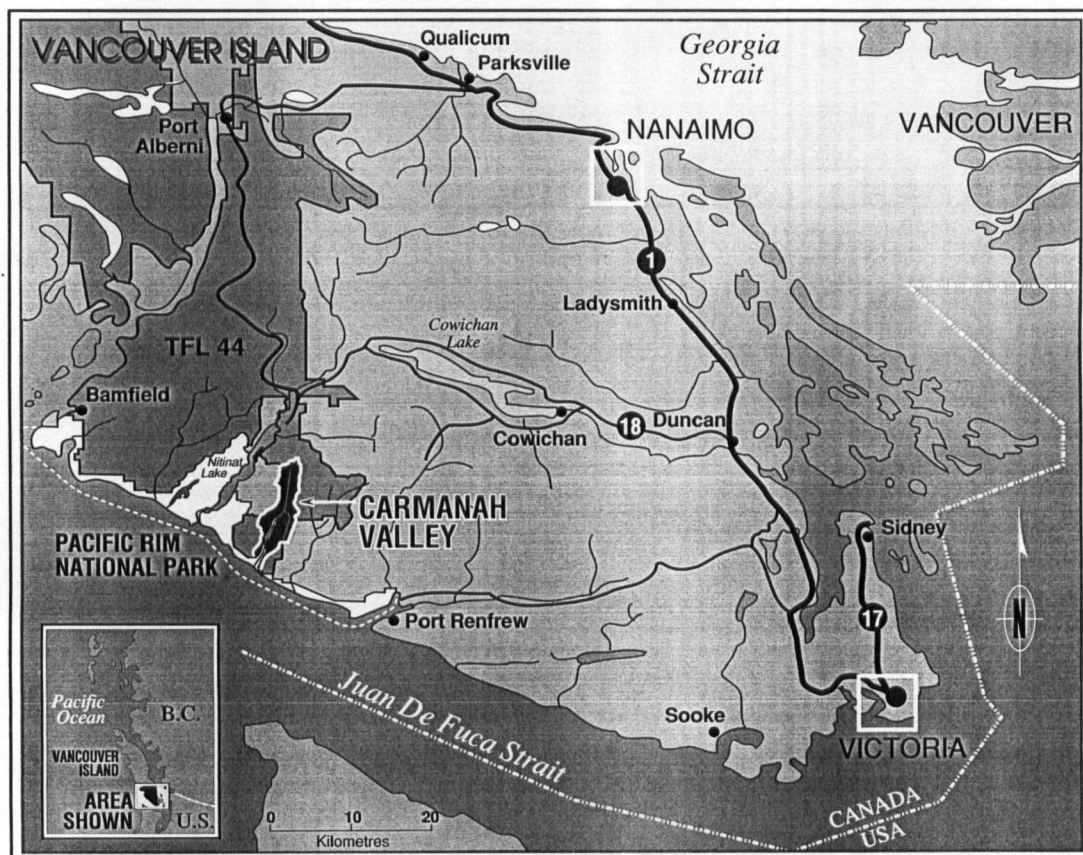


Figure 1.1: Location of the Carmanah Valley

It is widely believed that single-thread alluvial channels tend towards a configuration which is in equilibrium with the independent variables. This is known as the concept of the graded river (Mackin, 1948). Such rivers are said to be in a state of dynamic equilibrium continuously adjusting their geometry to annual, seasonal, and short-term fluctuations in the independent variables. Furthermore the development of a river is punctuated by infrequent catastrophic events which can cause severe disruption of the channel geometry.

Timber harvesting activity in the upper watershed has the potential to alter the hydrologic regime of the catchment. Because the valley slope and the size of the sediment supplied to the channel remain constant, the possible changes to the independent variables are the amount of runoff, the size and timing of peak flows, and the sediment yield of the upper catchment.

1.1.1 Runoff

Evidence from Carnation Creek (Hetherington, 1982; 1988) and Oregon (Harr *et al*, 1974) indicate that the volume of runoff, and the magnitude and timing of flood waters from rain-only events will not be significantly affected by timber harvesting activities in the upper watershed.

Increased storm runoff can be expected from clearcuts within the *transient snow zone* between about 350 - 1100 metres above sea level (Harr, 1986) due to rain-on-snow events. This includes significant areas of the upper Carmanah and August Creek valleys. The recently harvested areas are prone to develop significant snowpacks which can melt rapidly during the subsequent passage of warm, moist storm fronts. The storm runoff produced by these rain-on-snow events includes the precipitation in the form of rain from the storm, together with melt water from the snowpack.

An increase in the magnitude of isolated extreme flows as a result of rain-on-snow

events has been observed at the nearby Carnation Creek experimental watershed (Hetherington, 1988). The impact of these events would be expected to increase with the percentage of the watershed which has been cleared. The probable rate of harvesting in the Carmanah Valley of 1 - 2 % per year should minimize any effect of rain-on-snow events.

1.1.2 Sediment Yield

Potential sediment yield increases can be subdivided into chronic and pulse sedimentation (Grant, 1988; Grant *et al*, 1984).

Chronic Sedimentation

Chronic sedimentation is comprised of surface erosion from roads and landings, clearcut areas with exposed mineral soil, and landslide scars. Much of the sediment is fine material which is transported in suspension and will exert little stress on the fluvial regime.

Past work suggests that the load of suspended sediment can increase sharply following road construction, harvesting, and slash burning (eg Megahan, 1972). However the suspended load rates tend to return to near pre-harvest levels within a few years (Beshta, 1978).

While the increased load of suspended sediment may pose a threat to fisheries resources, it is unlikely to result in downstream channel adjustment.

Pulse Sedimentation

Pulse sedimentation is comprised of large periodic inputs of coarse sediment and organic debris, and occurs as a result of debris slides or debris flows which enter directly into the major channels, or from debris torrents which are initiated by slides in steep low order

tributaries.

Pulse sedimentation occurs as rapid, episodic events which are usually associated with relatively low frequency, high magnitude hydrological events. During these events the increased incidence of landslides, coupled with the high transporting power of the fluvial network, is capable of delivering and transporting large volumes of coarse bedload sediment.

There is little doubt that an acceleration of landslide activity occurs as a result of timber harvesting and road construction. For example Swanston and Swanson (1976) found that for coastal regions of the Pacific Northwest from Oregon to B.C. clearcutting can increase the incidence of landsliding by two to four times over unlogged forest. Road construction can increase landslides by 25 to 350 times.

Recent improvements in road construction techniques and increased awareness amongst industry personnel may have reduced the incidence of logging related landslides in recent years. However no comprehensive study has been undertaken to confirm this.

It must therefore be concluded that the potential exists for a significant increase in the supply of coarse sediment to the Carmanah Creek channel following the commencement of extensive logging activity within the upper Carmanah and August creek valleys.

1.2 THESIS PROPOSAL

Timber harvesting activity in the upper watershed has the potential to significantly increase the supply of coarse bedload sediment to the channel.

The channel will adjust its geometry in response to the increase sediment load. This may produce a negative impact on the stands of Sitka Spruce which colonize the banks and floodplain of the channel.

A necessary component of any management strategy for the watershed is to predict

the magnitude of the channel changes which are likely to result from any proposed land-use changes.

In this thesis it is proposed to develop a method which will permit a quantitative assessment of the magnitude of the channel response to variations in the sediment supply resulting from timber harvesting upstream of the Sitka Spruce trees.

Chapter 2

MODEL TYPES

2.1 INTRODUCTION

This chapter gives a brief description of the 3 categories of river response models: qualitative, regime, and analytical.

2.2 QUALITATIVE MODELS

Qualitative models have been developed largely through field observations by river engineers and fluvial geomorphologists. The qualitative models or formulae do not permit quantification of river responses. These formulae only indicate the general trend of river adjustments.

The formulae of Lane (1955a) and Schumm (1969) are presented below.

2.2.1 Lane's Model

Lane (1955a) suggested that the following expression is very useful when analysing changes in stream morphology:

$$\frac{G_b}{Q} \propto \frac{S}{D} \quad (2.1)$$

G_b is the sediment load, Q is the dominant discharge, S is the channel slope, and D is the sediment size.

Equation 2.1 indicates that if the sediment load increases while maintaining the original discharge and sediment size, then the channel will adjust by increasing its gradient

to restore equilibrium.

Equation 2.1 also indicates that if the dominant discharge is increased while maintaining the original sediment load and size, the channel will adjust by decreasing its gradient.

2.2.2 Schumm's Model

Schumm (1969) proposed several qualitative equations which illustrate the relationship between the dependent hydraulic variables including the width/depth ratio (W/Y), the meander wavelength (L), and sinuosity (Z), and the independent variables Q and G_b .

The relationship between the dominant discharge (taken by Schumm to be the mean annual flood or the mean annual discharge) and the channel geometry is given by:

$$\frac{W Y Z L}{S} \propto Q \quad (2.2)$$

Equation 2.2 indicates that an increase in the dominant discharge will produce an increase in the width, W , depth, Y , sinuosity, Z , and meander wavelength, L , and a decrease in channel slope, S . Note that an increase in Z is equivalent to a decrease in S .

The relationship of channel geometry to sediment load for constant Q is:

$$\frac{W L S}{Y Z} \propto G_b \quad (2.3)$$

Equation 2.3 indicates that an increase in the sediment load will result in the channel adjusting by increasing the W , L , S , and W/Y , and decreasing Y and Z . This suggests a tendency towards a braided channel morphology for increased sediment load.

2.2.3 Discussion of the Qualitative Models

The qualitative formulae presented above are based upon observations from natural rivers. They have been widely referenced and are generally accepted. These formulae are used in Chapter 5 as partial verification of the quantitative model developed in

this thesis.

2.3 REGIME MODELS

Regime *theory* applied to channel geometry was initially developed by Lacey (1930) based on observations of silt-lined canals in India. Empirical relations were defined to aid in the design of canals which would transport the introduced sediment without appreciable deposition or scour. Canals which behaved in this manner were said to be *in regime*.

Regime is equivalent to the concept of a *graded river* (Mackin, 1948).

Regime type analyses were later applied to natural alluvial rivers by workers such as Leopold and Maddock (1953), Nixon (1959), Simons and Albertson (1963), Kellerhals (1967), Bray (1982b), and Hey and Thorne (1986).

The equations for width and depth are often expressed in the form:

$$W \propto Q^a$$

$$Y \propto Q^b$$

The value of a ranges between 0.45 - 0.55 with a typical value of 0.5. The value of b ranges between 0.33 - 0.41.

More sophisticated regime equations may include sediment size and load in the regime equations.

The equations of Hey and Thorne (1986) will be reviewed here as they were derived from data from stable gravel rivers with mobile beds. The Hey and Thorne study is the first to consider the effect of sediment load on the regime geometry.

2.3.1 Width

The general equation for channel width is:

$$W = 3.67 Q_b^{0.45} \quad (2.4)$$

Q_b = the bank-full discharge. The coefficient of determination, r^2 , for Equation 2.4 is 0.7884. This equation is very similar to the original Lacey equation.

Hey and Thorne determined that the channel width was independent of sediment size and load. Bray (1982b) found that width varied slightly with grain diameter.

The width in the Hey and Thorne study was strongly influenced by the type and density of the bank vegetation. Bank vegetation was subdivided into 4 categories from vegetation Type I (grassy banks) to vegetation Type IV (> 50 % tree/shrub cover). The effect of the increased density of trees and shrubs was to decrease the channel width.

The revised equation for channel width is:

$$W = \alpha Q_b^{0.5} \quad (2.5)$$

α ranged from 2.34 for vegetation type IV, to 4.33 for vegetation type I. The coefficient of determination, r^2 , for Equation 2.5 is 0.9577. r^2 has increased significantly over Equation 2.4.

The effect of the bank vegetation is to alter the bank strength and thus its ability to withstand shear stresses exerted by the flowing water.

The effect of channel slope on width was not assessed.

2.3.2 Depth

The simple hydraulic geometry relation gives:

$$Y = 0.33 Q_b^{0.35} \quad (2.6)$$

The coefficient of determination, r^2 , for Equation 2.6 is 0.8045.

The coefficient of determination is increased to $r^2 = 0.8712$ with the inclusion of grainsize:

$$Y = 0.22 Q_b^{0.37} D_{50}^{-0.11} \quad (2.7)$$

The regime depth was not significantly effected by bank vegetation or sediment load.

2.3.3 Slope

The channel slope equation determined by the Hey and Thorne study is:

$$S = 0.087 Q_b^{-0.43} D_{50}^{-0.09} D_{84}^{0.84} G_b^{0.10} \quad (2.8)$$

The coefficient of determination, r^2 for Equation 2.8 is 0.6285.

The low coefficient of determination indicates considerable unexplained variance in Equation 2.8. In addition the exponent of 0.10 for G_b suggests that the channel slope is quite insensitive to the sediment load. It is shown in Chapter 5 however that the channel slope is strongly influenced by the sediment load.

The attempt by Hey and Thorne to incorporate sediment load into their regime analysis was not successful. This is probably due largely in part to the absence of data on the subpavement grainsize distribution which is necessary to calculate sediment transport rates.

Note that the exponent for discharge in Equation 2.8 can be obtained theoretically by a stable channel analysis (See Appendix D).

2.3.4 Effect of Slope on Channel Width

Because the channel slope is considered a dependent variable it has not been included in the regression analyses when determining the regime equations for channel width. Thus

for a given discharge, sediment size, and bank vegetation type, the regime equations predict a single channel width which will develop, independent of the channel slope.

Henderson (1966, p 449) showed that to maintain sediment continuity along a channel, the ratio of unit discharge to unit sediment discharge, q/q_s , must be constant. Wider reaches of the channel must have steeper gradients to transport the same volume of sediment as a narrower channel. He states that increase in the channel gradient with local increases in the channel width is feature which is observed in natural rivers.

From a consideration of bank stability, an increase in the channel gradient would be expected to increase the streampower available to attack the banks, and a wider channel would be expected.

2.3.5 Analysis of the Data of Wolman and Brush

To test the influence of channel gradient on channel width an analysis is performed on the experimental data of Wolman and Brush (1961). Only the mobile-bed channels in the 0.67 mm sand will be used. The data is presented in Appendix A. This experimental data is used so that the influence of the channel slope will not be masked by other variations which are present in natural rivers such as variations in the bank strength.

Wolman and Brush used an inclined bed comprised of well sorted sand and measured the equilibrium channel geometry which developed for various discharges and channel slopes. Sediment was fed into the upstream end of the channel and adjusted until equilibrium was established.

Width equations were determined in the form:

$$W = \alpha Q^a$$

The simplest case corresponds to the case where a is a constant. Regression analysis of

the experimental data yielded the following equation for channel width:

$$W = 5.59 Q^{0.45} \quad (2.9)$$

The coefficient of determination, r^2 , for Equation 2.9 is 0.7283. The coefficient of determination indicates considerable unexplained variance.

In the second trial the coefficient α is considered a function of channel slope. A linear relationship was established between α and S . This relationship yields:

$$W = \alpha Q^{0.60} \quad (2.10)$$

where:

$$\alpha = 1364 S + 11.59$$

The coefficient of determination, r^2 , for Equation 2.10 is 0.9383.

A scatter plot of Equations 2.9 and 2.10 is shown in Figure 2.1. The data from Equation 2.10 has collapsed towards the line of perfect agreement relative to Equation 2.10. The coefficient of determination of Equation 2.10 shows a large increase over Equation 2.9 in which the influence of channel slope was not considered.

Equation 2.10 indicates that by increasing the slope of a channel with a constant discharge and uniform bank material, the value of α will increase, and a wider channel will develop.

The above analysis indicates that the channel slope does influence the stable channel width. The wider channel predicted by Equation 2.10 for steeper channel slopes agrees with the observations of Henderson (1966) discussed in the previous section.

2.3.6 Discussion of Regime Equations

The empirical regime equations indicate that the width and depth of alluvial channels are principally controlled by the bankfull discharge. Furthermore the channel width, and

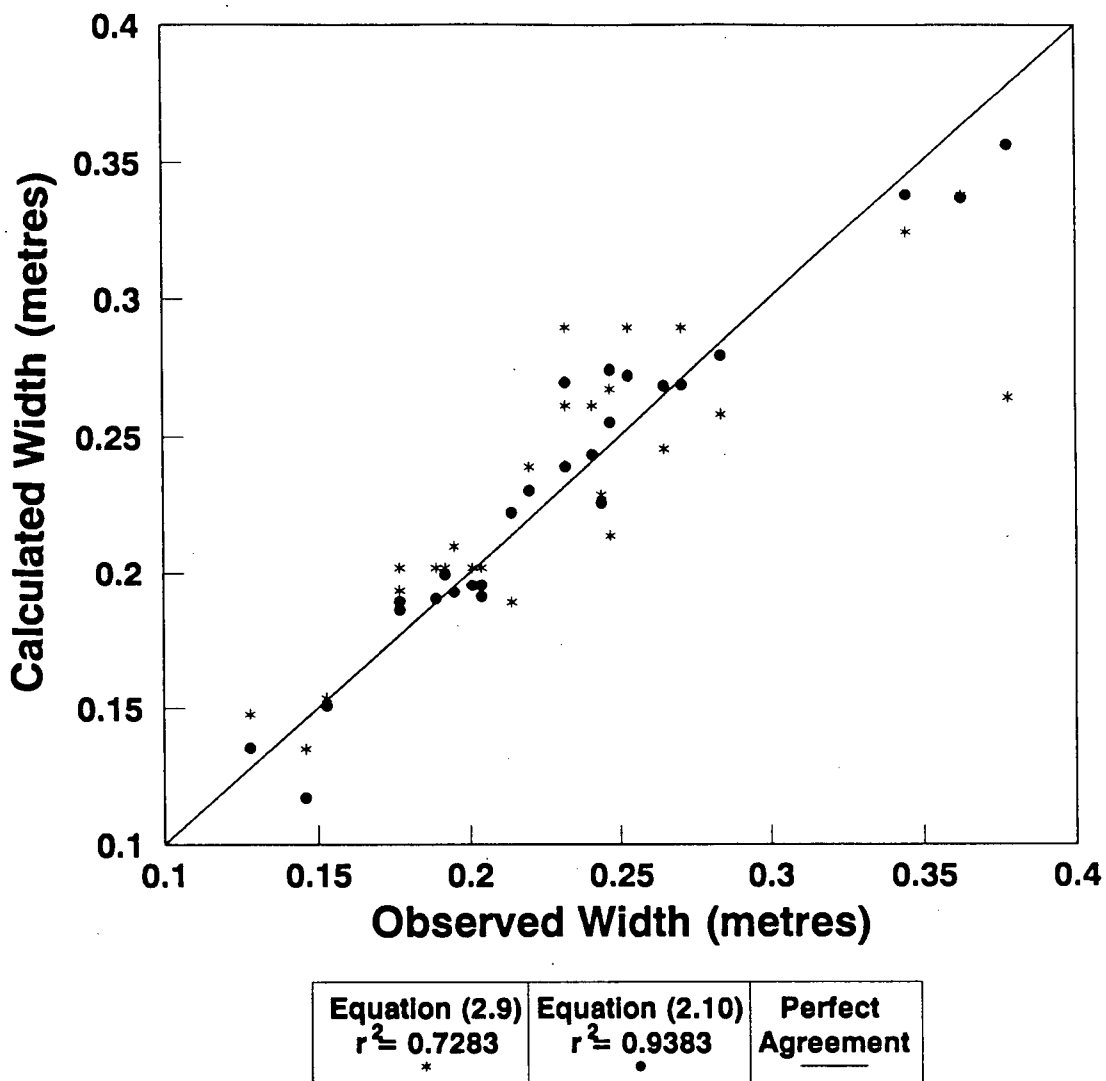


Figure 2.1: Comparison of Channel Widths Calculated by Equations 2.9 and 2.10 with the Observed Channel Widths for the Flume Data of Wolman and Brush (1961).

presumably also the channel depth, are strongly modified by the ability of the bank to resist erosion.

The channel slope is a function of discharge, sediment size, and sediment load, although the effect of sediment load has not yet been successfully incorporated into a regime analysis.

The channel width and depth do not appear to be directly influenced by the sediment load. However it was shown that the width will respond to variations in the channel slope, and is therefore indirectly affected by the sediment load.

2.4 ANALYTICAL MODELS

Analytical models are based on the simultaneous solution of the equations governing the movement of water and sediment through a channel.

2.4.1 Stable Channel Models

The stable channel method of the USBR (Lane, 1955b) was the first example of a process-based model for channel design. This method combines equations for flow resistance, the threshold of sediment motion, and bank stability to derive equations which result in a solution for the stable channel geometry. This model applies to the threshold channel where the rate of sediment transport approaches zero.

An explicit solution is only possible for the *Type B* channel (See Lane, 1955b) because W and R can then be expressed as functions of the maximum channel depth, thus reducing the number of unknown variables.

The wider *Type A* channels require an additional regime width equation to obtain a solution (See Appendix D).

2.4.2 Mobile-Bed Models

Mobile-bed models require the solution of a sediment transport equation in place of the threshold condition of the stable channel models.

The unknown dependent variables generally considered are width, depth, velocity and channel gradient. The equations available for solution are flow resistance, continuity, and sediment transport, so that there are only three equations to solve for four unknown variables.

Explicit solutions are only possible if the value of one of the dependent variables is known. Fixed-width models of river response assume that the channel width remains unchanged while the river is responding to an altered regime. Alternatively the channel width can be estimated using an empirical regime equation, such as Equation 2.4.

To obtain a fourth equation, an approach which has been used by several authors is to incorporate an extremal hypothesis which contends that a channel develops towards a geometry such that some feature is maximized or minimized.

Yang (1976) incorporates the theory of minimum unit stream power as the required closure hypothesis. Chang (1979, 1980) and Thorne *et al* (1988) use the theory of minimum streampower which is similar to the approach of Yang. The general outcome of the theories of minimum unit stream power and minimum stream power is that the channel will develop at the minimum slope that is required to transport the imposed water and sediment load.

White *et al* (1982) combined the above equations with the theory of maximum transport capacity. The hypothesis of maximum transport capacity states that a channel develops a width where the sediment transport capacity of the channel is a maximum.

Extremal hypotheses are discussed further in Chapter 3.

The models of Chang and White *et al* have had reasonable success in predicting the

channel geometry of alluvial rivers despite the absence of stream bank stability analysis in their models. However the errors associated with their models precludes the use for engineering applications.

An alternative approach to the above analytical models of river channel development is that of Parker (1978a,b). In his model for gravel rivers (1978b), Parker considers the lateral stability of the channel and uses perturbation techniques to develop rational regime equations. By considering the bank stability, Parker was able to determine the geometry of alluvial channels without resorting to an extremal hypothesis. Bettess *et al* (1988) have shown however that the equations of Parker do not appear to be totally consistent with the empirical regime relations derived from observations of canals and rivers.

2.5 CONCLUSIONS

The mobile-bed analytical models offer the most potential for successfully quantitative modelling of river response. The models of Chang (1979, 1980) and White *et al* (1982) have produced reasonable results. The errors associated with these models however, preclude their use for engineering applications.

As these models are largely process-based, they can be refined by the inclusion of additional aspects of river channel development. Potential refinements might include the distribution of the boundary shear stress and the stability of the channel banks. Such refinements should increase the accuracy of the modelled channel geometries, and may remove the necessity for an extremal hypothesis.

The importance of the qualitative and empirical regime models is that they have improved our understanding of river channel development, and serve as an important verification of analytical model outputs. The successful analytical model must reproduce

the responses predicted by the qualitative and regime models.

Chapter 3

THEORETICAL BACKGROUND

3.1 INTRODUCTION

This chapter reviews the theory required for the development of an analytical river response model.

3.2 DOMINANT DISCHARGE

The empirical regime equations discussed in section 2.3 were initially derived from canal data where the equilibrium conditions were maintained under highly uniform flow conditions. In contrast the hydraulic geometry of rivers is formed under a highly variable flow regime.

Inglis (1947), quoted by Nixon (1959), defined the concept of a dominant discharge which is the steady discharge which represents the variable flow of the natural river. It is generally accepted that for single-thread rivers the dominant discharge is equal to the bankfull discharge (Wolman, 1955; Wolman and Leopold, 1957; Nixon, 1959).

3.2.1 Bankfull Discharge

A thorough review of the definitions of bankfull discharge is given by Williams (1978). The most significant definition of bankfull discharge from the aspect of channel geometry is the the stage at which the width/depth (W/Y) ratio is a minimum (Wolman, 1955). For relatively steep sided channels which are not incised, this stage is generally equivalent

to the height of the active floodplain (Wolman and Leopold, 1957).

At the bankfull stage the hydraulic radius of the channel becomes a maximum.

3.2.2 Frequency of Bankfull Discharge

Several authors have suggested that the dominant discharge can be defined by a characteristic recurrence interval. Wolman and Leopold (1957) determined that the recurrence interval of bankfull discharge was 1.4 years based upon the annual maximum series. Subsequent work by Williams shows that, while the recurrence interval has a median value of about 1.5 years (annual maximum series), the wide scatter of values about this mean makes the 1.5 year flood a poor estimate of bankfull conditions. Despite this Bray (1982b) has successfully based his regime equations for gravel-bed rivers on 2 year flood flows.

3.2.3 Bankfull Flow and Sediment Transport

Several researchers have reported that during overbank conditions the velocity and discharge of the in-channel flow actually may actually decrease with increased stage above the bankfull condition. Barishnikov (1967) states:

The phenomenon of the decrease of discharge in the main channel when considered with that of the alluvial plain has been discovered and proved experimentally by Soviet hydrologists within the last 10 - 15 years.

This has been confirmed more recently by Smith (1989), and others, who note an increase in the flow resistance within the channel due to flow exchange between the channel and the out of bank flow.

Barishnikov (1967) determined experimentally that the sediment transport capacity of the channel decreases under conditions of out of bank flow and that this decrease was

greater as the floodplain roughness was increased. These reductions may be up to 20 - 25% of the bankfull capacity.

3.2.4 Discussion

It is clear that the bankfull stage as defined by the minimum W/Y ratio or the height of the active floodplain represents a hydraulically significant discharge because the hydraulic radius, velocity, discharge, and sediment transport capacity of the channel are all maximized.

The bankfull discharge will be used in this thesis to represent the formative discharge for the modelled alluvial channel.

3.3 FLOW RESISTANCE

This discussion of flow resistance theory will be limited to high Reynolds numbers where fully turbulent flow has developed. In this fully rough zone flow resistance is independent of the Reynolds number (Henderson, 1966; p. 92-94).

Flow resistance formulae are generally expressed as either logarithmic or power-law functions of relative roughness R/k_s . k_s is a measure of the effective boundary roughness, such as the diameter of the bed sediment, with the dimension of length.

Nikuradse (1933) and Colebrook and White (1937), quoted by A.S.C.E. (1963), Keulegan (1938), Leopold *et al* (1964) and Limineros (1970)) have developed logarithmic forms of the flow resistance equation. The Manning-Strickler equation, and the relationship derived by Kellerhalls (1967, see equation (3.8) this paper) are well known examples of power-law flow resistance formulae.

3.3.1 Logarithmic Flow Resistance Equations

Experimental measurements on sand-coated pipes by Nikuradse (1933) and others resulted in the following equation which is recommended by the A.S.C.E. Task Force on Flow Resistance (1963):

$$\frac{1}{\sqrt{f}} = 2 \log \left(\frac{12 R}{k_s} \right) \quad (3.1)$$

Leopold *et al* (1964) and Limerinos (1970) have fitted natural river data to the logarithmic form of the flow resistance equation:

Leopold *et al*:

$$\frac{1}{\sqrt{f}} = 2.03 \log \left(\frac{3.11 Y}{D_{84}} \right) \quad (3.2)$$

Limerinos:

$$\frac{1}{\sqrt{f}} = 2.03 \log \left(\frac{3.72 R}{D_{84}} \right) \quad (3.3)$$

Both equations (3.2) and (3.3) are associated with considerable scatter. Note that the constant 2.03 which appears ahead of the logarithmic term is fixed by theory and is equal to $2.3/\sqrt{8}\kappa$ where 2.3 represents the conversion factor from natural to base 10 logarithms, and κ is the *Von Karman* universal constant which is equal to 0.4.

Hey (1979) showed that flow resistance and discharge estimates for gravel-bed rivers, based on the relative roughness, are successful only at riffle sections. Errors for the discharge estimates at pool sections are quite large which Hey attributed to backwater effects. The riffle sections in gravel rivers act as hydraulic control sections, and only at these sections will the flow depth and velocity be a function of the local hydraulic geometry.

Data collected by Hey at riffle sections (see Appendix B) was used to derive Equation 3.4:

$$\frac{1}{\sqrt{f}} = 2.03 \log \left(\frac{3.78 R}{D_{84}} \right) \quad (3.4)$$

Equation (3.4) is virtually identical to the Limineros relationship (equation (3.3)). Equation 3.4 is shown together with the field data in Figure 3.1.

Bray (1982a) determined that k_s was equal to $3.5 D_{84}$ and $6.8 D_{50}$. From these relationships Equation (3.4) can be rewritten as:

$$\frac{1}{\sqrt{f}} = 2.03 \log \left(\frac{1.94 R}{D_{50}} \right) \quad (3.5)$$

when the D_{50} fraction is used. Bray (1982a) indicates that there is no advantage in using D_{84} over D_{50} when calculating the flow resistance.

3.3.2 Power-Law Flow Resistance Equations

The flow resistance coefficient from the Manning-Strickler relationship is as follows:

$$\frac{1}{\sqrt{f}} = k \left(\frac{R}{D} \right)^{1/6} \quad (3.6)$$

where k is an empirical constant.

When fitted to the riffle data in Appendix B Equation 3.6 becomes:

$$\frac{1}{\sqrt{f}} = 1.93 \left(\frac{R}{D_{84}} \right)^{1/6} \quad (3.7)$$

Kellerhalls (1967) found that for immobile gravel rivers with very low sediment transport the flow resistance was best explained by:

$$\frac{1}{\sqrt{f}} = k \left(\frac{R}{D} \right)^{1/4} \quad (3.8)$$

When fitted to the riffle data in Appendix B Equation (3.8) becomes:

$$\frac{1}{\sqrt{f}} = 1.67 \left(\frac{R}{D_{84}} \right)^{1/4} \quad (3.9)$$

Equations 3.7 and 3.9 are plotted together with the field data in Figure 3.1.

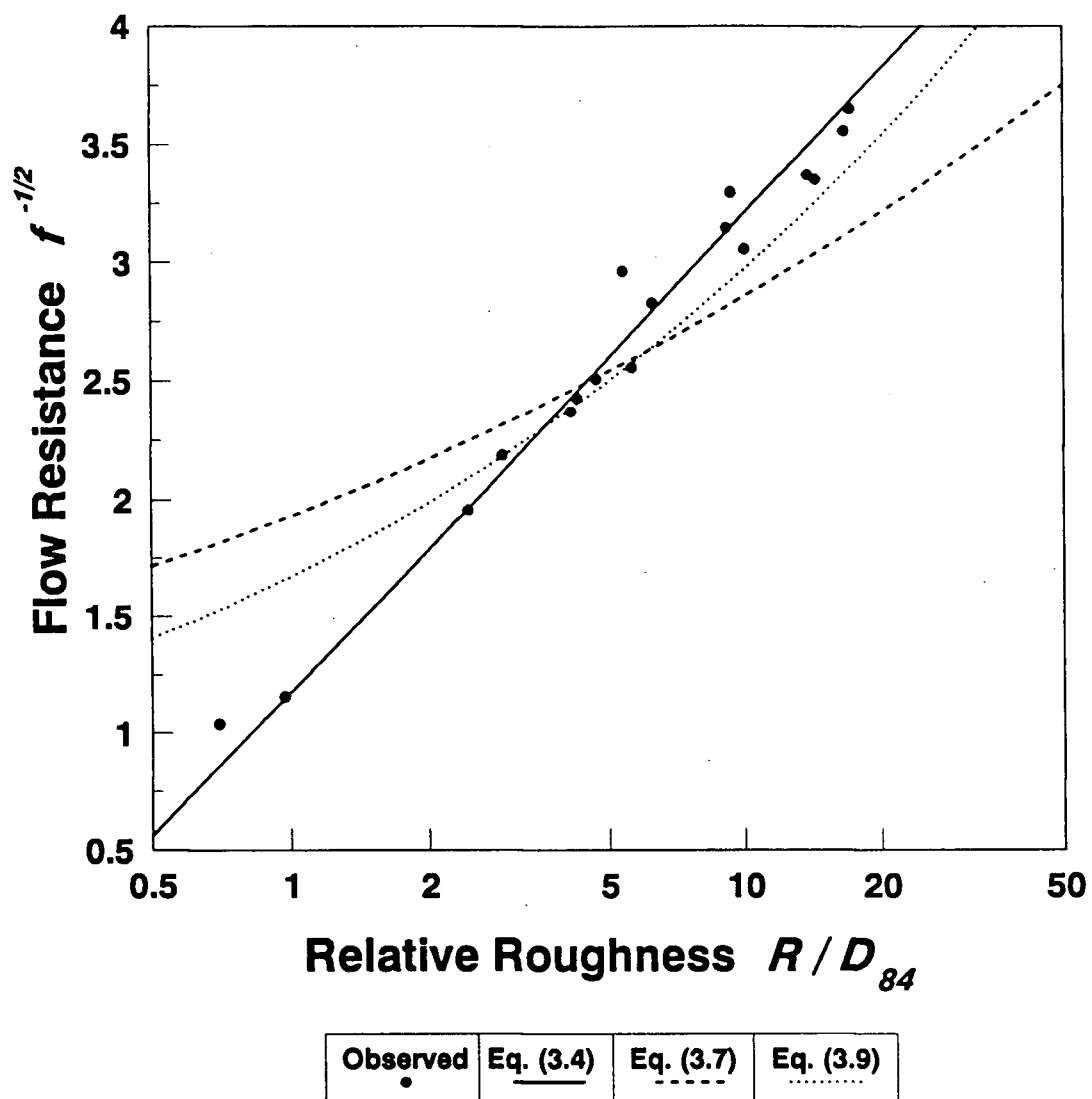


Figure 3.1: Logarithmic and Power-Law Flow Resistance Equations Fitted to the Riffle Data of Hey (1979).

3.3.3 Discussion

Figure 3.1 shows that the logarithmic Equation (3.4) closely approximates the variation in the observed flow resistance. This form of the flow resistance equation is theoretically sound and has been successfully applied to open channel and pipe flow. The power-law equations do not explain the observed flow resistance.

The power-law equations have been favoured for open channel flow where they are widely used. These equations are empirical with no theoretical basis.

Figure 3.2 shows the behavior of the functions $y = \log x$, $y = x^{1/6}$, and $y = x^{1/4}$. Depending upon the x range considered, the logarithmic relationship can be approximated by a power-law equation. For example the 1/4 power-law relationship of Kellerhalls (1967) was developed from immobile gravel rivers with relative roughness values, R/D_{50} , between 6.1 – 44.1. Data from rivers with larger relative roughness values (deeper and/or finer bed material) will be more closely approximated by the widely accepted 1/6 power-law relationship of Manning-Strickler.

The power-law flow resistance equations are thus only approximations of the actual logarithmic relationship. These empirical power-law equations are derived by fitting a curve to a limited range of data. Outside of this range the power-law approximation will not hold.

The logarithmic form of the flow resistance equation is recommended.

3.4 THRESHOLD OF MOVEMENT

In order to model the transport of sediment and to assess the stability of channel banks it is necessary to determine the conditions at which a particle will become mobilized. The following section presents several approaches to the onset of sediment motion.

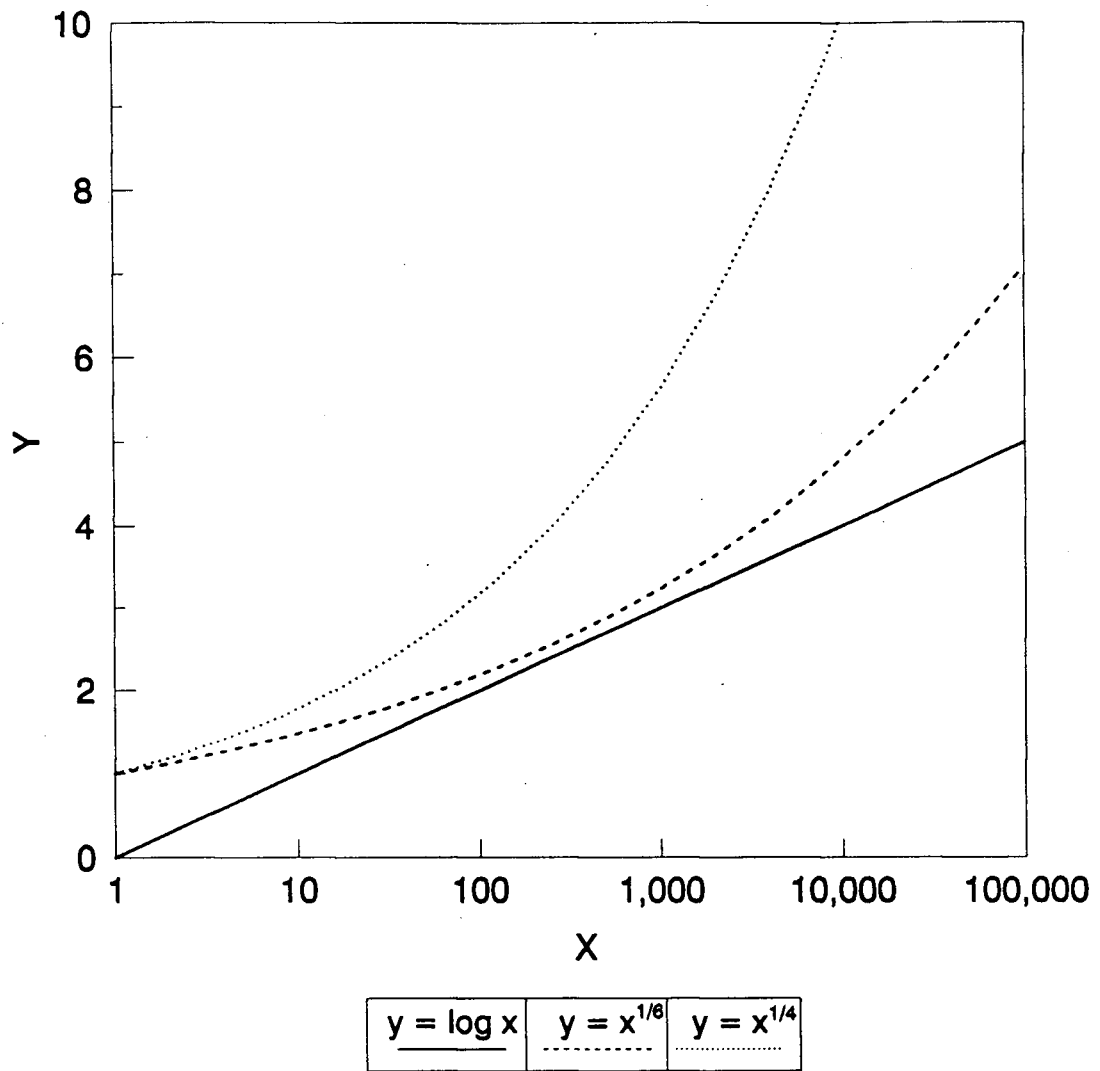


Figure 3.2: Semi-log plots of the Functions $y = \log x$, $y = x^{1/6}$, and $y = x^{1/4}$.

3.4.1 Dimensionless Shear Stress Approach

In his classic paper, Shields (1936), quoted by Henderson (1966, p 411-413), derived his dimensionless bed shear stress function, τ^* :

$$\tau^* = \frac{\tau_o}{\gamma (S_s - 1) D} \quad (3.10)$$

which can, for a wide channel, be stated more simply as:

$$\tau^* = \frac{R S}{1.65 D} \quad (3.11)$$

where τ_o = mean bed shear stress which for a wide channel is $\approx \gamma R S$; γ =unit weight of water; S_s =specific gravity of the grains (assumed here to equal 2.65); D is the diameter of the grains.

Shields (1936) also defined the particle Reynolds Number as;

$$R_e^* = \frac{v^* D}{\nu} \quad (3.12)$$

where v^* is the average shear velocity = $\sqrt{g R S}$; ν is the kinematic viscosity; R_e^* is the particle Reynolds Number.

Shields plotted his data in the $\tau^* - R_e^*$ plane resulting in a simple relationship between the two dimensionless groups whereby for $R_e^* \geq 400$ (which corresponds to a grain size greater than about 6 mm), the value of τ^* is constant and equal to 0.056.

Neill (1967) determined that for gravels, $\tau_c^* = 0.03$. This is the generally accepted value for the breakup of the pavement¹ layer for gravel rivers, based upon the mobility of the median pavement grain size, D_{50} .

¹The term pavement used in this thesis is that of Parker *et al* (1982) who define pavement as the coarse layer which develops on the bed of gravel rivers and becomes mobile only during relatively high flows. In contrast armour is defined as a coarse layer which never moves.

3.4.2 Excess Stream Power Approach

Bagnold (1977, 1980) derived a sediment transport relationship where the rate of sediment transport is expressed as a power-law function of excess unit stream power, $\omega - \omega_o$, where ω equals the stream power in mass units/unit bed area = $\rho q S$; ω_o equals the threshold stream power below which no sediment transport is possible.

Equation 3.13 relates ω to τ^* . The derivation is presented in Appendix C.

$$\omega = 38200 \tau^{*1.5} D^{1.5} \log \left(\frac{3.20 \tau^*}{S} \right) \quad (3.13)$$

Substituting $\tau^* = 0.03$ into Equation 3.13 yields:

$$\omega_o = 200 D^{1.5} \log \left(\frac{0.10}{S} \right) \quad (3.14)$$

A similar equation was derived by Bagnold (1980).

3.4.3 Threshold of Movement from Field Studies

In contrast to the work of Shields (1936), Neill (1967), and others, Parker *et al* (1982) and Andrews (1983) have studied the inception of particle movement by analysing bedload transport measurements in gravel rivers.

This method differs significantly from the flume studies of Shields, Neill, and others in that the sediment mixture is highly non-uniform, the discharge variable, and a coarse layer of surficial pavement shields the finer subsurface material from the flow at low discharges.

Parker *et al* (1982) and Andrews (1983) derived the following equations for the critical dimensionless shear stress:

Parker *et al* (1982):

$$\tau_{ci}^* = 0.0876 \left(\frac{d_i}{d_{50}} \right)^{-1} \quad (3.15)$$

Andrews (1983)

$$\tau_{c_i}^* = 0.0834 \left(\frac{d_i}{d_{50}} \right)^{-0.872} \quad (3.16)$$

$\tau_{c_i}^*$ = the critical dimensionless shear stress of the i^{th} size fraction of the subpavement sediment; d_i = the diameter of the i^{th} size fraction of the subpavement sediment; d_{50} = the median grain diameter of the subpavement sediment.

Equations 3.15 and 3.16 can be approximated with little error by:

$$\tau_{c_i}^* = 0.09 \left(\frac{d_i}{d_{50}} \right)^{-1} \quad (3.17)$$

$$\frac{\tau_{c_i}}{\gamma (S_s - 1) d_i} = 0.09 \left(\frac{d_{50}}{d_i} \right) \quad (3.18)$$

$$\frac{\tau_{c_i}}{\gamma (S_s - 1)} = 0.09 d_{50} \quad (3.19)$$

(The above analysis was shown to the author by Dr Michael Church.)

Thus when the i^{th} fraction is set equal to d_{50} , Equation 3.19 simplifies to:

$$\tau_{c_{d_{50}}}^* = 0.09 \quad (3.20)$$

where $\tau_{c_{d_{50}}}^*$ = the critical dimensionless shear stress of the subpavement median grainsize.

Two features of the above analysis are noteworthy.

1. Equation 3.19 indicates that the mobility of the subpavement sediment is independent of the grain diameter of the individual size fractions, and depends only upon the median grainsize of the sediment mixture.
2. Equation 3.20 indicates that the subpavement median grainsize will become mobile at a constant value of τ^* .

At the point of pavement mobilization $\tau_{D_{50}}^* = 0.03$ and $\tau_{d_{50}}^* = 0.09$. Thus:

$$\frac{\frac{\tau}{\gamma (S_s - 1) d_{50}}}{\frac{\tau}{\gamma (S_s - 1) D_{50}}} = \frac{0.09}{0.03} \quad (3.21)$$

which simplifies to:

$$\frac{D_{50}}{d_{50}} = 3.00 \quad (3.22)$$

The median pavement grain diameter, D_{50} , is on average 3 times the diameter of the subpavement grain diameter, d_{50} . Thus when the pavement layer becomes mobile, all subpavement sediment up to 3 times the median subpavement grainsize would be expected to become mobilized instantaneously. Parker *et al* (1982) Andrews (1983) found however that grains up to 4.2 times the diameter of d_{50} became mobile at the same stage. This can only be explained by a decrease in τ_c^* following the breakdown of the pavement layer, and this conclusion is discussed below.

3.4.4 Discussion

According to Andrews (1983), Equations 3.15 and 3.16 are valid for particle diameters less than 4.2 times d_{50} . For particles larger than 4.2 times d_{50} , the critical dimensionless shear stress approached a constant value of 0.02. This agrees with the results of Ramette and Heuzel (1962), quoted by Andrews (1983), who found that the critical shear stress of the largest radioactively marked grains introduced into the Rhone River approached a lower limit of 0.02.

The results presented by Parker *et al* (1982), and Andrews (1983) are somewhat misleading. The critical shear stress of a sediment size was determine from its first appearance in the bed load samples. The presence of a coarse bed pavement layer shields the finer fractions of the subpavement sediment from the flow. This finer sediment

would have become mobilized at lower shear stresses if it had been exposed to the flow. Thus at the shear stress required for the break-up of the pavement layer, much of the sediment becomes instantaneously mobilized. The critical shear stresses suggested by Equations 3.15 and 3.16 are in effect only apparent.

The relationships determined by Parker *et al* and Andrews are consistent with $\tau_c^* \approx 0.02$ following breakup of the pavement. Equation 3.20 indicates that the $\tau_{d_{50}}^*$ is 0.09 at the breakup of the pavement layer. Thus, consistent with a critical dimensionless shear stress of 0.02, all particles up to approximately 4.5 times the median subpavement grainsize will become mobile instantaneously upon breakdown of the pavement layer. This is in agreement with the observations of Andrews and Parker *et al*.

The variation in the critical shear stress can be explained in terms of exposure of the grain to the flow. Fenton and Abbot (1977) mounted a test grain on a rod which protruded through the base of an artificially roughened flume. When the grain was fully exposed the critical dimensionless shear stress was 0.01. The critical shear stress increased dramatically as the exposure of the grain to the flow was reduced.

3.4.5 Conclusions

Variations in the critical dimensionless shear stress must be accounted for during modelling of sediment transport and bank stability. It appears that the pavement layer appears to break down at $\tau_{D_{50}}^* = 0.03$. Once this layer is broken the subpavement sediment becomes mobilized at $\tau_{c_i}^* = 0.02$ due to increased exposure of the grains to the flow. This results in most of the subsurface sediment becoming active at the stage of pavement breakup.

On the falling limb of the flood the bed will remain mobile at stages less than what was required to initiate breakup of the pavement.

It is likely that the critical dimensionless shear stress for the channel banks will be

much higher than for the bed. As the banks are essentially immobile, with time the unstable and highly exposed grains will tend to be selectively removed from the bank. This will result in a more stable bank pavement layer which will require higher stresses to initiate movement.

Two questions which remain unanswered at this point are:

1. Why does the subpavement appear to become consistently mobilized at a critical dimensionless shear stress of 0.09 for the median subpavement grain diameter ?
2. Why is the ratio of pavement to subpavement median grain diameters typically close to 3 ?

3.5 BANK STABILITY

A stable bank is a requirement of an equilibrium channel. River banks can be broadly classified into 3 types:

1. Non-cohesive banks which are formed from sand and gravel alluvium similar to the bed material.
2. Cohesive banks which are formed from cohesive silts and clays.
3. Composite banks are comprised of a lower non cohesive unit (often point-bar deposits) overlain by a cohesive layer of clay, silt, and fine sand.

The mechanics of bank erosion and failure are markedly different for the three bank types. Erosion of non-cohesive banks occurs as fluvial entrainment of discrete grains. The stability of non-cohesive banks can be assessed from the stability of the individual grains (eg Lane, 1955b).

Erosion and failure of cohesive banks occurs as fluvial entrainment of grains or aggregates of grains, and through mass failure (Thorne, 1988). Mass failures can occur when bank becomes oversteepened or the channel depth exceeds a critical depth for bank stability.

Composite banks retreat through fluvial entrainment of grains from the lower non-cohesive unit resulting in undercutting of the upper cohesive unit. This may be followed by mass failure of the upper unit.

The following discussion will consider only the stability of non-cohesive bank sediment. This includes composite river banks, as the bank stability is principally controlled by fluvial erosion of the lower non-cohesive unit.

The stability of non-cohesive banks is an area of active research. An example of recent work can be found in Osman and Thorne (1988) and Thorne and Osman (1988).

3.5.1 USBR Method for Non-Cohesive Banks

A summary of the United States Bureau of Reclamation method is given in Lane (1955b). This method resolves the forces acting on a particle on the sides of a channel. These forces are:

1. The force of the water tending to move the particle down the canal in the direction of flow.
2. The force of gravity tending to move the particle down the sloping channel bank.

These forces are opposed by a resisting force which is proportional to the vertical component of the particle weight multiplied by the coefficient of internal friction.

Analysis of these forces leads to the following expression for K , the bank stability factor:

$$K = \frac{\tau_o}{\tau_c} = \cos \theta \sqrt{1 - \frac{\tan^2 \theta}{\tan^2 \phi}} \quad (3.23)$$

This expression was later simplified by Henderson (1966, p 419) to:

$$K = \sqrt{1 - \frac{\sin^2 \theta}{\sin^2 \phi}} \quad (3.24)$$

τ_o = the mean shear stress acting on the bank of the channel, τ_c = the critical shear stress required to move the grain on a horizontal bed, θ = the angle of the bank slope from the horizontal, ϕ = the angle of repose of the bank sediment.

The USBR method assumes that the shear stress acting on the particle is horizontal. This may not hold when secondary currents are present.

Equation 3.24 can be expressed in a dimensionless form:

$$\frac{\bar{\tau}_{bank}}{\gamma (S_s - 1) D_{50_{bank}}} = 0.056 \sqrt{1 - \frac{\sin^2 \theta}{\sin^2 \phi}} \quad (3.25)$$

$\bar{\tau}_{bank}$ = the mean bank shear stress; $D_{50_{bank}}$ = the median bank grain diameter; 0.056 = the critical dimensionless shear stress for the bank sediment.

3.5.2 Modification of ϕ

USBR data (Lane, 1955b) indicates that the angle of repose for coarse gravel approaches a maximum of approximately 40° . Due to the presence of bank shear stresses, a riverbank comprised of gravel would require a bank slope of somewhat less than 40° to remain stable. However stable banks comprised of gravel are observed to have bank slopes in excess of 40° .

Wolman and Brush (1961) observed that the admixture of small amounts of cohesive silts and clays produce steeper side slopes than would be expected in non-cohesive material. Thus the effective *insitu* angle of repose of the bank sediment will often be much

greater than the equivalent material forming the gravel bar in the same channel.

3.5.3 Vegetation

The effect of the bank vegetation on stream bank stability may be significant. The vegetation effect depends on many factors including the type and density of the vegetation, the depth and density of the root mass, and probably the size of the channel.

When determining empirical regime equations for gravel rivers (see section 2.3) Hey and Thorne (1986) found that for the same discharge a river with a grass covered bank was on average 1.85 times wider than a river with > 50% coverage of trees and shrubs on the banks. The more densely vegetated banks were able to withstand higher shear stresses than the grass covered banks. Similarly Andrews (1984) found that rivers described as having thin bank vegetation were 1.26 times wider than those having thick bank vegetation.

Conversely Zimmerman *et al* (1967) found that the widths of the small streams in their study decreased for streams flowing through meadows, but were wider when flowing through forested areas. In this case the channel banks in the meadows were stabilised by dense networks of grass roots. In the forested areas the larger tree roots were less capable of binding the bank material.

3.6 DISTRIBUTION OF THE BOUNDARY SHEAR STRESS

The mean boundary shear stress can be determined from:

$$\tau = \gamma R S \quad (3.26)$$

Or for wide channels

$$\tau = \gamma Y S \quad (3.27)$$

τ = the mean boundary shear stress; γ = the unit weight of water (typically 9810 N/m³); R = the hydraulic radius; Y the average depth; S = the slope of the energy grade line which is generally assumed to equal the slope of the free surface, or the channel bed in the case of uniform flow. The derivation of the above equations can be found in any hydraulics text such as Henderson (1966) or Chow (1959).

The boundary shear stress is not uniformly distributed along the wetted perimeter. The distribution of the shear stress must be known in order to determine a stable channel geometry.

The USBR as part of their program to investigate methods for designing unlined canals was the first successful attempt at determining the distribution of the boundary shear stress (an earlier attempt by Leighly (1932) was inconclusive due to a lack of data). This work by the USBR is summarized by Lane (1955b).

The USBR, and subsequent investigations has shown that the distribution of boundary shear stress is influenced by the aspect ratio (W/Y) of the channel, the slope of the side walls, and any roughness variation along the wetted perimeter.

The development of secondary currents makes analytical solution of the shear stress distribution very difficult. Consequently empirical equations have been fitted to experimental data.

Knight (1981) and Knight *et al* (1984) considered the distribution of the shear force (SF):

$$SF = SF_{bed} + SF_{bank}$$

Which equals:

$$\bar{\tau}P = \bar{\tau}_{bed}P_{bed} + \bar{\tau}_{bank}P_{bank}$$

where P is the perimeter. Experimental data were used to obtain an expression for $\%SF_{bank}$ which is the percentage of the shear force acting on the banks. From this the

average shear stresses acting on the bank and the bed can be determined.

The method of Knight was limited to straight rectangular channels with uniform boundary roughness. It was extended by Flinham and Carling (1988) to include trapezoidal channels with non-uniform roughness. The equations of Flinham and Carling are presented here.

The percentage of the shear force being carried by the banks of the channel with uniform bed and bank roughness is given by:

$$\log \%SF_{bank} = -1.4026 \log \left(\frac{P_{bed}}{P_{bank}} + 1.5 \right) + 2.247 \quad (3.28)$$

The following relations were derived for the mean bank and bed shear stresses:

$$\frac{\bar{\tau}_{bank}}{\gamma Y S} = 0.01 \%SF_{bank} \left[\frac{(W + P_{bed}) \sin \theta}{4 Y} \right] \quad (3.29)$$

$$\frac{\bar{\tau}_{bed}}{\gamma Y S} = 1 - .01 \%SF_{bank} \left[\frac{W}{2 P_{bed}} + 0.5 \right] \quad (3.30)$$

The data used to derive the above equations was obtained from artificially roughened plywood channels with P_{bed}/P_{bank} ratios between 0.5 - 10, with bank angles of 45°, 68°, and 90°. Equations 3.28 to 3.30 are displayed graphically in Figures 3.3 to 3.5.

Natural channels are typically have P_{bed}/P_{bank} ratios much greater than 10, and bank angles typically less than 35°. While these values are outside of the range of experimental data used to derive Equations 3.28, 3.29, and 3.30, it is assumed that the exponential character of these equations permits extrapolation beyond the limits of the experimental data.

3.7 SEDIMENT TRANSPORT

Following a review of the numerous sediment transport equations available, it was concluded that the equations of Parker, Klingeman, and MacLean (1982) were most suitable

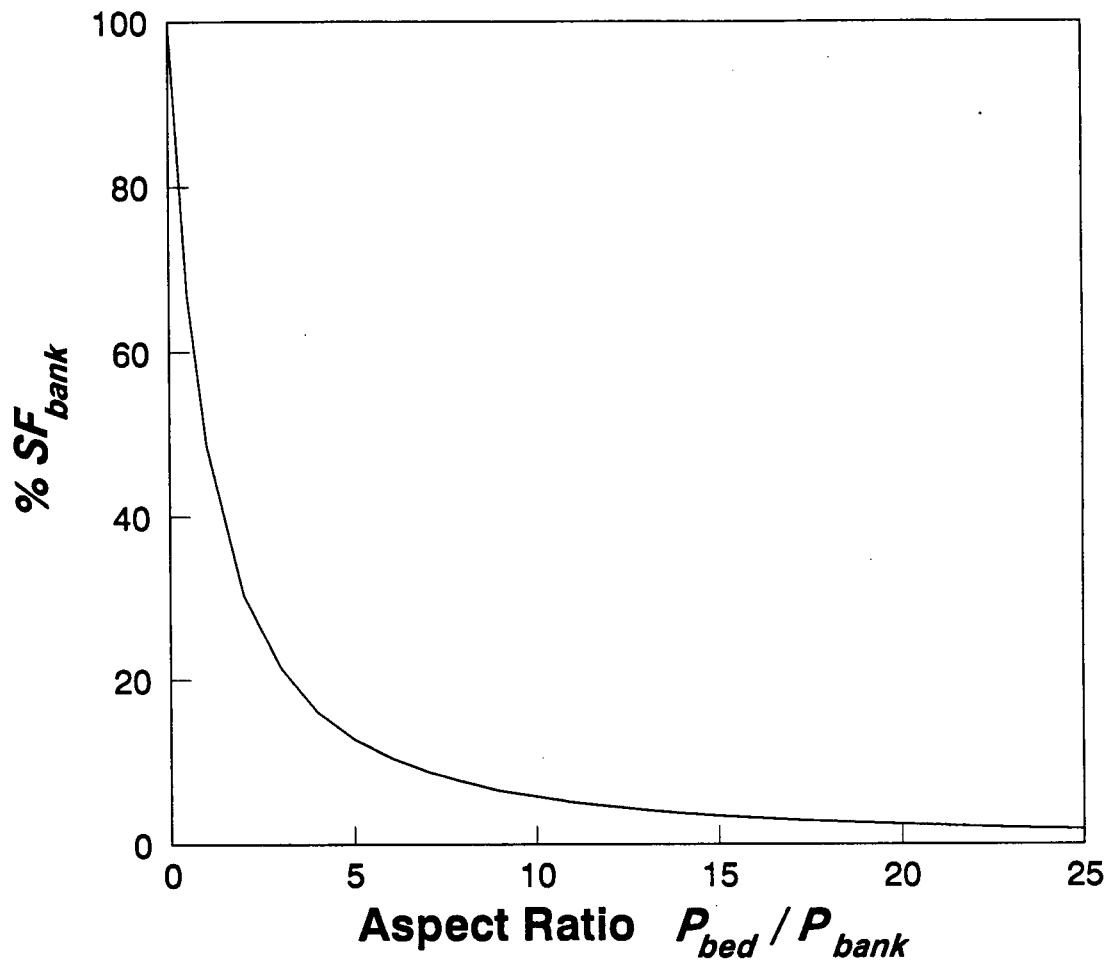


Figure 3.3: $\%SF_{bank}$ as a Function of The Aspect Ratio P_{bed}/P_{bank} from Equation 3.28.

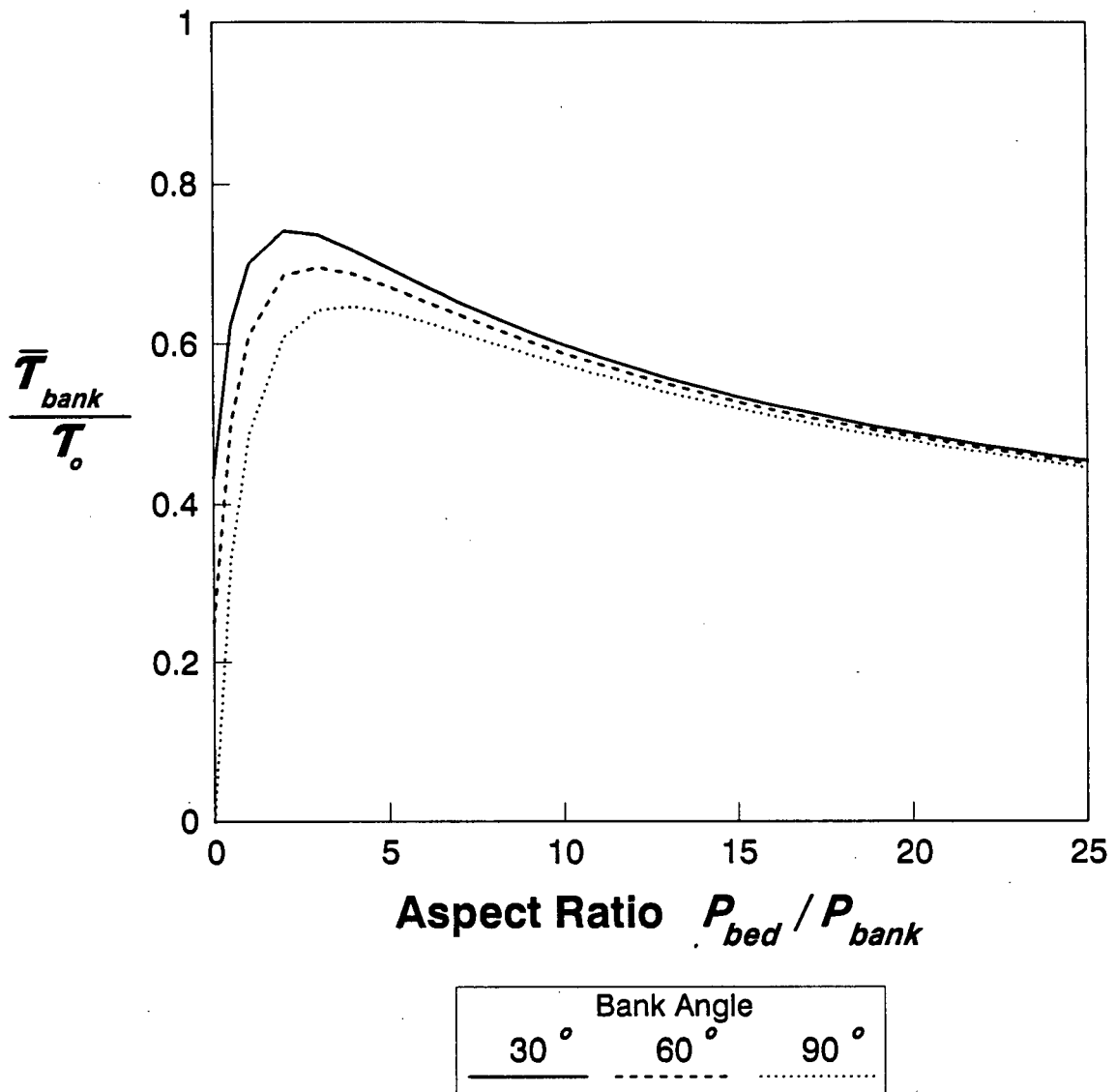


Figure 3.4: The Relationship Between the Non-Dimensional Mean Bank Shear Stress and the Aspect Ratio P_{bed}/P_{bank} from Equation 3.29. Y_o is the Maximum Channel Depth. The Non-Dimensional shear stress is given by $\tau_{bank}/\gamma Y_o S$.

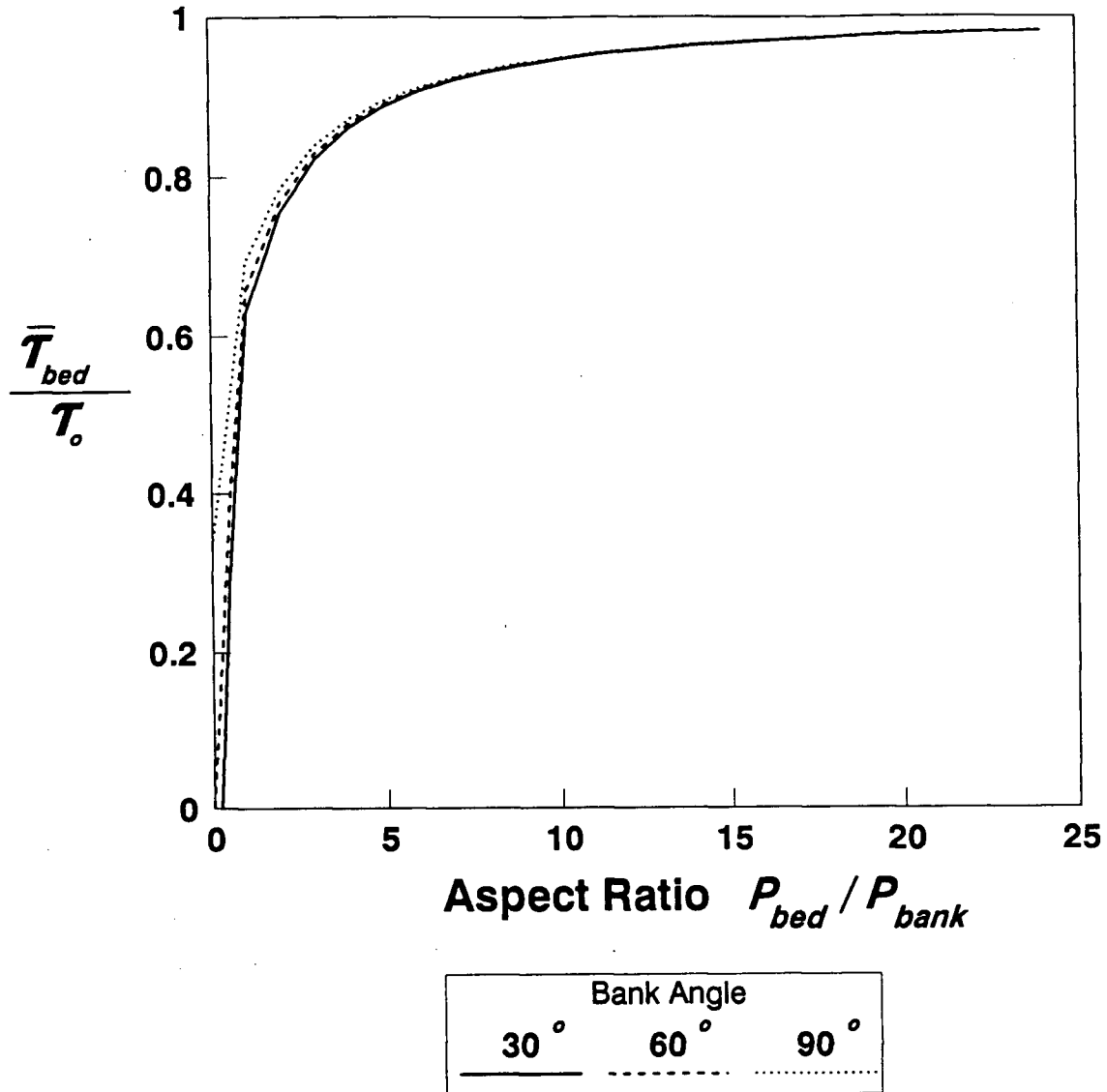


Figure 3.5: The Relationship Between the Non-Dimensional Mean Bed Shear Stress and the Aspect Ratio P_{bed}/P_{bank} from Equation 3.30. Y_o is the Maximum Channel Depth. The Non-Dimensional shear stress is given by $\tau_{bed}/\gamma Y_o S$.

for modelling gravel rivers. The PKM equations are rationally based and derived from high quality bedload transport measurements from natural gravel rivers.

The PKM equations assume that the d_{50} of the subpavement is representative of the bedload. No sediment transport is assumed until $\tau_{d_{50}}^*$ approaches 0.0876 (see Section 3.4.3 for discussion).

The bedload measurements are used to derive equations for W^* , which Parker *et al* term the total dimensionless bedload:

$$W^* = \frac{q_s^*}{\tau^{*3/2}} \quad (3.31)$$

q_s^* = Einstein bedload parameter (dimensionless) = $q_s / (D \sqrt{(S_s - 1) g D})$; q_s = the volumetric bedload per unit bed width; τ^* = dimensionless bed shear stress.

W^* is a bedload efficiency term as defined by Bagnold (1966). Equation 3.31 which can be reduced to (see Appendix F):

$$W^* = \sqrt{\frac{8g}{f}} \frac{i_b}{\omega} \quad (3.32)$$

i_b = unit bedload transport rate by immersed weight (kg/sec); ω = unit stream power in mass units (kg/sec); f = Darcy-Weisbach friction factor.

The equations for W^* are expressed as $f(\phi_{50})$ where $\phi_{50} = \tau_{d_{50}}^* / 0.0876$. The equations are:

$$W^* = \begin{cases} 0.0025 \exp[14.2 (\phi_{50} - 1) - 9.28 (\phi_{50} - 1)^2] & 0.95 < \phi_{50} < 1.65 \\ 11.2 \left(1 - \frac{0.822}{\phi_{50}}\right)^{4.5} & \phi_{50} \geq 1.65 \end{cases} \quad (3.33)$$

A full discussion is presented in Parker *et al* (1982).

3.8 EXTREMAL HYPOTHESES

In order to determine a unique solution for the governing equations of continuity, flow resistance, sediment transport, and bank stability, it is presently necessary to resort to an extremal hypothesis.

An extremal hypothesis, sometimes referred to as a variational principle (White *et al*, 1982), are based upon upon an assumption that the geometry of a channel develops such that some feature is maximised or minimized. Often there is no physical justification or theoretical support for these hypotheses. However extremal hypothesis have been combined with equations of flow and sediment transport to produce reasonable predictions of channel geometry (Chang, 1980; White *et al*, 1982).

The principal extremal hypotheses are summarized below.

3.8.1 Minimization Hypotheses

This grouping includes 3 similar hypotheses: the theory of minimum stream power (MSP) (Chang 1979, 1980), the theory of minimum unit stream power (MUSP) (Yang, 1976), and the theory of minimum energy dissipation rate (MEDR) (Yang and Song, 1979).

These three hypotheses are generally equivalent under conditions of imposed discharge and sediment load. The MSP and MUSP are special cases of the more general MEDR (Yang and Song, 1979).

When applied to natural rivers these hypotheses imply that the channel will develop at the minimum slope required to transport the imposed load of water and sediment.

3.8.2 Maximum Transport Capacity

The hypothesis of maximum transport capacity (MTC) (White *et al*, 1982) is based upon the assumption that, for a given slope, a channel will adjust its width until the sediment

transport capacity is maximized.

The existence of sediment transport maximum can be obtained through the iterative solution of a sediment transport equation for various channel widths (Pickup, 1976; White *et al*, 1982).

For a given channel gradient, this hypothesis gives a unique channel geometry and sediment transport capacity.

If the sediment transport capacity of the channel does not equal the imposed sediment load the channel will increase or decrease its slope (simultaneously dynamically adjusting the other dependent variables including width), until the sediment transport capacity of the channel is equal to the imposed sediment load.

3.8.3 Discussion

As previously stated the three minimization hypotheses are generally equivalent under normal conditions and imply a minimization of the channel slope. Furthermore the TC hypothesis was shown by White *et al* (1982) to be equivalent to the minimization of channel slope.

Chang (1980) and White *et al* (1982) have included their respective extremal hypotheses in analytical models to predict the geometry of alluvial rivers with reasonable success.

3.9 Conclusions

The theory required for the development of an analytical model of river response was presented in this chapter. The model to be developed in this thesis will be of the type developed by Chang (1979, 1980), and White *et al* (1982). This model type is based upon the iterative solution of the governing equations which describe the channel processes.

The results of the Chang and the White *et al* models agreed fairly well with the observed channel geometries, however the degree of scatter was too excessive for these models to be used for engineering applications.

The stability of the channel banks must be addressed. It was shown in Section 3.5.2 that the bank vegetation (which represents only one component of the bank stability) can influence the channel width by a factor of 2. This indicates that the bank vegetation alone can influence the channel width to the same order as a four-fold increase or decrease in the bankfull discharge (from Equation 2.4).

The model to be proposed in this thesis will include additional channel processes, principally the distribution of the boundary shear stresses, and bank stability analysis.

Chapter 4

DEVELOPMENT OF RIVERMOD

4.1 INTRODUCTION

RIVERMOD is an analytical computer model designed to predict the response of an alluvial channel to changes in the input variables, principally dominant discharge and sediment load. The model structure is based on simplified physical processes. RIVERMOD outputs the stable channel geometry which is required to transport the imposed water and sediment load.

This chapter explains the theoretical development of RIVERMOD.

4.2 SIMPLIFYING ASSUMPTIONS

Alluvial rivers are dynamic, highly complex systems. The following simplifying assumptions are incorporated into RIVERMOD.

1. The channel geometry can be modelled on the bankfull discharge.
2. The sediment transport capacity of the channel at the bankfull stage is representative of the total bedload.
3. A trapezoidal channel develops with a mobile bed and stable, immobile banks.
4. The banks develop at the threshold of sediment movement at the bankfull stage.

5. Secondary currents are not significant. Thus the bed and bank shear stresses, while not equal in magnitude, are both assumed to be uniformly distributed across their respective channel perimeters.
6. The flow resistance is due to grain roughness only.

4.3 MODEL THEORY

This section contains a brief discussion of the equations and concepts used in RIVERMOD.

4.3.1 Flow Resistance

The following flow resistance equation was developed in Section 3.3.1:

$$\frac{1}{\sqrt{f}} = 2.03 \log \left(\frac{1.94 R}{D_{50}} \right) \quad (3.5)$$

Previous attempts at analytically modelling river channel changes such as Chang (1979, 1980) assumed that the pavement grainsize distribution, usually represented by D_{50} or D_{85} , remains unchanged. It is known however that a river has the capacity to modify the pavement grainsize distribution and thus the channel roughness.

Consider a channel which has a vanishingly small bedload transport rate. The channel will have adjusted to a threshold condition at the bankfull stage where the dimensionless bed stress, $\tau_{D_{50}}^* = 0.03$. If a change is imposed onto the channel such as an increase in slope or width due to channellization, the channel will respond by dynamically adjusting its depth and pavement grainsize distribution such that $\tau_{D_{50}}^*$ will, after a period of adjustment, be again equal 0.03.

By analogy it is proposed that for mobile bed channels, $\tau_{D_{50}}^*$ will also remain constant during channel adjustments.

Assuming that the specific gravity of the transported sediment equals 2.65, the Shields equation can be written as (see section 3.4.1):

$$\tau^* = \frac{R \cdot S}{1.65 D_{50}} \quad (3.11)$$

Substituting equation 3.11 into 3.5 yields:

$$\frac{1}{\sqrt{f}} = 2.03 \log \left(\frac{3.2 \tau^*}{S} \right) \quad (4.1)$$

The assumption of constant $\tau_{D_{50}}^*$ is probably valid when the channel is not responding to large changes in the sediment input. The present version of RIVERMOD will assume that equation 4.1 will apply to any channel adjustments. The relationship between subpavement and pavement median grainsizes, and sediment transport rates is an area for future research.

4.3.2 Continuity

The equation for steady continuity is:

$$Q = v R (P_{bed} + P_{bank}) \quad (4.2)$$

The mean channel velocity, v , is calculated from open channel form of the Darcy-Weisbach equation:

$$v^2 = \frac{8 g R S}{f} \quad (4.3)$$

Substituting equations 3.5 and 4.3 into 4.2 gives:

$$Q' = 5.74 \log \left(\frac{3.2 \tau^*}{S} \right) \sqrt{g R S} R (P_{bed} + P_{bank}) \quad (4.4)$$

Q' is the theoretical discharge capacity of the channel which assumes that the total channel roughness is given by equation 3.5.

In order to eliminate the error which is due to the presence of roughness elements other than grain roughness such as macro bed forms, coarse organic debris, spill roughness *etc*, Q'_{bank} is calculated from the initial channel geometry using equation 4.4 and is used in preference to the actual Q_{bank} . Thus it is implicitly assumed in RIVERMOD that the non grain roughness remains constant during channel adjustment.

The use of Q'_{bank} rather than Q_{bank} is a valid approach as tractive force theory is used in RIVERMOD to calculate the sediment transport rates and in the bank stability analysis. Therefore it is more important to accurately model the depth of flow, from which the shear stress is calculated, rather than the velocity, stream power, or actual discharge.

4.3.3 Distribution of the Boundary Shear Stress

The method of Knight (1981) and Knight *et al* (1984) modified by Flinham and Carling (1988) is used. The method is discussed in some detail in section 3.6. The performance of their formula are shown graphically in Figures 3.3 - 3.5.

Figure 3.4 indicates that for a particular slope, increasing the aspect ratio not only reduces the total shear stress, $\gamma R S$, but also the fraction of the total shear stress acting on the banks also decreases.

Figure 3.5 indicates that for aspect ratios typical of natural rivers ($P_{bed}/P_{bank} > 10$), the bed shear stress approaches $\gamma Y_o S$.

4.3.4 Bank Stability

The bank stability analysis strictly applies only to banks comprised of noncohesive sediment. The method was developed by the USBR and is discussed in Lane (1955 b) and in section 3.5.

Equation 3.25 is rewritten here:

$$\frac{\bar{\tau}_{bank}}{\gamma (S_s - 1) D_{50_{bank}}} = 0.056 \sqrt{1 - \frac{\sin^2 \theta}{\sin^2 \phi}} \quad (3.25)$$

This equation defines the threshold of bank stability.

Equation 3.25 indicates that as the bankangle θ approaches the angle of repose of the bank sediment ϕ , the expression on the right approaches zero, and the shear stress that can be tolerated by a stable bank also approaches zero. Conversely as θ decreases, the stable bank can tolerate larger shear stresses.

This approach to bank stability has some limited capacity for dealing with weak intergranular cohesion. Unconsolidated gravel has a maximum ϕ of about 40° (eg see Henderson, 1964; p. 420). Due to intergranular fines, root masses, or packing of the bank sediment, the effective angle of repose, ϕ' , may be much greater than 40° . A ϕ' of up to 90° can be used with Equation 3.25.

4.3.5 Sediment Transport

The equations of Parker, Klingeman, and McLean (1982) are used in RIVERMOD. The equations are given in section 3.7. These equations are used to model the sediment transport capacity of the channel at the bankfull stage. These equations assume that the mobile sediment can be represented by the subpavement median grainsize.

The sediment transport is restricted to the channel bed. The banks are assumed to develop at the threshold of stability. Any sediment which becomes mobilized on the banks will move instantaneously down the bank to the bed. The bed shear stress used to calculate the sediment transport rate is calculated by the method of Flinham and Carling (1988, see equations 3.28 - 3.30).

It is assumed that the bedload capacity of the channel at the bankfull stage is representative of the total bedload. For example the response of a channel to an increase of

25% in the sediment supplied to the channel would be modelled as a 25% increase in the sediment transport capacity of the channel at the bankfull stage.

4.3.6 Extremal Hypothesis

There are 5 unknown variables which must be solved in order to determine a stable, equilibrium channel geometry: P_{bed} , P_{bank} , θ , S , and the boundary shear stress distribution, in particular $\bar{\tau}_{bank}$. There are essentially only 4 equations available to solve these variables: continuity, boundary shear stress distribution, bank stability, and the sediment transport equations.

An additional hypothesis is required and is usually referred to as an extremal hypothesis, as discussed in section 3.8.

White *et al* (1982) used the hypothesis of maximum transport capacity (MTC) in their model, to predict river geometry with relative success. Similarly Chang (1979, 1980) used the hypothesis of minimum stream power (MSP).

The bedload transport capacity, G_b , is shown as a function of the bed width for stable channels for a range of channel slopes in Figure 4.1. The PKM sediment transport equations, and the bank stability analysis discussed in preceeding sections were used to generate the data for Figure 4.1. The existance of a sediment transport maximum for a selected channel slope is evident. This agrees with the observations of Gilbert (1914) and the findings of Pickup (1976) and White *et al* (1982).

The MTC hypothesis of White *et al* implies that a channel will adjust its slope such that the sediment transport capacity maximum is equal to the sediment load imposed on the channel. Thus in the case of the hypothetical channel modelled in Figure 4.1, if the imposed sediment load is 44 kg/sec the channel will develop at a slope of .006 and surface width of approximately 35 metres as shown by the dashed lines.

The following examination of Figure 4.1 shows that the MTC hypothesis is generally

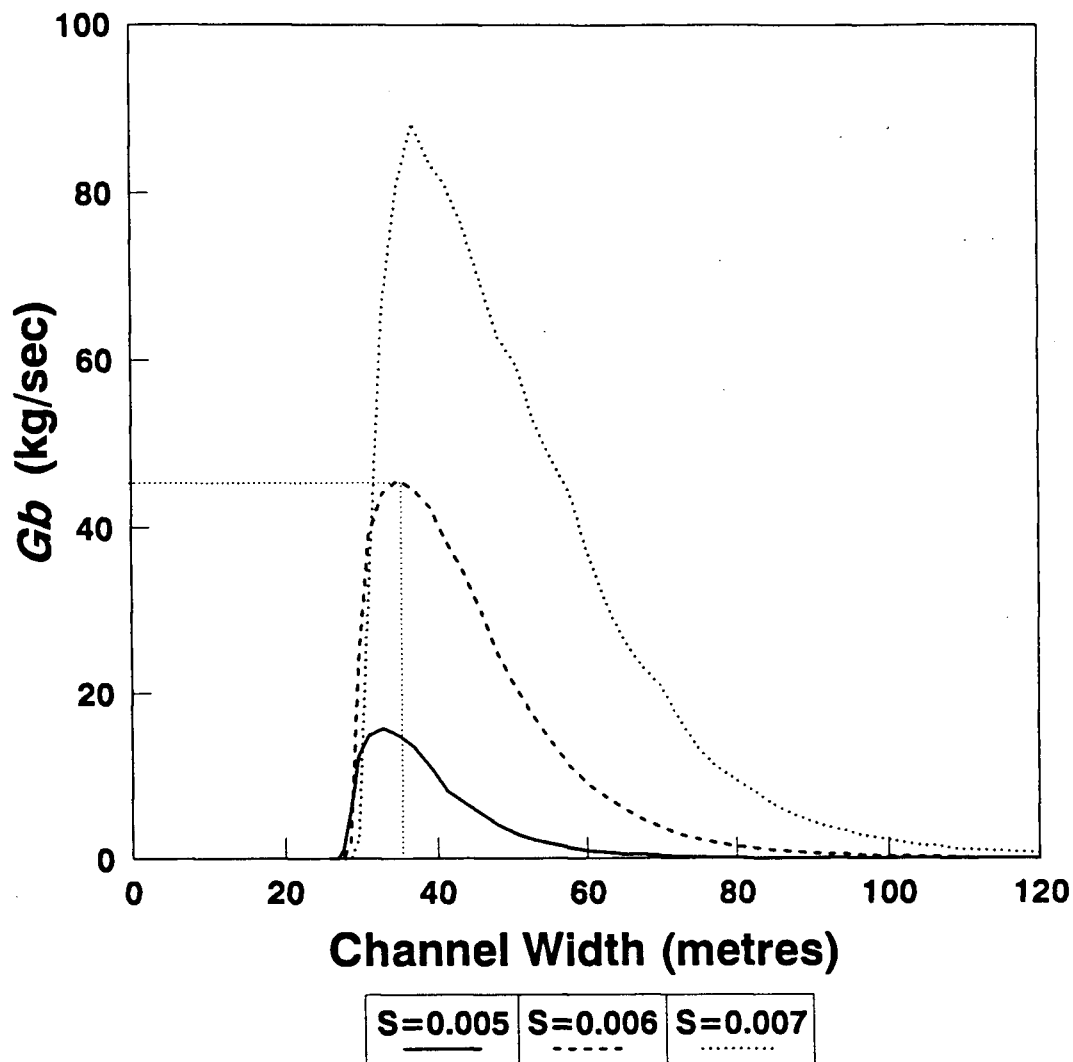


Figure 4.1: Bed-Load Transport Capacity for A Stable Channel as a Function of Bed Width for an Hypothetical Channel. $Q'_{bank} = 100 \text{ m}^3/\text{sec}$, $D_{50} = 0.075 \text{ metres}$, $D_{50_{bank}} = 0.075 \text{ metres}$, $d_{50} = 0.025 \text{ metres}$, $\phi = 40^\circ$.

equivalent to the MSP hypothesis.

In general the sediment transport capacity of a channel decreases with reduced channel slope. The minimum channel slope which can transport the imposed sediment load of 44 kg/sec is 0.006. A channel which develops at a slope less than 0.006 will be unable to transport all of the imposed sediment.

At the minimum channel slope of 0.006 the channel geometry must correspond to the MTC condition.

For slopes greater than the minimum required, the sediment load can be accommodated by two possible channel widths. In Figure 4.1 sediment continuity will be maintained for a channel slope of 0.007 for channel widths of approximately 32 or 60 metres. Clearly neither of these widths correspond to the MTC condition.

The equivalence of the MTC and MSP hypothesis was recognized by White *et al* (1982) following a different line of reasoning.

During the development of RIVERMOD it was found that poor predictions of channel geometry were obtained when using a sediment transport equation to predict the MTC condition.

The Einstein bedload function derived from laboratory data is shown graphically in Figure 4.2. The relation indicates that when the threshold condition is approached the sediment transport rate is strongly influenced by the threshold condition. For what may be described as fully mobile beds where $\tau^* > 0.1$, the transport rate is independent of the threshold condition. Brown (1950) and Kalinske (1947) have shown that for a given sediment and fluid, the transport rate for the fully mobile condition is given by:

$$G_b \propto P_{bed} \bar{\tau}_{bed}^3 \quad (4.5)$$

Neill (1968) determined that for gravel sediments the critical dimensionless bed shear stress is 0.03, not the 0.056 indicated by Figure 4.2.

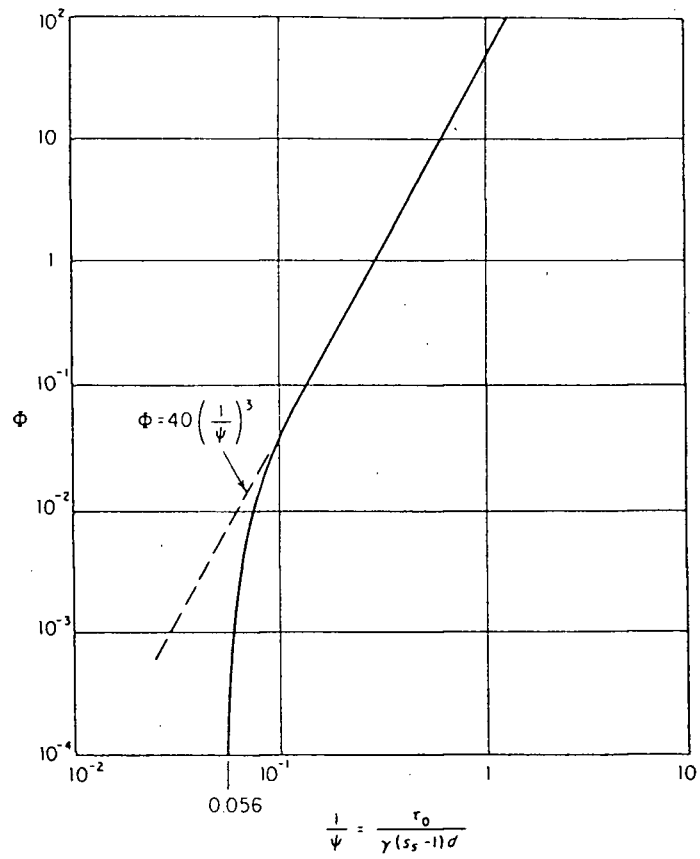
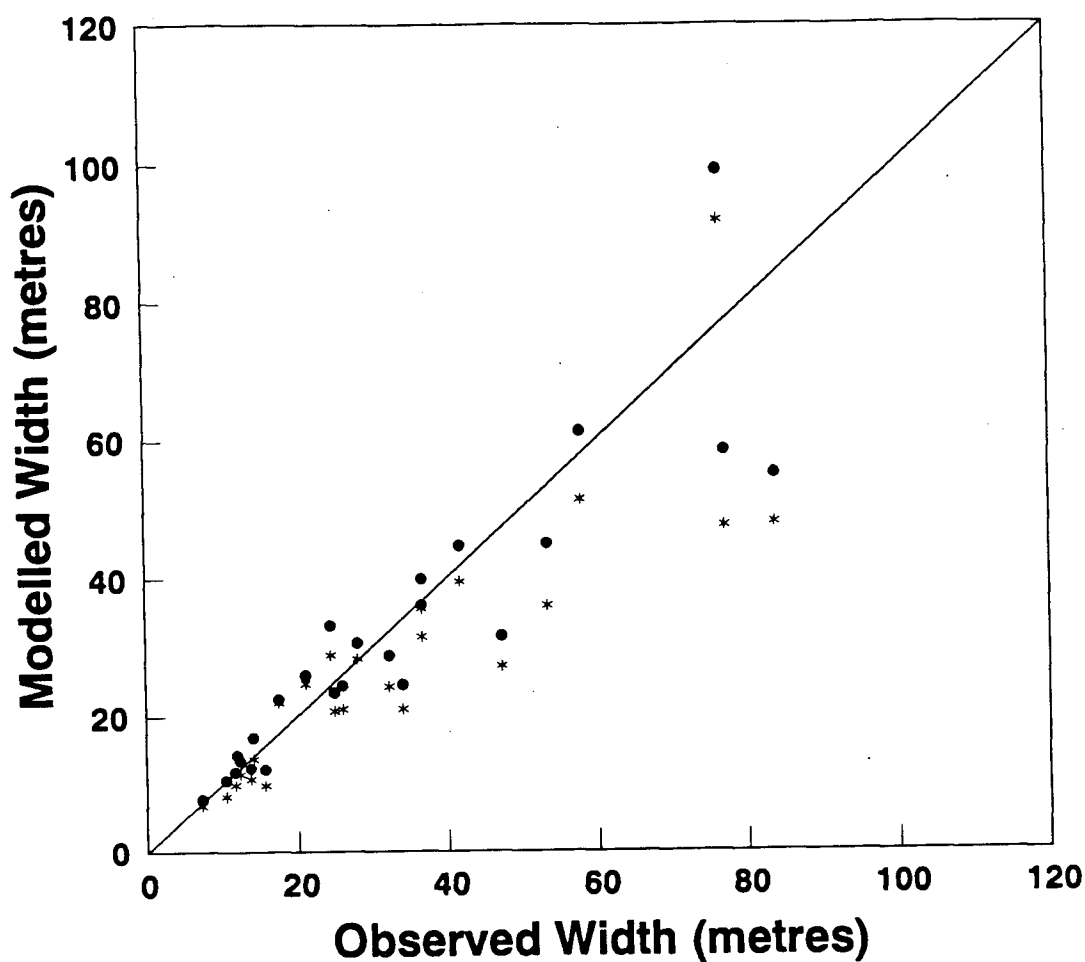


Figure 4.2: The Einstein Bed-Load Function (Einstein, 1942)



Eq. 4.6	PKM	Perfect Agreement
$r^2 = 0.8143$	$r^2 = 0.7552$	
•	*	

Figure 4.3: Comparison of Channel Widths Modelled Using the Sediment Transport Equations of Parker *et al* (1982) and Equation 4.6 to Assess the MTC Condition. The mean error for the MSTP predictions is +0.6%, compared to -12% for the MTC. The mean absolute error for the MSTP predictions is $\pm 16\%$, compared to $\pm 19.3\%$ for the MTC.

Gravel rivers typically have relatively small τ^* at the bankfull stage. For example Andrews (1984) found that for 24 gravel rivers with mobile beds, the mean bankfull $\tau_{D_{50}}^*$ was 0.046. It was argued in Section 3.4 that, as a result of increased grain exposure, τ^* approaches 0.02 following breakup of the pavement layer. Thus at the bankfull stage, $\tau_{d_{50}}^*$ will have an average value of 0.138 (assuming $d_{50} = D_{50}/3$), which is well in excess of the critical value of $\tau^* = 0.02$. It seems probable that the potential for a channel to transport sediment should be described by the proportionality given by Equation 4.5.

During the development of RIVERMOD the MTC condition was assessed using the sediment transport relations of Parker *et al* (1982) and by Equation 4.5. The results obtained using the Brown-Kalinske relationship (Equation 4.5) were superior. An example is shown in Figure 4.3. The channel widths calculated using Equation 4.5 scatter evenly about the line of perfect agreement with a mean error of only 0.6 %¹. Using the Parker *et al* equations the channel width is consistently underpredicted to give a mean error of -12 %.

The variation of the MTC hypothesis of White *et al* proposed here is that for a given slope a channel will adjust its cross sectional geometry such that the index of sediment transport potential, M , which represents the potential which a channel has to transport sediment, is a maximum. M is defined as:

$$M = P_{bed} \bar{\tau}_{bed}^3 \quad (4.6)$$

This is referred to as the Hypothesis of Maximum Sediment Transport Potential (MSTP). The principal difference between the MSTP and the MTC and MSP hypotheses is the latter use a sediment transport equation to determine the maximum sediment transport capacity or the minimum slope condition. MSTP uses Equation 4.6 to calculate the

¹The term mean error used in this thesis is the arithmetic mean of the residual errors as calculated by Equation 5.1. The mean of two residual errors +35% and -35% is 0%. This is an indication of the symmetry of the errors. The term mean absolute error is the arithmetic mean of the absolute values of the errors. The mean absolute error of the two residuals +35% and -35% is $\pm 35\%$.

index M , which is defined as the potential which a channel has to transport sediment. The actual sediment transport rate will depend on the efficiency with which the sediment transport potential is transferred to the sediment.

4.4 RIVERMOD

Flowcharts for RIVERMOD and subfunction STABLECHANNEL are shown in Figures 4.4 and 4.5. A definition sketch is shown in Figure 4.6.

The data required for RIVERMOD is Q_{bank} , G_b , d_{50} , D_{50} , $D_{50_{bank}}$, ϕ , and τ^* . All of these inputs can be measured in the field or readily calculated from field measurements. The channel response is modelled at the bankfull discharge.

4.4.1 STABLECHANNEL

The key component of RIVERMOD is the subfunction STABLECHANNEL.

STABLECHANNEL calculates the stable channel cross section for a trial channel slope, S , and bed perimeter, P_{bed} . The steps are as follows:

1. The subfunction is initialized by setting the bank angle, θ , equal to the angle of repose of the bank sediment, ϕ .
2. θ is decreased, and $Y = 0$.
3. Y is incremented.
4. The friction factor, f , the hydraulic radius, R , the bank perimeter, P_{bank} , and the discharge capacity of the channel, Q' , are calculated.
5. Steps 3 and 4 are repeated until $Q' = Q_{bank}$.
6. The boundary shear stress distribution is calculated.

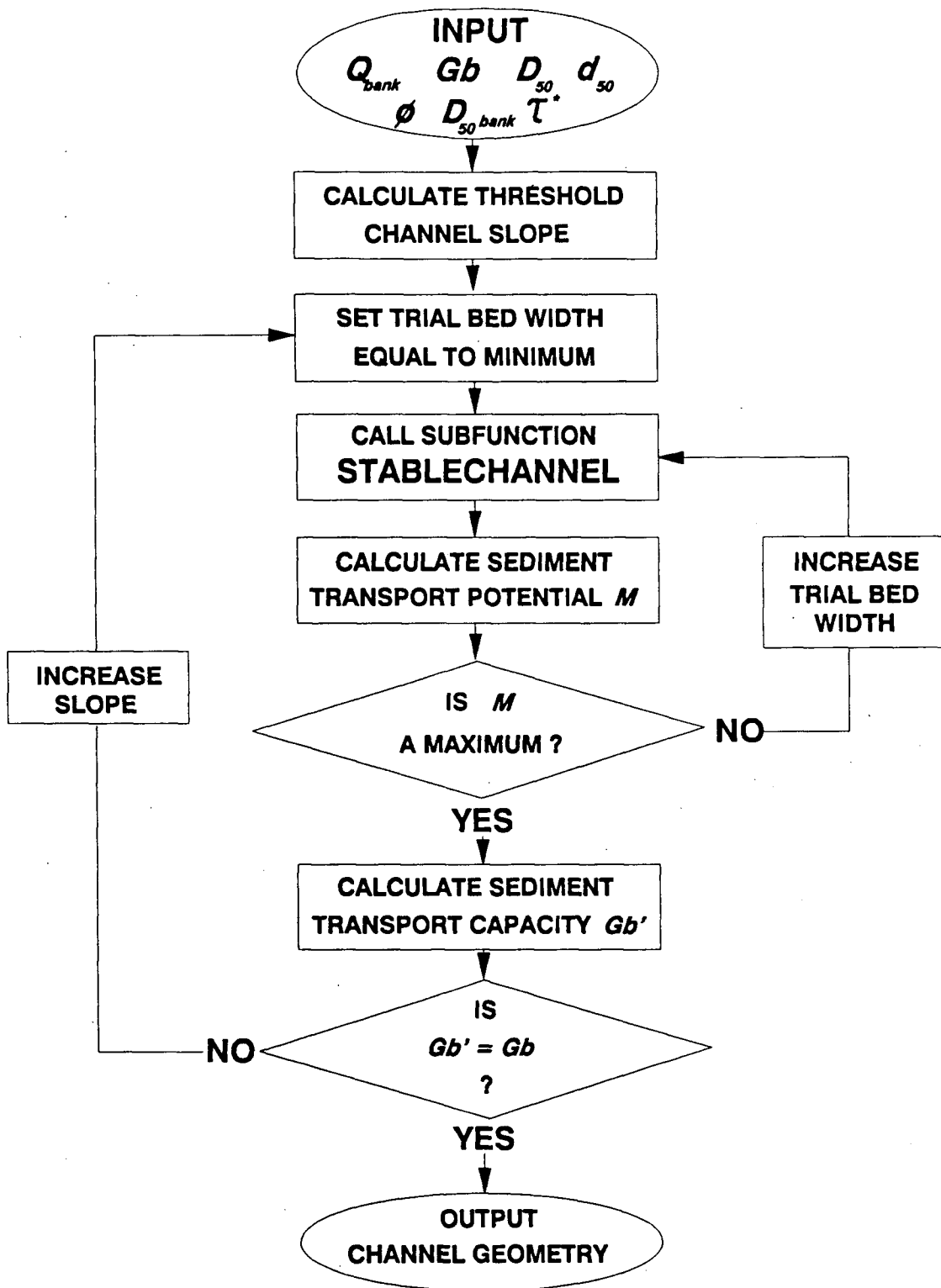


Figure 4.4: Flow Chart of RIVERMOD

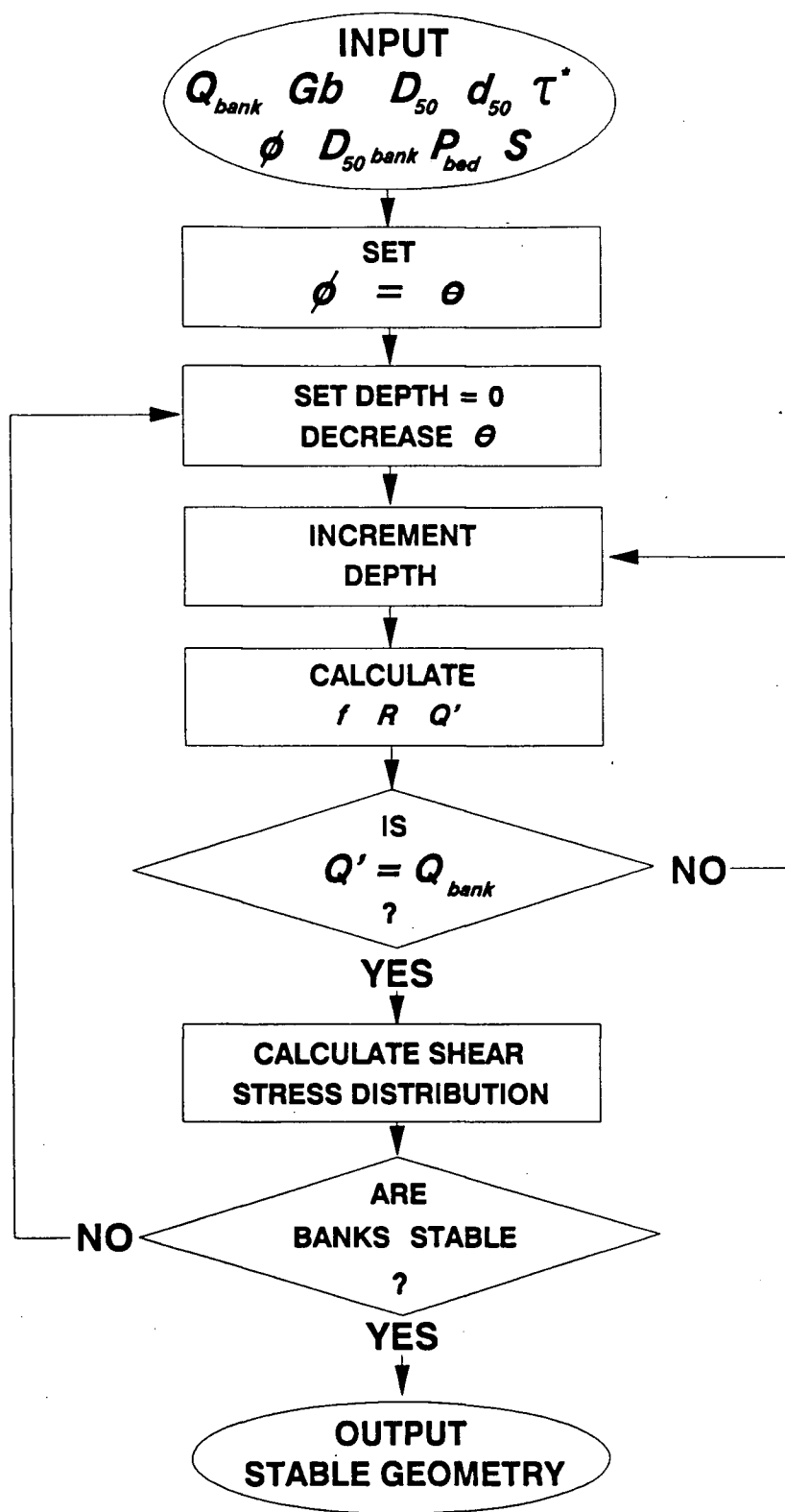


Figure 4.5: Flow Chart of Subfunction STABLECHANNEL

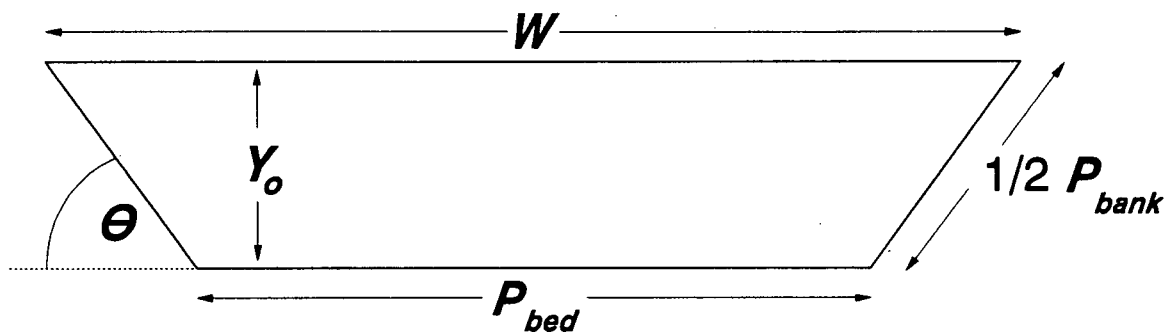


Figure 4.6: Definition Sketch for RIVERMOD

7. The bank stability is assessed.

8. If the banks are not stable then θ is decreased, Y set equal to zero, and steps 2 - 6 are repeated.

This continues until a stable channel configuration is obtained.

4.4.2 RIVERMOD

Figure 4.4 shows the location of STABLECHANNEL within RIVERMOD. The subfunction STABLECHANNEL is recalled for a range of trial bed widths. For a given slope, potentially an infinite number of stable channel configurations can be determined, one corresponding to each trial bed width (The exception is when solving for small bed widths with steep channel slopes where a stable configuration may not be possible).

The range of possible channel configurations is shown in Figure 4.7. Note the existence of a sediment transport maximum. As the bed width increases the angle of the banks increase and approach the angle of repose of the bank sediment ϕ .

A sediment transport potential index, M , is calculated for the stable channel configuration corresponding to each trial bed width. The stable channel configuration corresponding to the maximum M is selected in accordance with the Hypothesis of Maximum Sediment Transport Potential.

A sediment transport capacity, G'_b is calculated for the channel geometry which corresponds to the maximum M .

This process is repeated for a range of increasing channel slopes commencing with the threshold channel slope which is given by:

$$S = 0.36 D_{50}^{1.28} Q_{bank}^{-0.43} \quad (4.7)$$

The derivation of Equation 4.7 is given in Appendix D.

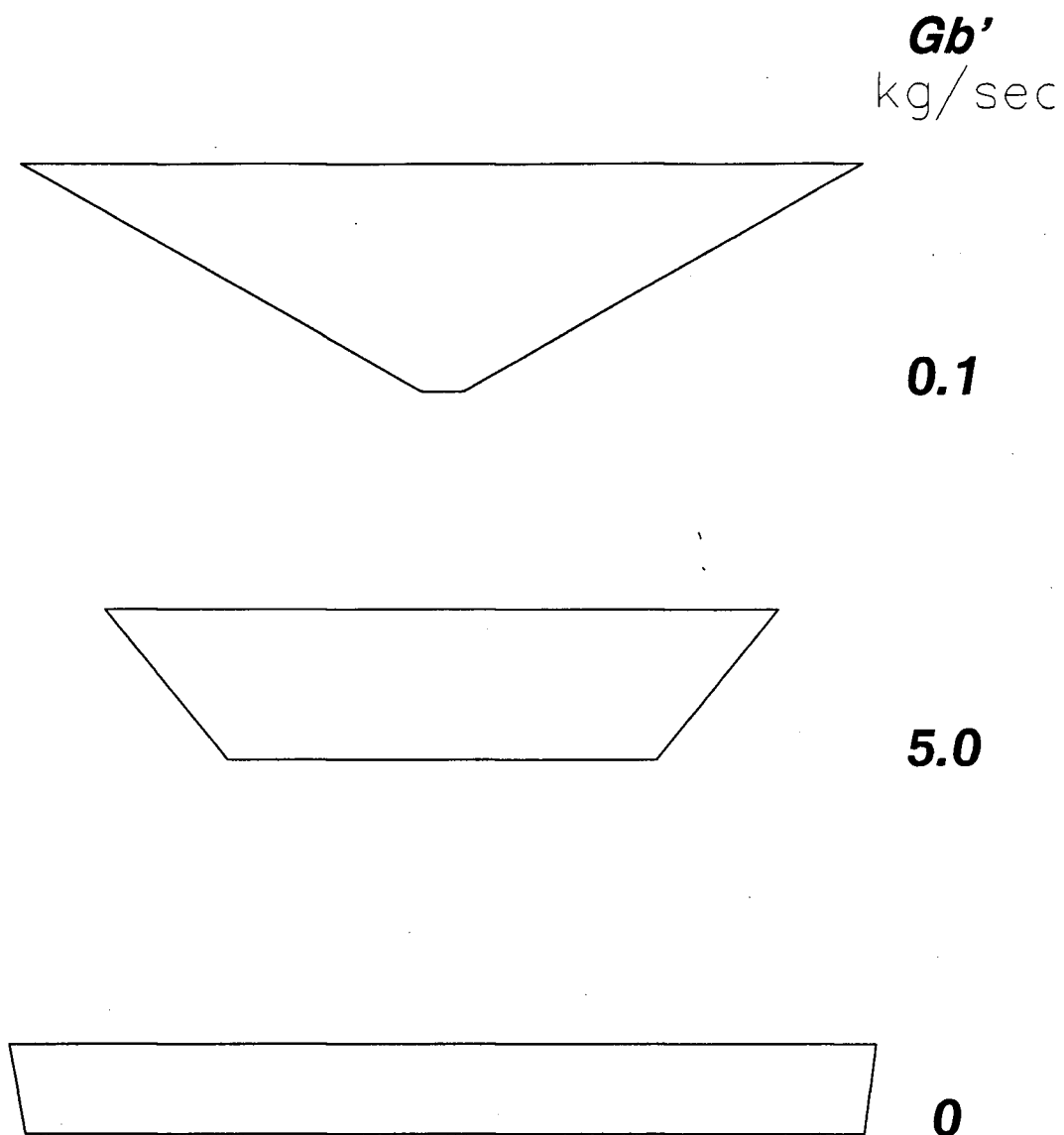


Figure 4.7: Possible Stable Channel Configurations for a Given Slope. The Sediment Transport Capacity is Indicated to the Right of Each Channel. Not to Scale.

RIVERMOD continues to adjust the trial channel slope until the sediment transport capacity G'_b is equal to the input sediment load G_b . The channel geometry corresponding to $G'_b = G_b$ is then output, and the program ends.

4.5 CONCLUSIONS

The theory incorporated into RIVERMOD was presented in this chapter. RIVERMOD is based on a simplified trapezoidal channel geometry which assumes a mobile bed and stable banks. A stable, equilibrium channel geometry is obtained through the iterative solution of equations for flow resistance, continuity, the distribution of the boundary shear stress, bank stability, and a sediment transport relationship, together with the hypothesis of maximum sediment transport potential (MSTP).

The basic concept of RIVERMOD is similar to the models of Chang (1979, 1980) and White *et al.* The errors associated with these models, however, preclude their use for engineering applications. The inclusion of the bank stability analysis in RIVERMOD is seen here as a considerable improvement in model design.

A further improvement is the use of the effective bankfull discharge, Q'_{bank} , rather than the actual bankfull discharge, Q_{bank} . This eliminates the errors associated with the calculation of the flow resistance, and allows the model to be used on ungauged rivers.

An additional refinement is the idea of a constant dimensionless bed shear stress, $\tau_{D_{50}}^*$, which allows the grain size distribution of the pavement layer to dynamically adjust together with the slope and depth. A channel can therefore adjust the boundary roughness.

The MSTP hypothesis is a variation of the maximum transport capacity hypothesis (MTC) of White *et al* (1982). In preliminary trials the MSTP hypothesis was found to give significantly better predictions of channel geometry than the MTC hypothesis which

used the sediment transport equations of Parker *et al* (1982).

For a trial channel slope RIVERMOD calculates the sediment transport capacity index, M , stable channel configurations corresponding to a range of trial bed widths until a maximum M is determined. The sediment transport capacity, G'_b , is calculated for the stable channel configuration corresponding to the maximum M . G'_b is compared to the input sediment load. The slope is then adjusted, and the procedure repeated until G'_b is equal to the input sediment load. When this occurs the stable, equilibrium channel geometry is output.

RIVERMOD is applicable only to stable, single-thread channels which are flowing through their own alluvium. The analysis does not extend to braided or bedrock controlled channels.

RIVERMOD has been programmed in MicroSoft QuickBasic 4.0. The code is presented in Appendix H.

Chapter 5

VERIFICATION OF RIVERMOD

5.1 INTRODUCTION

Only preliminary testing and verification of RIVERMOD will be attempted at this stage of the model development. Data from selected gravel-bed rivers will be input into RIVERMOD, and a comparison of the modelled and observed channel geometries will be made. In addition the responses of a river channel predicted by RIVERMOD for a variety of conditions will be compared to the regime and qualitative models discussed in Chapter 2.

5.2 MODELLING EXISTING RIVERS

Gravel-bed river data from Andrews (1984) and Hey and Thorne (1986) are used. This data is presented in Appendix E. Both of these studies showed that the bank vegetation can have a strong influence on channel width, and hence indirectly on the channel depth and slope. Only those rivers with minimal bank vegetation were used as the effect of the bank vegetation on bank stability is not at present accounted for in the model.

For each river Q'_{bank} was calculated using Equation 4.4. G_b was calculated using the equations of Parker *et al* (1988) from the observed channel geometry. τ_{50}^* was calculated using Equation 3.11.

The subpavement median grainsize, d_{50} , was not given in the Hey and Thorne data set. $D_{50}/3$ was used in its absence.

The properties of the bank sediment, $D_{50_{bank}}$ and ϕ , were not available from either of the studies. As an approximation, D_{50} was used in place of $D_{50_{bank}}$, and a value of $\phi = 40^\circ$, which is a mean value for unconsolidated gravel which is 5-10 cm in diameter. These assumptions regarding the bank sediment properties are expected to result in considerable error. A sensitivity analysis of the bank sediment size and the angle of repose of the bank sediment, ϕ , in Section 5.4 indicate the strong control they may exert on the channel geometry.

The data was input into RIVERMOD and the channel geometry for each of the rivers modelled. The comparisons between the modelled and observed geometries are shown graphically in Figures 5.1 to 5.4, together with their respective coefficients of determination.

5.2.1 Discussion

The results show that RIVERMOD is able to predict the channel cross-sectional area and the channel slope with reasonable accuracy.

The channel area is constrained by continuity. Thus as long as the modelled channel slope is reasonably close to the observed slope, the flow resistance given by Equation 4.1 will not differ greatly from that calculated from the observed channel geometry. Thus any overprediction (underprediction) in the channel width will be offset by an underprediction (overprediction) in the channel depth. This results in a good prediction of channel area.

The channel slope is largely a function of the sediment load. A system of negative feedback appears to operate whereby errors in the width and depth have reduced effect on the sediment transport capacity, and hence the channel slope. An overestimation of the channel width, for example, will be accompanied by an underestimation of the depth. Thus while the sediment transport capacity of the channel per unit bed width will be underestimated, this appears to be largely compensated by the greater width of

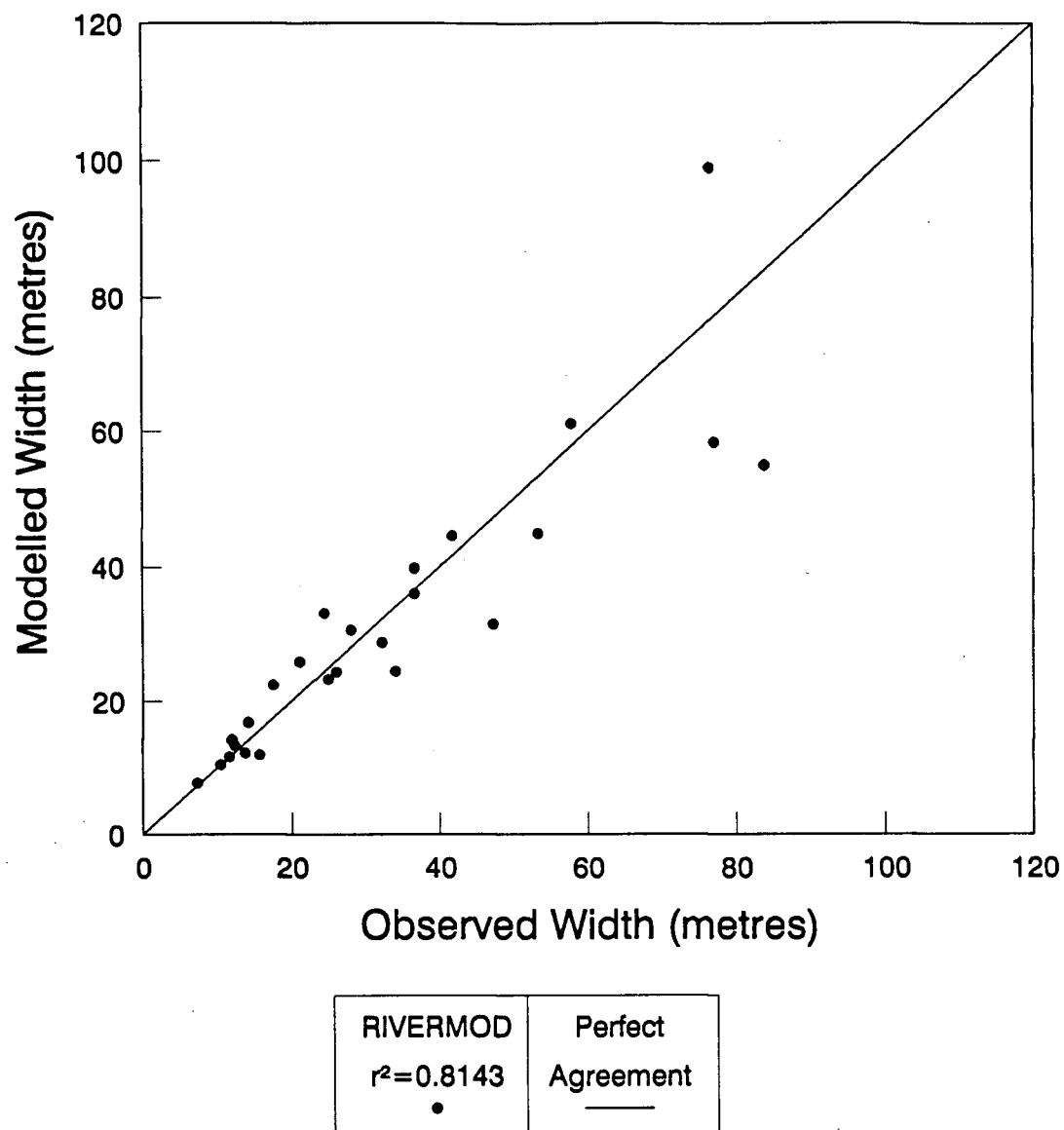


Figure 5.1: Comparison of Modelled and Observed Surface Channel Widths for Selected Gravel-Bed Rivers

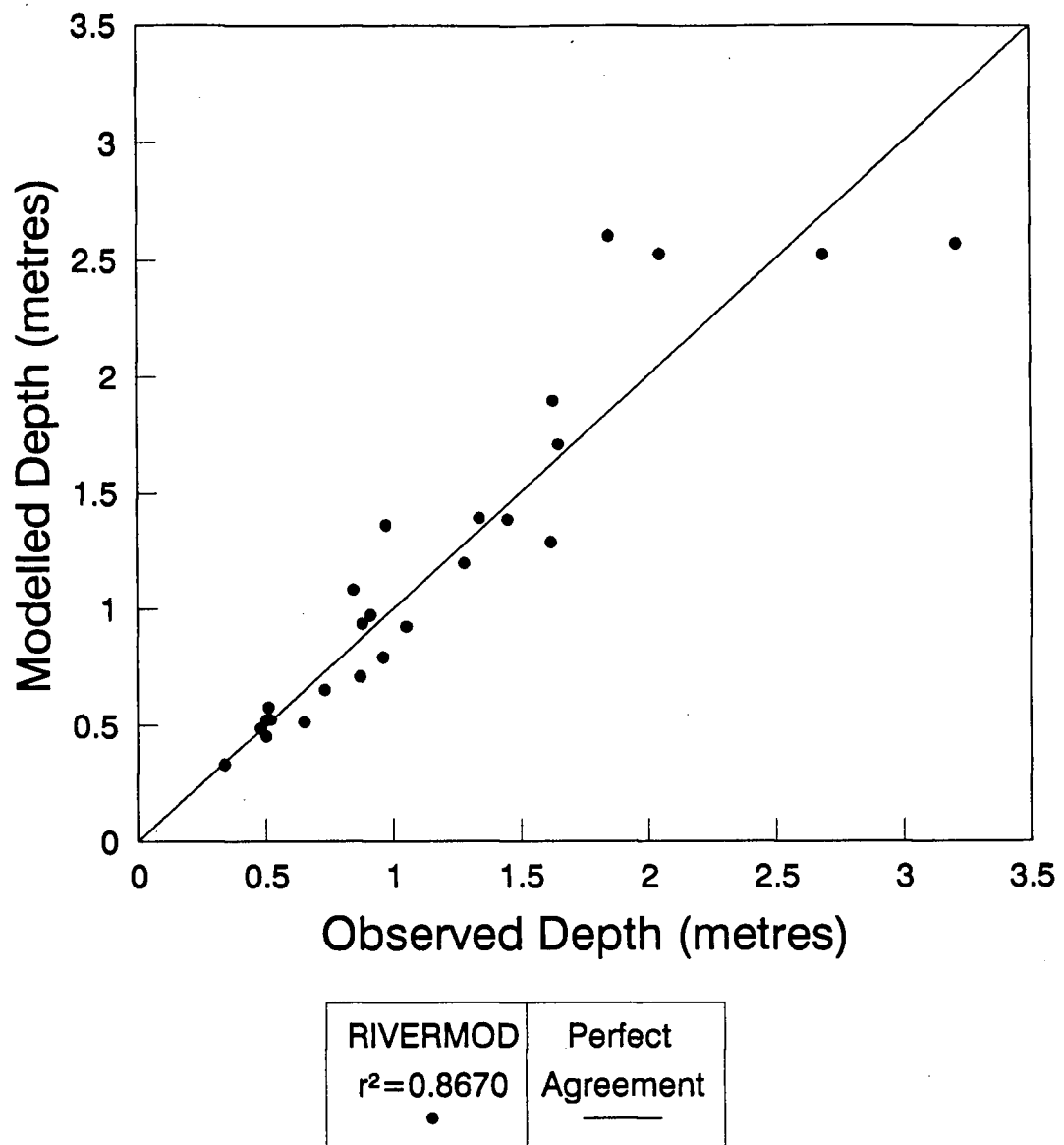


Figure 5.2: Comparison of Modelled and Observed Average Channel Depths for Selected Gravel-Bed Rivers

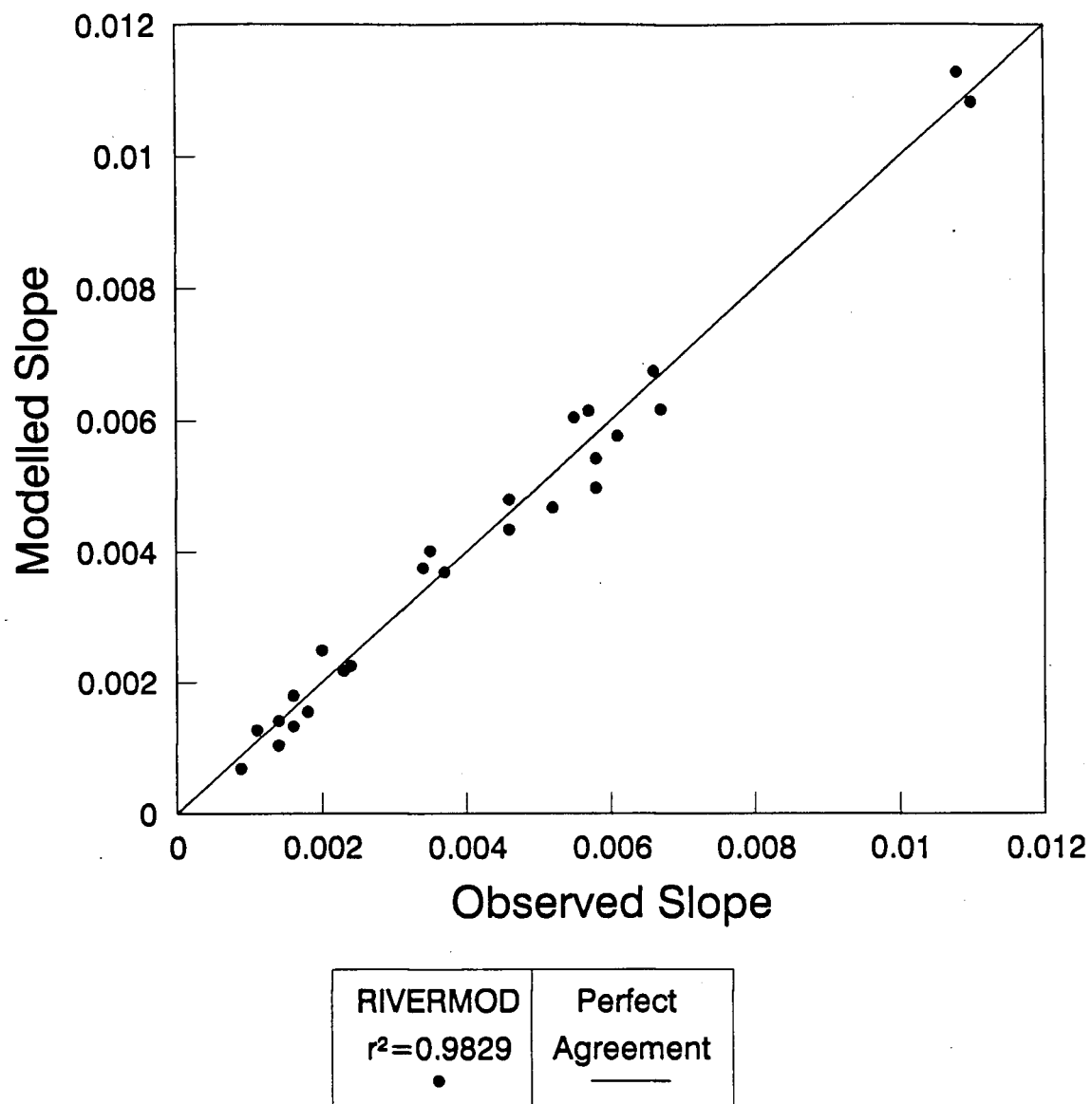


Figure 5.3: Comparison of Modelled and Observed Channel Slopes for Selected Gravel-Bed Rivers

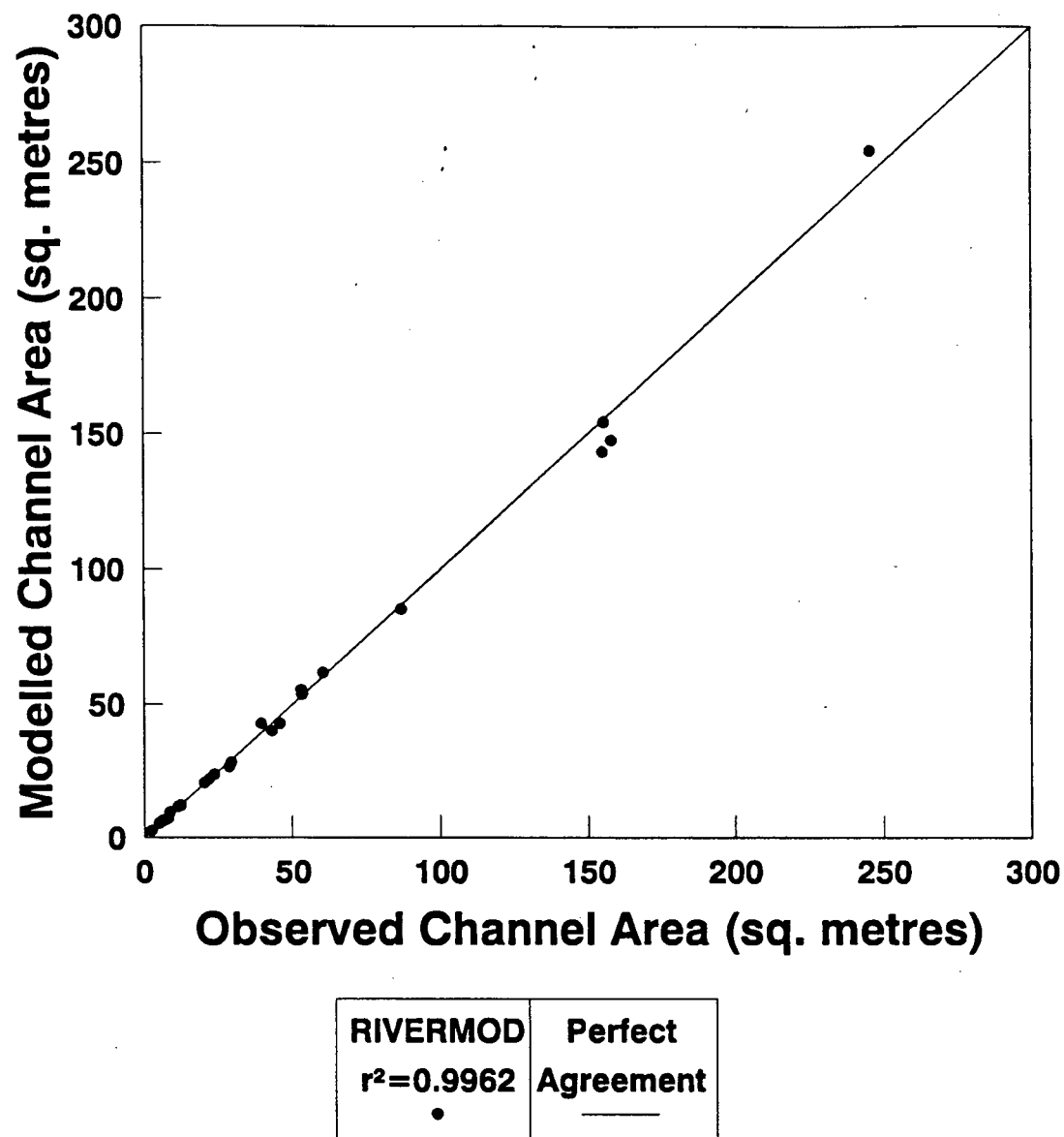


Figure 5.4: Comparison of Modelled and Observed Channel Cross-Sectional Areas for Selected Gravel-Bed Rivers

the active bed.

As the data necessary for the bank stability analysis was not available significant errors in the modelled channel width and depth were expected. Nonetheless the agreement between the observed and modelled widths and depths are considered good.

A detailed examination of the residual errors is given in the following section.

5.3 RESIDUAL ERRORS

The residual errors were determined from the following equation:

$$\epsilon_x = \frac{X_m - X_o}{X_o} * 100\% \quad (5.1)$$

where X is the variable concerned, ϵ_x = the residual error as a percentage of the observed variable, and the subscripts $_o$ and $_m$ denote the observed and modelled values respectively.

The residual errors for the RIVERMOD output were determined for the channel surface width, average depth, slope, and cross-sectional area. The results are presented in Table 5.1.

Best fit regime type equations were derived by regression analysis of the river data in Appendix E. The equations are presented below:

$$W = 4.81 Q'_{bank}{}^{0.46} \quad (5.2)$$

$$Y = 0.24 Q'_{bank}{}^{0.39} \quad (5.3)$$

$$S = 0.83 D_{50}^{1.30} Q'_{bank}{}^{-0.45} \quad (5.4)$$

The residual errors for the regime equations were calculated as described in the preceding section and are presented in Table 5.2.

Run Number *	Width (%)	Depth (%)	Slope (%)	Area (%)
1.01	1.7	1.4	(5.7)	3.1
1.03	(33.2)	40.1	(25.7)	(6.4)
1.06	20.3	(10.7)	4.6	7.5
1.07	7.2	(3.2)	(1.5)	3.8
1.15	(27.9)	28.3	(13.9)	(7.5)
1.16	(6.2)	6.8	(7.9)	0.2
1.17	1.8	1.1	(5.3)	2.9
1.18	(6.1)	6.6	(6.3)	0.1
1.19	9.0	(4.4)	(0.1)	4.2
1.20	(15.7)	16.3	(13.8)	(1.9)
1.21	35.8	(20.4)	24.6	8.0
1.22	(34.3)	40.6	(22.0)	(7.6)
1.24	(1.4)	3.5	(6.3)	2.0
2.20	23.1	(17.6)	10.4	1.4
2.23	(9.8)	4.5	(5.4)	(5.8)
2.30	(22.3)	13.1	(9.7)	(12.2)
2.34	9.2	(9.6)	4.6	(1.3)
2.36	19.4	(18.3)	10.0	(2.4)
2.38	5.9	(6.2)	1.2	(0.8)
2.39	29.4	(20.0)	12.2	3.5
2.44	7.1	(6.4)	2.2	0.3
2.46	(10.7)	4.0	15.6	(7.1)
2.47	9.4	(12.1)	7.9	(3.9)
2.53	(24.2)	23.1	(16.4)	(6.7)
2.60	28.5	(21.0)	14.8	1.5
Mean	0.6	1.6	(1.3)	(1.0)
Max.	35.8	40.6	24.6	8.0
Min.	(34.3)	(21.0)	(25.7)	(12.2)

* 1. Denotes Andrews (1984) Data

() Denotes Negative Values

2. Denotes Hey and Thorne (1986) Data

Table 5.1: Residual Errors for the Outputs of RIVERMOD.

Run Number *	Width (%)	Depth (%)	Slope (%)	Area (%)
1.01	(7.4)	(7.8)	32.4	(14.6)
1.03	(35.8)	20.1	(25.1)	(22.9)
1.06	25.5	(12.3)	53.1	10.1
1.07	6.8	8.4	(0.8)	15.5
1.15	(21.2)	24.6	27.0	(1.7)
1.16	1.7	14.1	1.2	16.1
1.17	(0.5)	(0.6)	36.6	(1.1)
1.18	(0.3)	12.3	3.4	12.0
1.19	13.7	5.3	(25.6)	19.7
1.20	(12.6)	3.2	20.4	(9.8)
1.21	39.8	(20.3)	5.7	11.4
1.22	(32.0)	7.8	1.0	(26.7)
1.24	13.0	(7.9)	29.6	4.1
2.20	11.9	(1.6)	(38.1)	10.2
2.23	(9.4)	9.6	1.3	(0.7)
2.30	(20.4)	7.4	41.9	(14.5)
2.34	3.7	12.1	(15.7)	16.2
2.36	26.4	(14.5)	38.6	8.1
2.38	15.1	(15.5)	4.4	(2.7)
2.39	18.5	(7.9)	(41.8)	9.2
2.44	2.4	21.9	(35.7)	24.8
2.46	(9.3)	(15.6)	67.4	(23.4)
2.47	6.2	9.4	(32.9)	16.2
2.53	(17.8)	6.4	4.9	(12.6)
2.60	(3.5)	9.4	(58.1)	5.6
Mean	0.6	2.7	3.8	1.9
Max.	39.8	24.6	67.4	24.8
Min.	(35.8)	(20.3)	(58.1)	(26.7)

* 1. Denotes Andrews (1984) Data

() Denotes Negative Values

2. Denotes Hey and Thorne (1986) Data

Table 5.2: Residual Errors For The Regime Equations

5.3.1 Comparison Between The Output from RIVERMOD and the Regime Equations

Regime equations are currently widely used to model channel geometries. Equations 5.2 to 5.4 were derived to use as a yardstick to assess the performance of RIVERMOD. The magnitude of the residuals for the output from RIVERMOD and the regime equations are examined.

Channel Width

The mean absolute error is $\pm 16.0\%$ for the RIVERMOD output and $\pm 14.2\%$ for the regime equation output. The mean residual error is less than 1% for both the RIVERMOD output and the regime equation. The maximum errors are approximately $\pm 35\%$ for both. 60% of the residual errors for the RIVERMOD output lie within $\pm 20\%$ compared to 72% for regime equation. The coefficient of determination for the RIVERMOD output is $r^2 = 0.8143$ compared with $r^2 = 0.8482$ for the regime equation output.

Channel Depth

The mean absolute error is $\pm 13.6\%$ for the RIVERMOD output and $\pm 11.0\%$ for the regime equation output. The mean residual error is 1.6% and 2.7% for RIVERMOD and the regime equation respectively. The maximum errors are generally $\pm 25\%$ although RIVERMOD overpredicts the depth by up to 40%. 72% of the residual errors for the RIVERMOD output lie within $\pm 20\%$ compared to 84% for the regime equation. The coefficient of determination for the RIVERMOD output is $r^2 = 0.8670$ compared to the regime equation where $r^2 = 0.9364$.

Channel Slope

The mean absolute error is $\pm 9.9\%$ for the RIVERMOD output and $\pm 25.7\%$ for the regime equation output. The mean residual error is -1.3% and 3.8% for RIVERMOD and the regime equation respectively. The maximum errors for the RIVERMOD output are $\pm 25\%$ compared to $\pm 65\%$ for the regime equation. 88% of the RIVERMOD residual errors lie within $\pm 20\%$ compared to 37.5% for the regime equation. The coefficient of determination for the RIVERMOD output is $r^2 = 0.9829$ compared to $r^2 = 0.8042$ for the regime equation.

Cross-Sectional Area

The mean absolute error is $\pm 4.1\%$ for the RIVERMOD output and $\pm 12.4\%$ for the regime equation output. The mean residual error is -1.0% and 1.9% for the RIVERMOD output and the regime equation respectively. The maximum errors are $\pm 12\%$ for RIVERMOD and $\pm 25\%$ for the regime equation. 100% of the RIVERMOD residual errors, and 84% of the regime equation residual errors lie within $\pm 20\%$. The coefficient of determination for the RIVERMOD output is $r^2 = 0.9962$ compared to $r^2 = 0.9651$ for the regime equation.

Discussion

The regime approach provides slightly better predictions of the channel width and depth. As explained in the previous section the performance of RIVERMOD would be expected to improve if data regarding the bank sediment were available.

RIVERMOD provides markedly better predictions of the channel cross-sectional area and channel slope. The reasons for the success of RIVERMOD when modelling area and slope were discussed in the previous section. The relatively poor performance of the regime slope equation is due to the inability of regime equations to account for the effect

of sediment load which has a major control on the channel geometry.

The regime equations were derived from the data used in the comparison with RIVERMOD. These equations cannot be used with confidence for rivers not included in this study. RIVERMOD was employed without any calibration or adjusting of coefficients. It might therefore be reasonable to expect RIVERMOD to apply to a wider range of river conditions.

5.3.2 Systematic Variation of the Residuals

The residual errors for the modelled channel widths, W_m , plotted as functions of W_o , S_o , Q'_{bank} , g_b , and $\tau_{D_{50}}^*$ for both the RIVERMOD output and Equation 5.2 in Figures 5.5 to 5.9. With the exception of $\tau_{D_{50}}^*$, the residuals for both models appear randomly scattered. When plotted as a function of $\tau_{D_{50}}^*$, a definite trend in the residuals is evident. This indicates a source of systematic error which has yet to be accounted for in RIVERMOD. Resolution of this error will greatly increase the accuracy of the RIVERMOD predictions.

The residuals for Y_m , S_m , and A_m are shown as functions of $\tau_{D_{50}}^*$ in Figures 5.10 to 5.12.

Channel Depth The RIVERMOD shows a definite trend from overprediction of the depth at low values of $\tau_{D_{50}}^*$, to underprediction at high values of $\tau_{D_{50}}^*$. This is the inverse of the trend observed for the channel width. The residuals for the regime depth equation appear random.

Slope The trends displayed by the channel slope residuals for RIVERMOD and Equation 5.4 are highly dissimilar. The RIVERMOD residuals indicate a distinct trend from slight underpredictions of the channel slope for low values of $\tau_{D_{50}}^*$, to slight overpredictions for higher values of $\tau_{D_{50}}^*$. The regime residuals show the opposite trend from large

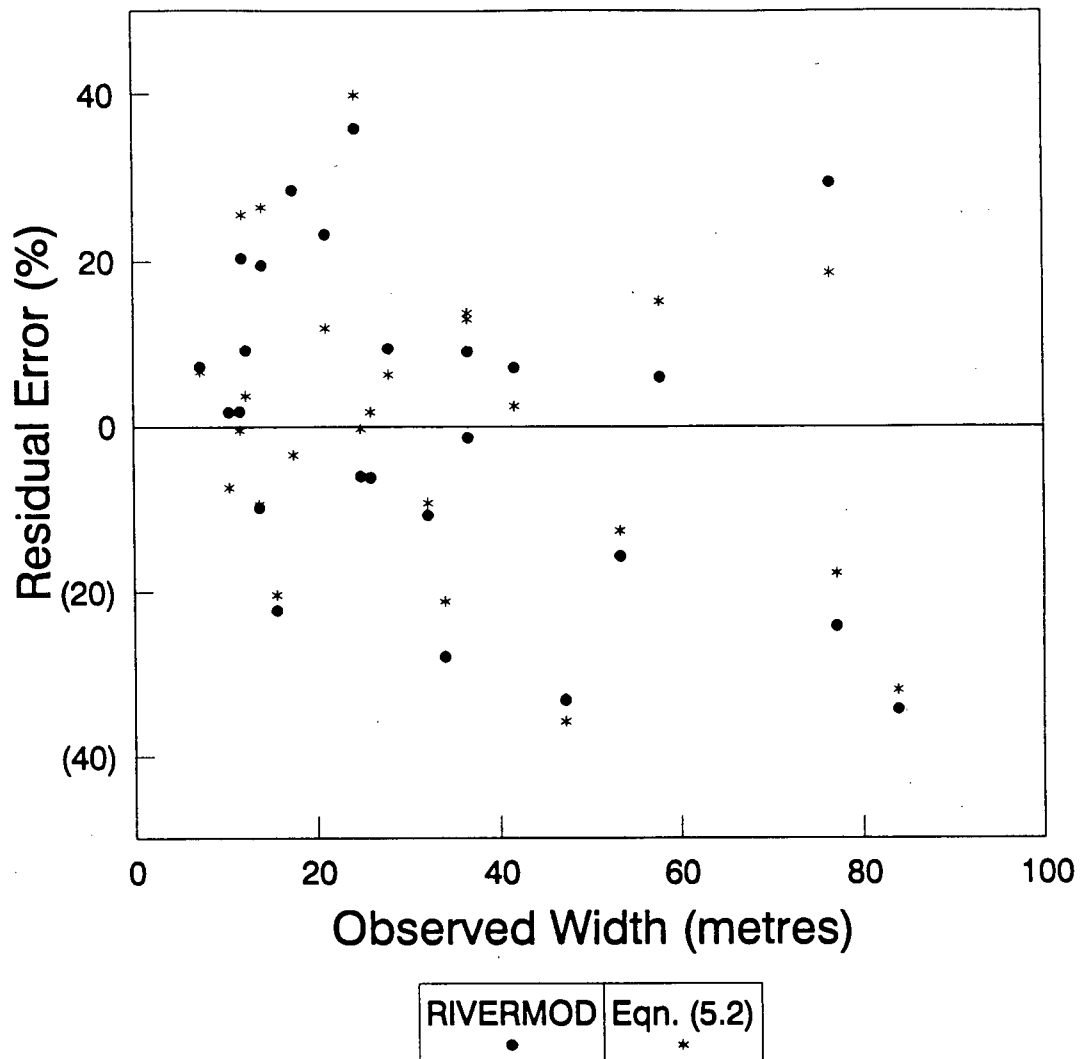


Figure 5.5: Residual Errors for the Channel Widths Modelled by RIVERMOD and from the Regime Channel Width Equation for Selected Gravel-Bed Rivers as a Function of the Observed Channel Width

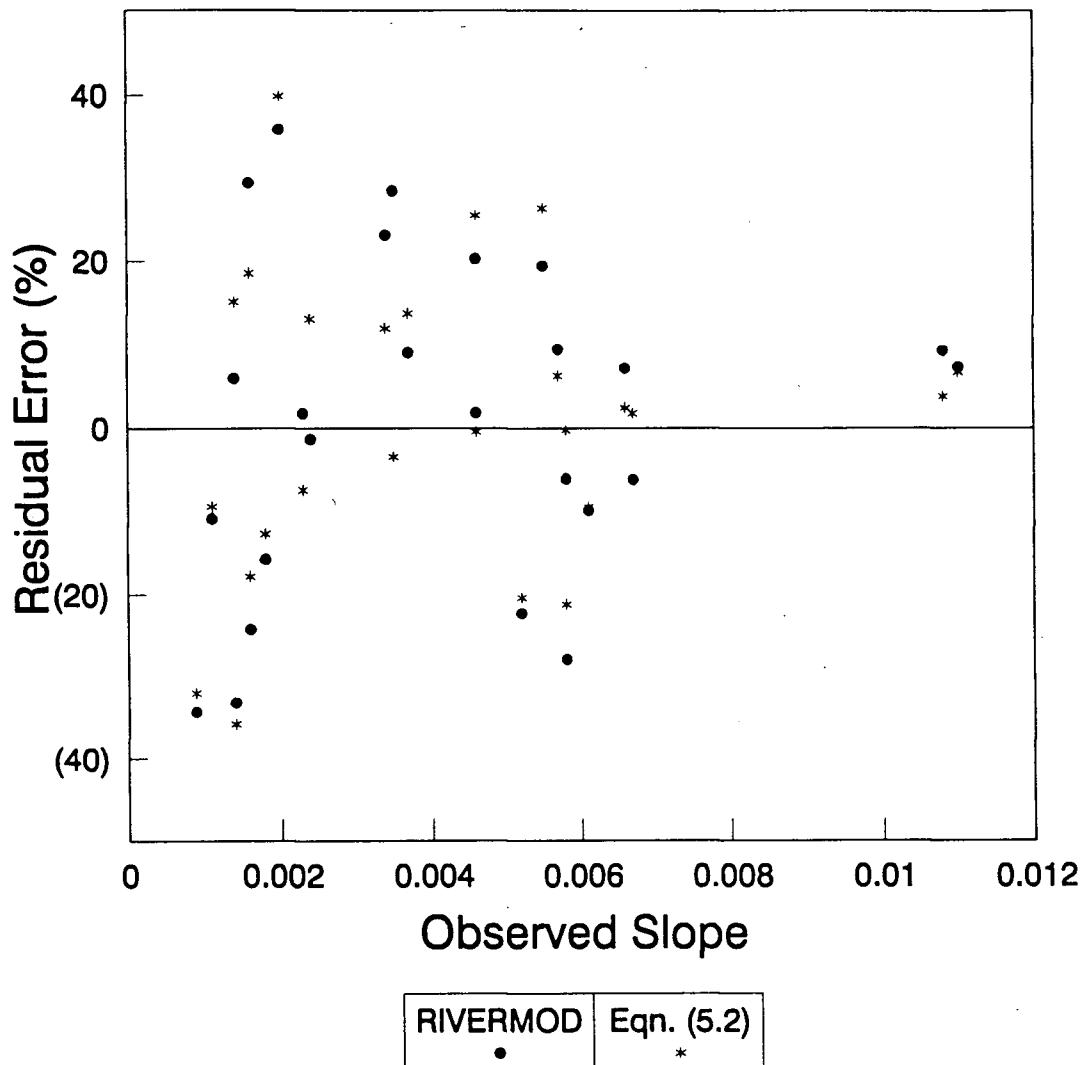


Figure 5.6: Residual Errors for the Channel Widths Modelled by RIVERMOD and from the Regime Width Equation for Selected Gravel-Bed Rivers as a Function of the Observed Channel Slope

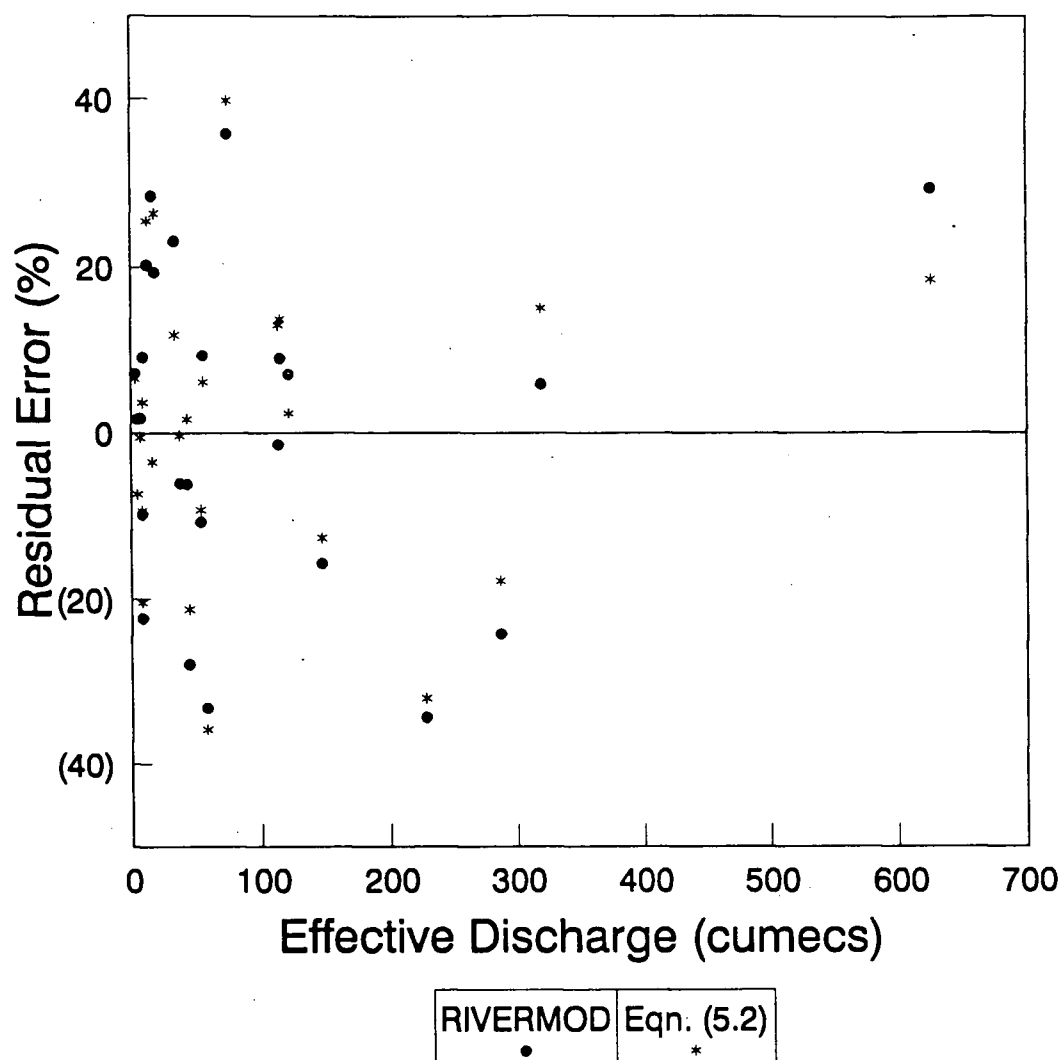


Figure 5.7: Residual Errors for the Channel Widths Modelled by RIVERMOD and from the Regime Width Equation for Selected Gravel-Bed Rivers as a Function of the Effective Discharge

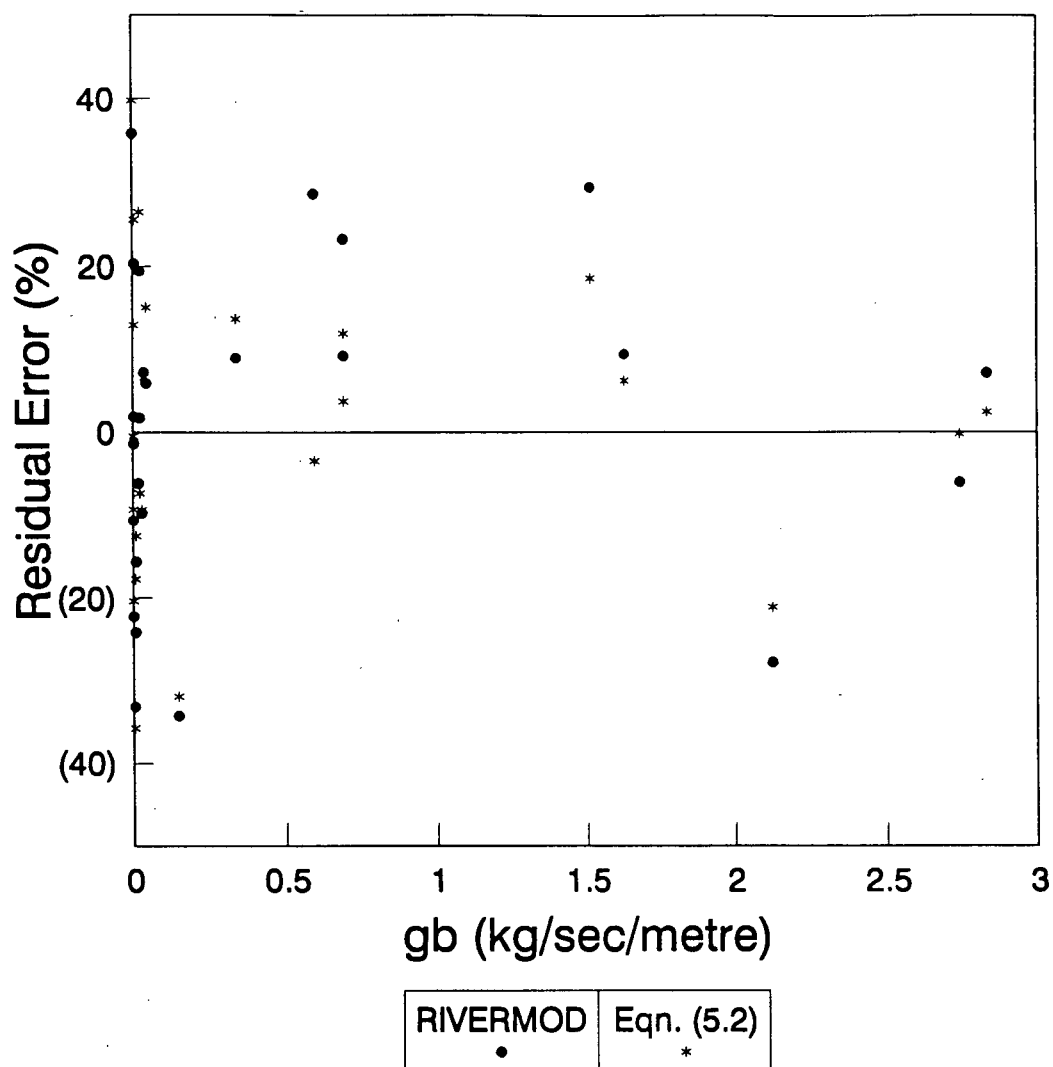


Figure 5.8: Residual Errors for the Channel Widths Modelled by RIVERMOD and from the Regime Width Equation for Selected Gravel-Bed Rivers as a Function of the Unit Sediment Discharge Capacity

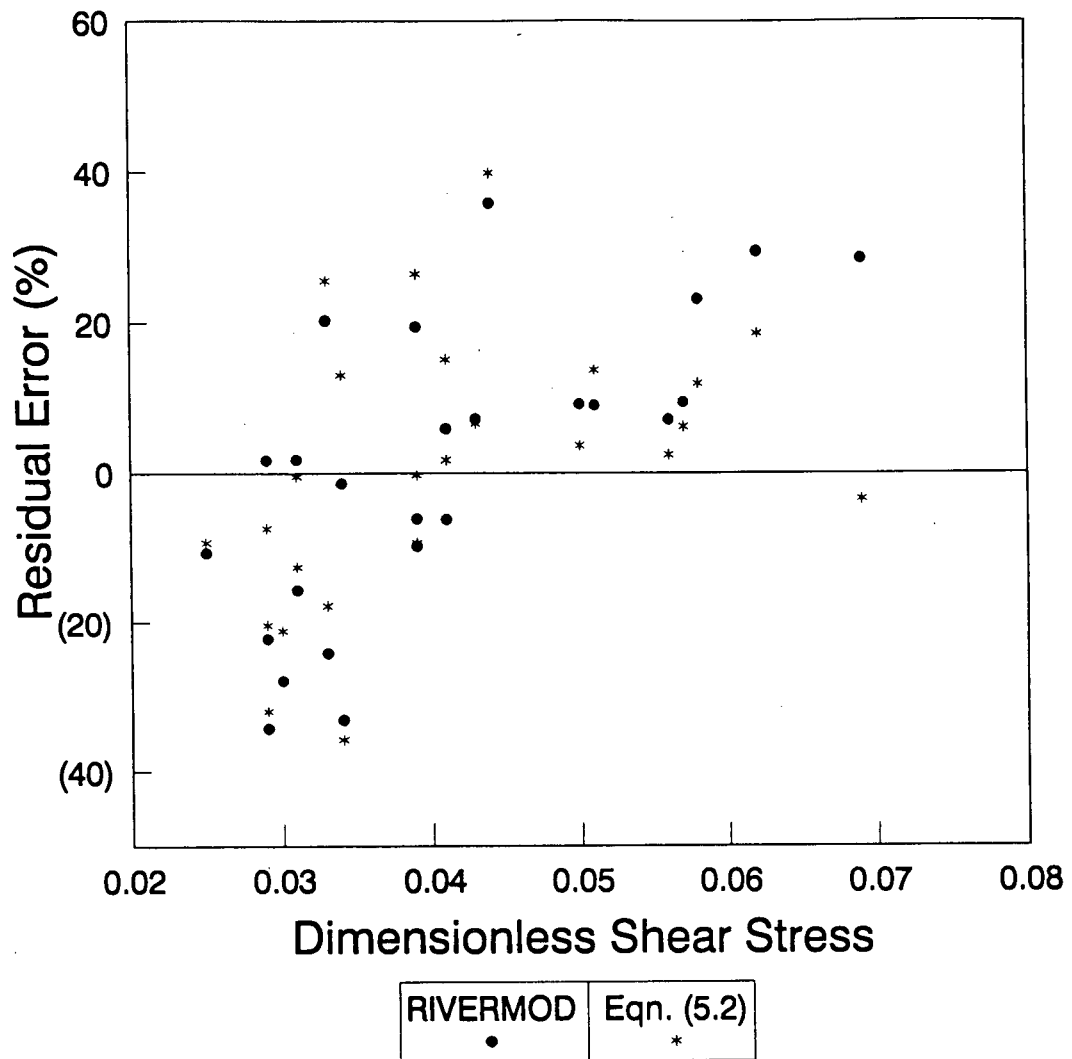


Figure 5.9: Residual Errors for the Channel Widths Modelled by RIVERMOD and from the Regime Width Equation for Selected Gravel-Bed Rivers as a Function of the Dimensionless Bed Shear Stress

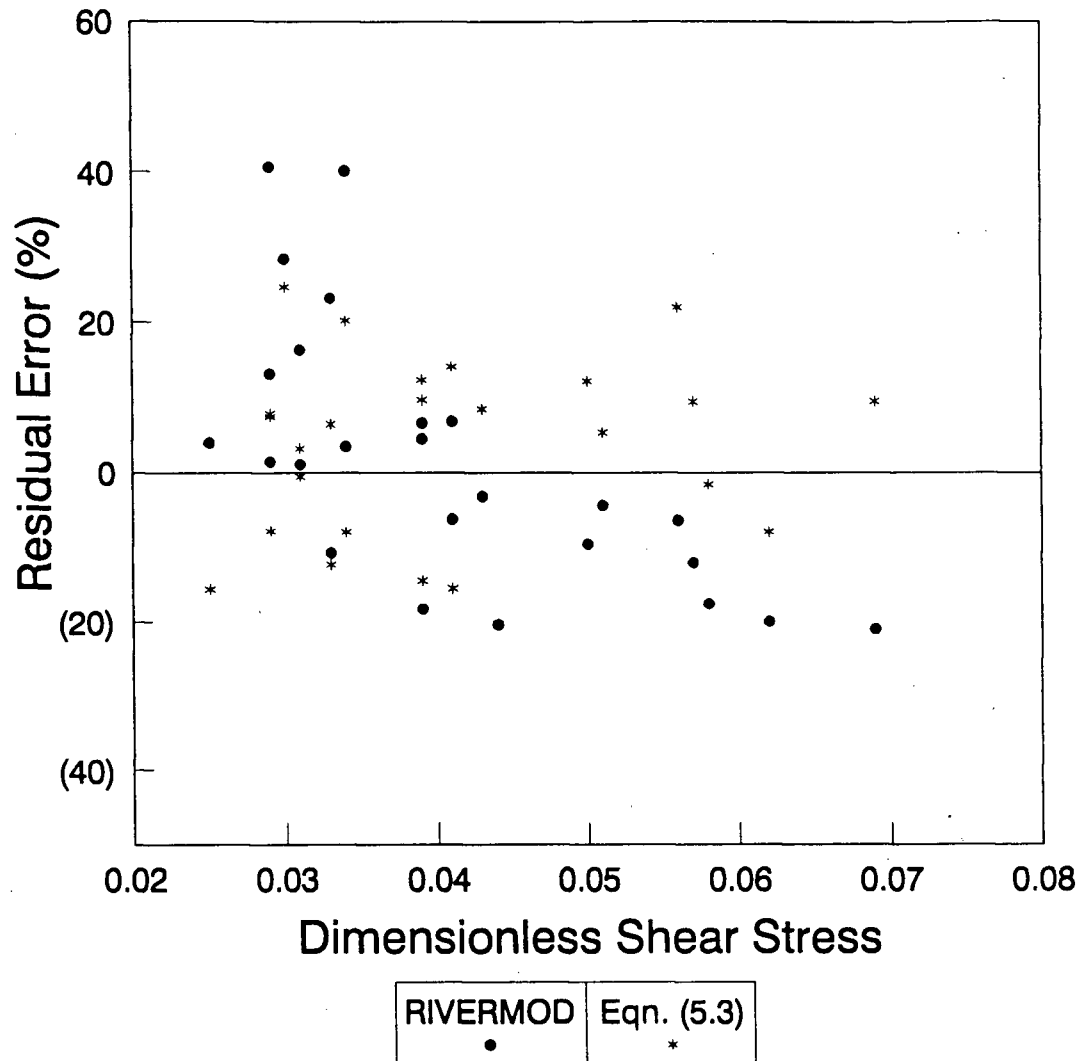


Figure 5.10: Residual Errors for the Channel Average Depths Modelled by RIVERMOD and from the Regime Depth Equation for Selected Gravel-Bed Rivers as a Function of the Dimensionless Bed Shear Stress

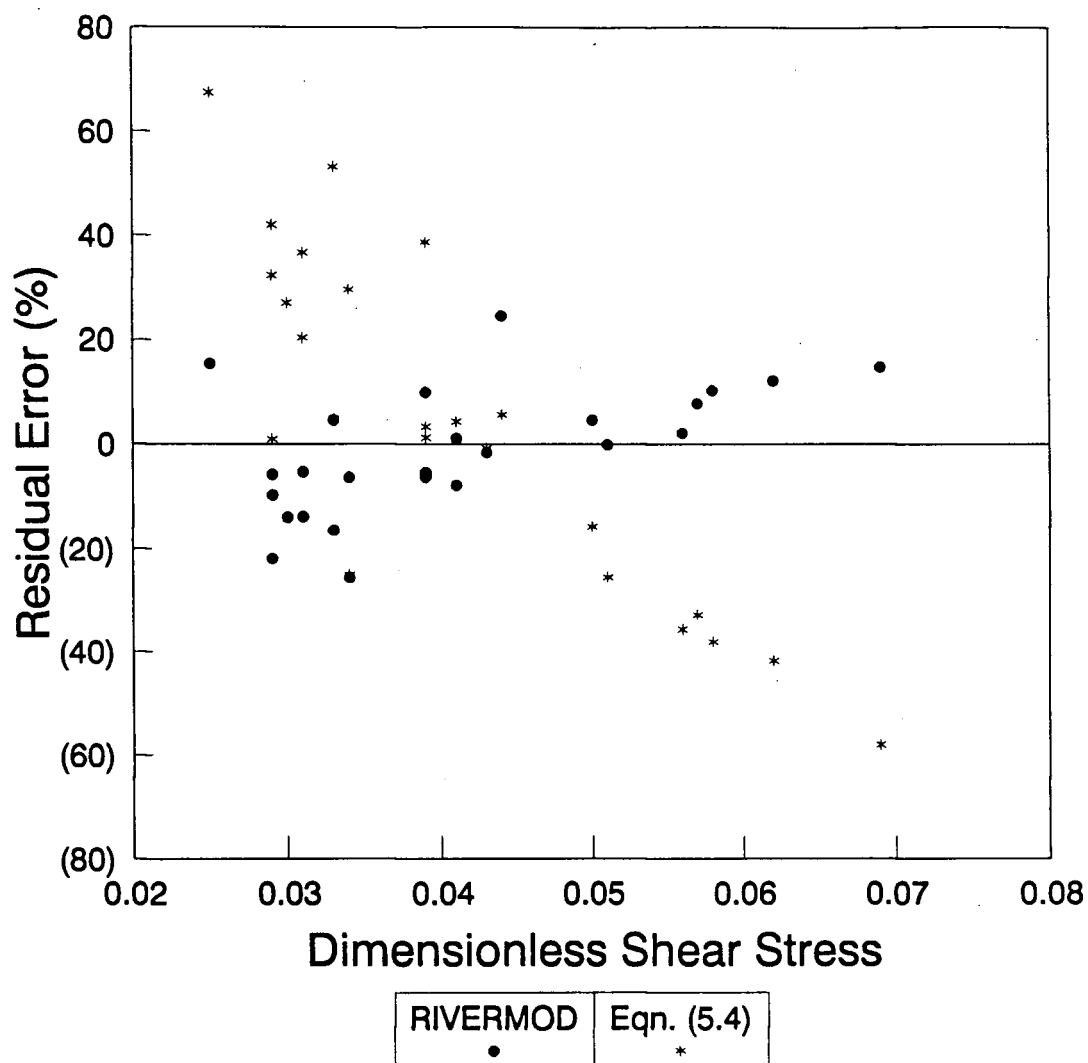


Figure 5.11: Residual Errors for the Channel Slopes Modelled by RIVERMOD and from the Regime Slope Equation for Selected Gravel-Bed Rivers as a Function of the Dimensionless Bed Shear Stress

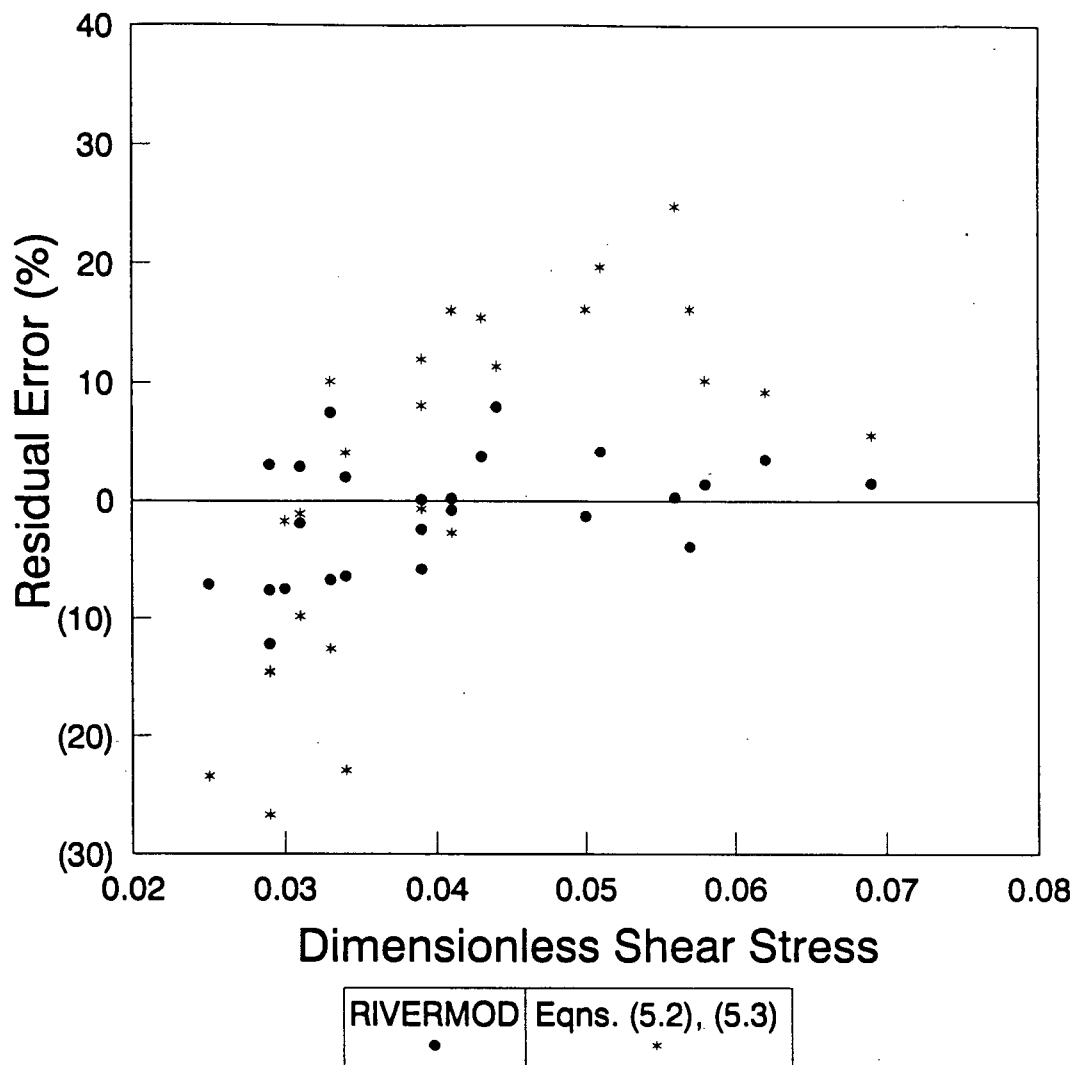


Figure 5.12: Residual Errors for the Channel Cross-Sectional Area Modelled by RIVERMOD and from the Regime Slope Equations for Selected Gravel-Bed Rivers as a Function of the Dimensionless Bed Shear Stress

overpredictions at low values of $\tau_{D_{50}}^*$, to large underpredictions for high values of $\tau_{D_{50}}^*$.

The trend of the regime residuals intersects the zero error line at $\tau_{D_{50}}^* = 0.042$ which is approximately equal to the mean value for the $\tau_{D_{50}}^*$ at the bankfull stage for the data used in this analysis. Equation 5.4 is unable to account for the effect of sediment load on the channel slope.

Cross-Sectional Area The RIVERMOD residuals are randomly scattered about the line of zero error. This indicates that an overprediction in the channel width is accompanied by an underprediction in the channel depth, and vice versa. The regime residuals show a trend which is sympathetic with that observed for the channel width. This is to be expected as the regime depth residuals were random.

5.4 PREDICTIONS OF CHANNEL ADJUSTMENTS

RIVERMOD is used to model the adjustment of a hypothetical river channel to a variety of disturbances. In each case only the independent variable being considered are permitted to vary, while all other variable remain constant. The independent variables considered are the median bank grainsize $D_{50_{bank}}$, the effective angle of repose of the bank sediment ϕ' , the bankfull discharge Q_{bank} , and the sediment load G_b . The dependent channel geometry variables W , Y , S , and θ are free to adjust to the varied conditions.

The purpose of this section is twofold. Firstly as a sensitivity test to determine the influence of the individual independent variables on the channel geometry, and secondly to compare the modelled reponse with observed channel changes and qualitative equations of river response.

5.4.1 Bank Sediment Size

The effect of the bank sediment size on the channel geometry are shown in Figures 5.13 to 5.15. With increasing $D_{50_{bank}}$ the channel responds through a decrease in W and S , and by an increase in Y . This is consistent with the ability of the banks to withstand greater shear stresses.

Decreasing $D_{50_{bank}}$ from 0.08 to 0.04 is shown to exert a large effect on the channel geometry. The width of the hypothetical river will increase by approximately 75% from 39 to 68 metres, the average depth will decrease by 35% from 1.38 to 0.90 metres, the slope increase by 35% from 0.0038 to 0.0051, and the aspect ratio W/Y will by increase 140% from 28 to 68.

If $W/Y = 60$ is taken as the threshold between single-thread and braided channels, it is shown above that the size of the bank sediment alone can determine whether the hypothetical river will develop a single-thread or braided channel.

The large potential effect on the channel geometry imposed by the bank sediment illustrates the necessity for this data when applying RIVERMOD.

5.4.2 Angle of Repose

The effect of varied ϕ' on the channel geometry is shown in Figures 5.16 to 5.18. With increasing ϕ' the channel responds through an decrease in W and S , and by an increase in Y . Increasing ϕ' is consistent with the ability of the banks to develop at a steeper bank angle for a given bank shear stress.

As with $D_{50_{bank}}$, ϕ' can exert a strong influence on the bank stability, and hence the channel geometry. ϕ' is influenced largely by the presence of intergranular fine material, and by vegetation root masses.

Hey and Thorne (1986) and Andrews (1984) have shown that the density of the bank

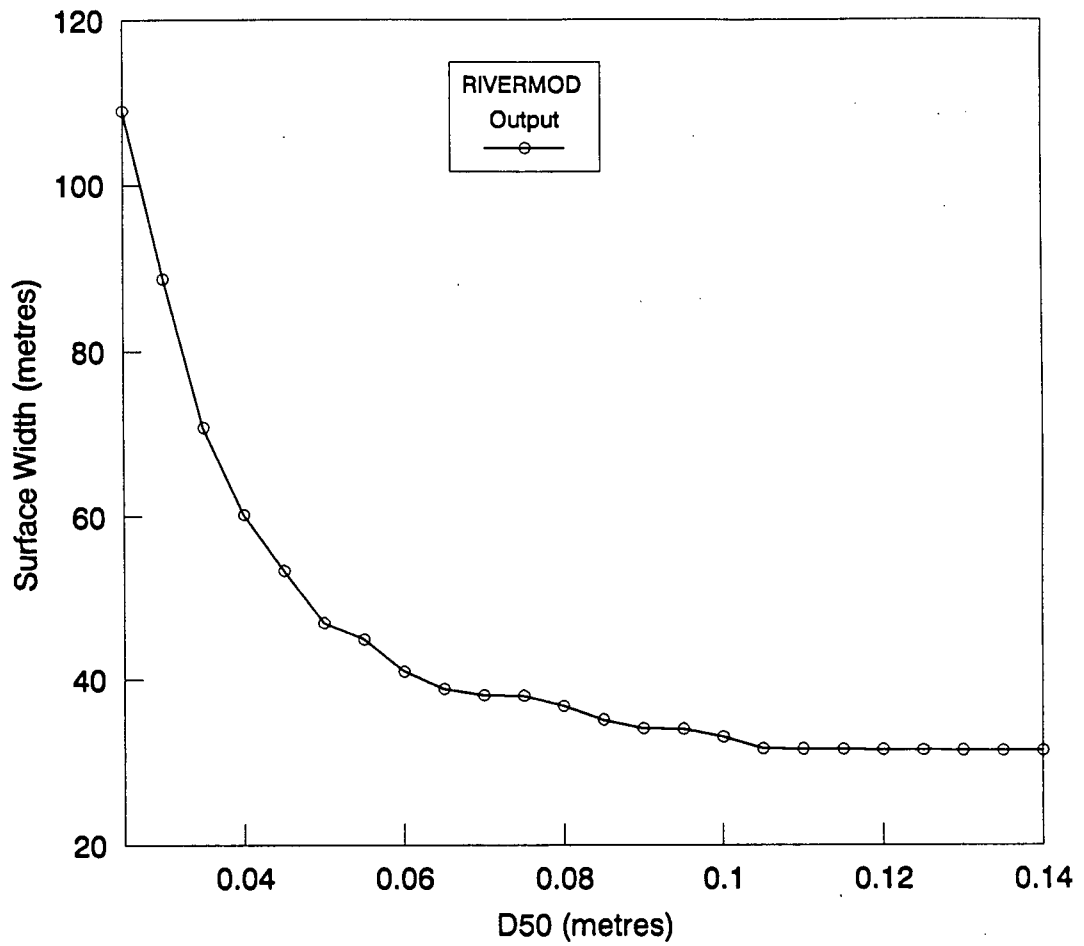


Figure 5.13: Effect of Bank Sediment Size on the Channel Surface Width. $Q = 100 \text{ m}^3/\text{sec}$, $d_{50} = 0.025 \text{ m}$, $D_{50} = 0.075 \text{ m}$, $\phi = 40^\circ$, $G_b = 9.2 \text{ kg/sec}$.

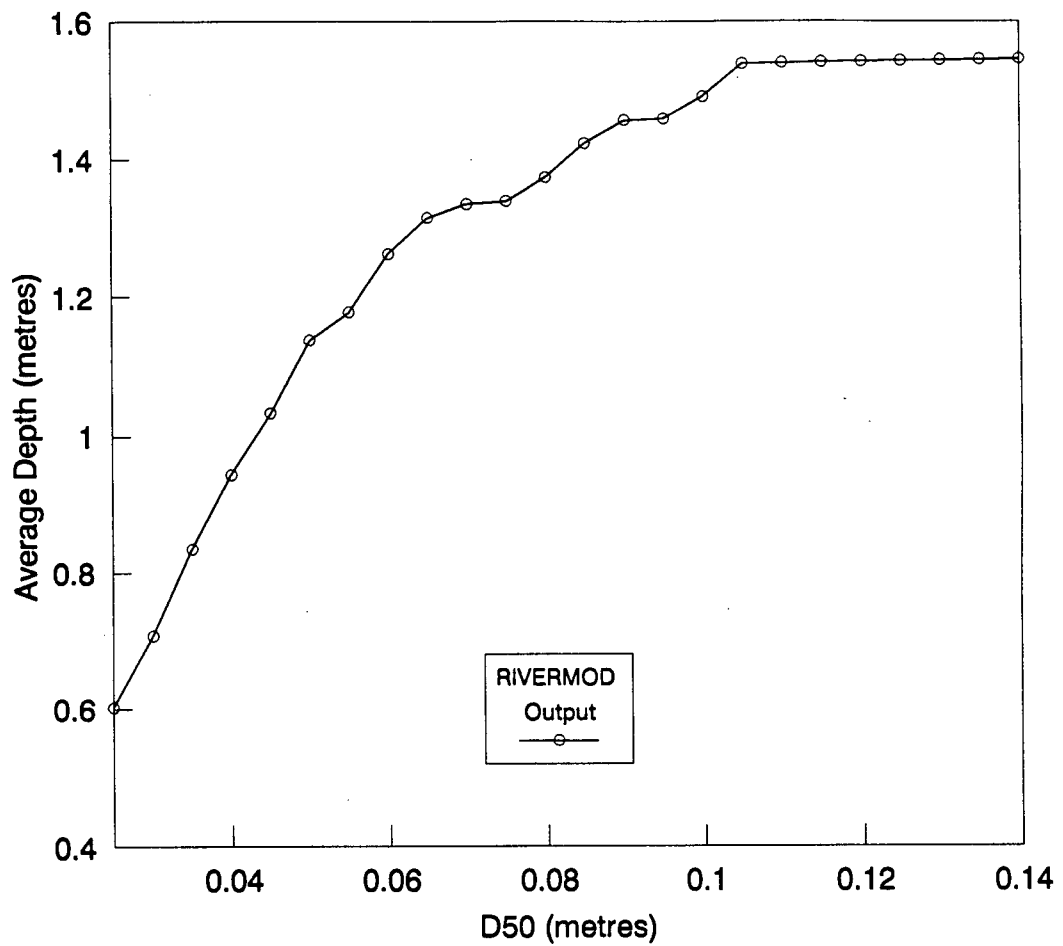


Figure 5.14: Effect of Bank Sediment Size on the Average Channel Depth. $Q = 100 \text{ m}^3/\text{sec}$, $d_{50} = 0.025 \text{ m}$, $D_{50} = 0.075 \text{ m}$, $\phi = 40^\circ$, $G_b = 9.2 \text{ kg/sec}$.

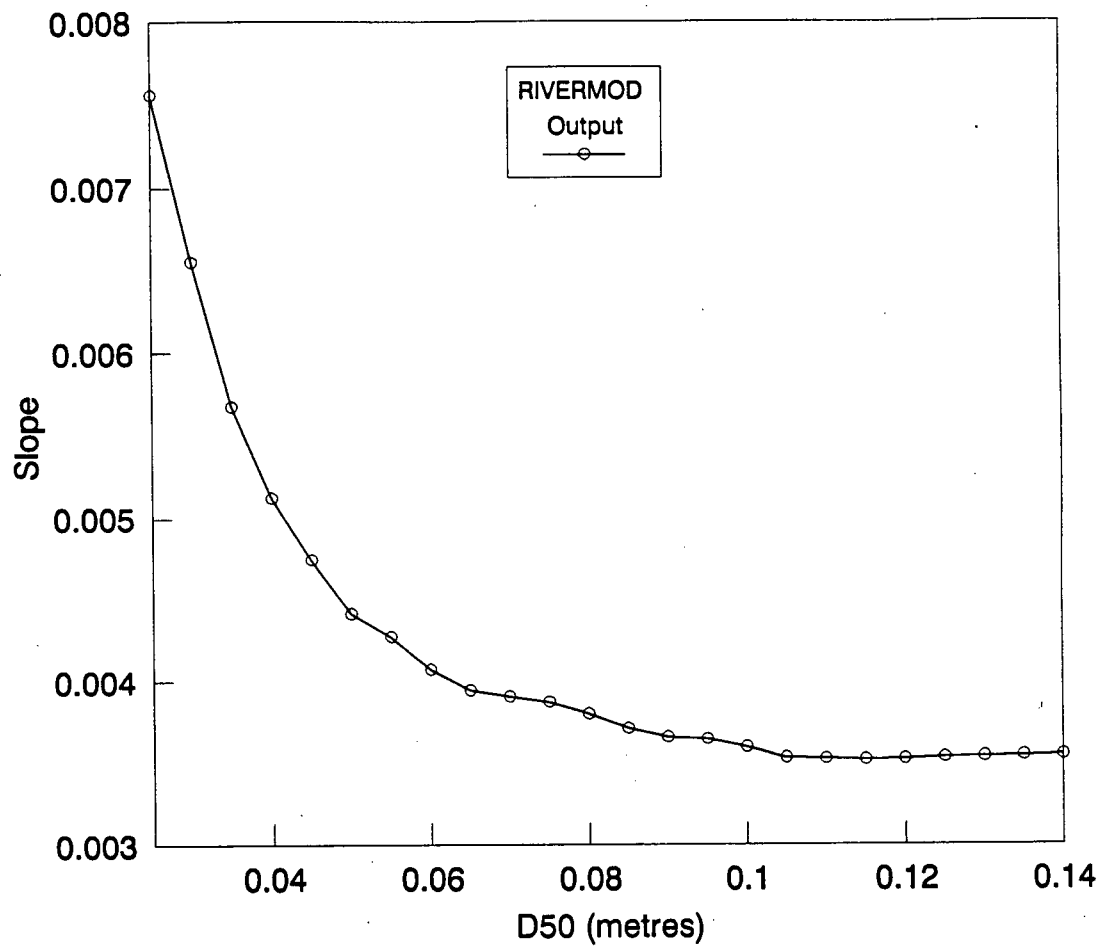


Figure 5.15: Effect of Bank Sediment Size on the Channel Slope. $Q = 100 \text{ m}^3/\text{sec}$, $d_{50} = 0.025 \text{ m}$, $D_{50} = 0.075 \text{ m}$, $\phi = 40^\circ$, $G_b = 9.2 \text{ kg/sec}$.

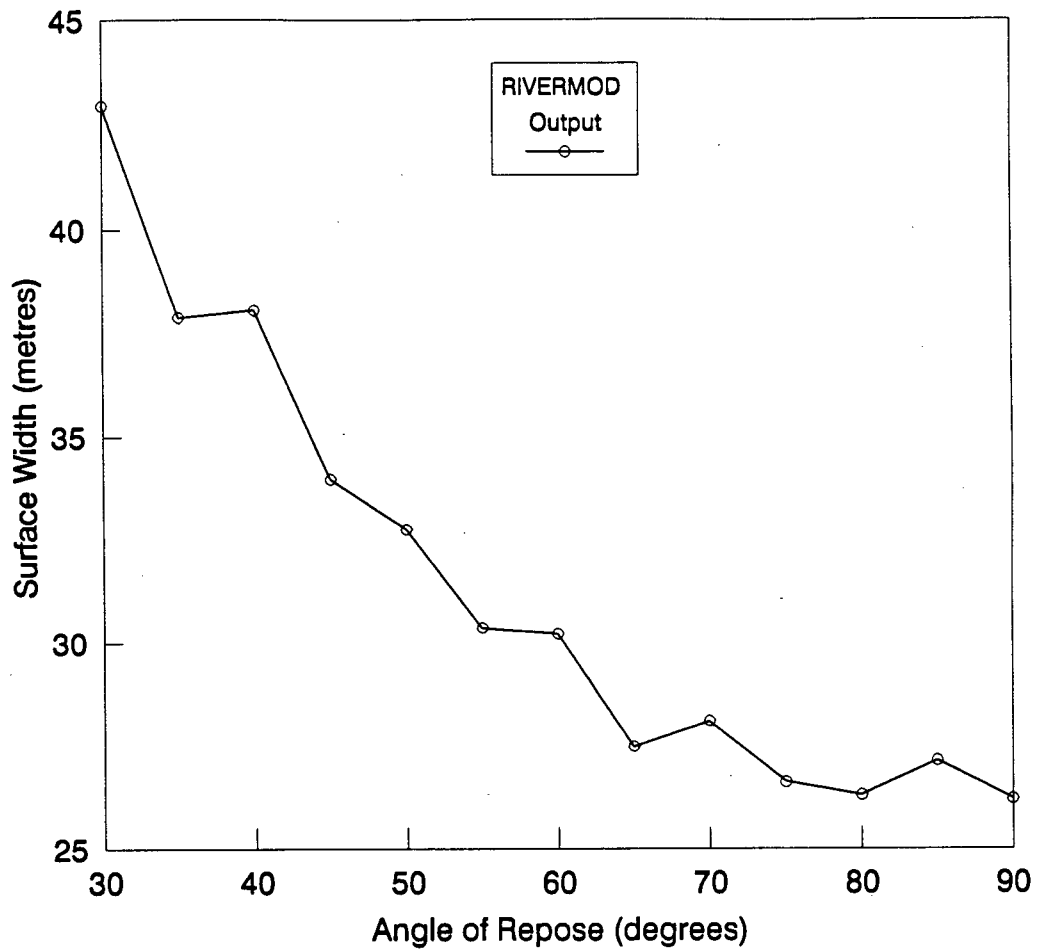


Figure 5.16: Effect of the Angle of Repose of the Bank Sediment on the Channel Surface Width. $Q = 100 \text{ m}^3/\text{sec}$, $d_{50} = 0.025 \text{ m}$, $D_{50} = 0.075 \text{ m}$, $D_{50_{bank}} = 0.075$, $G_b = 9.2 \text{ kg/sec}$.

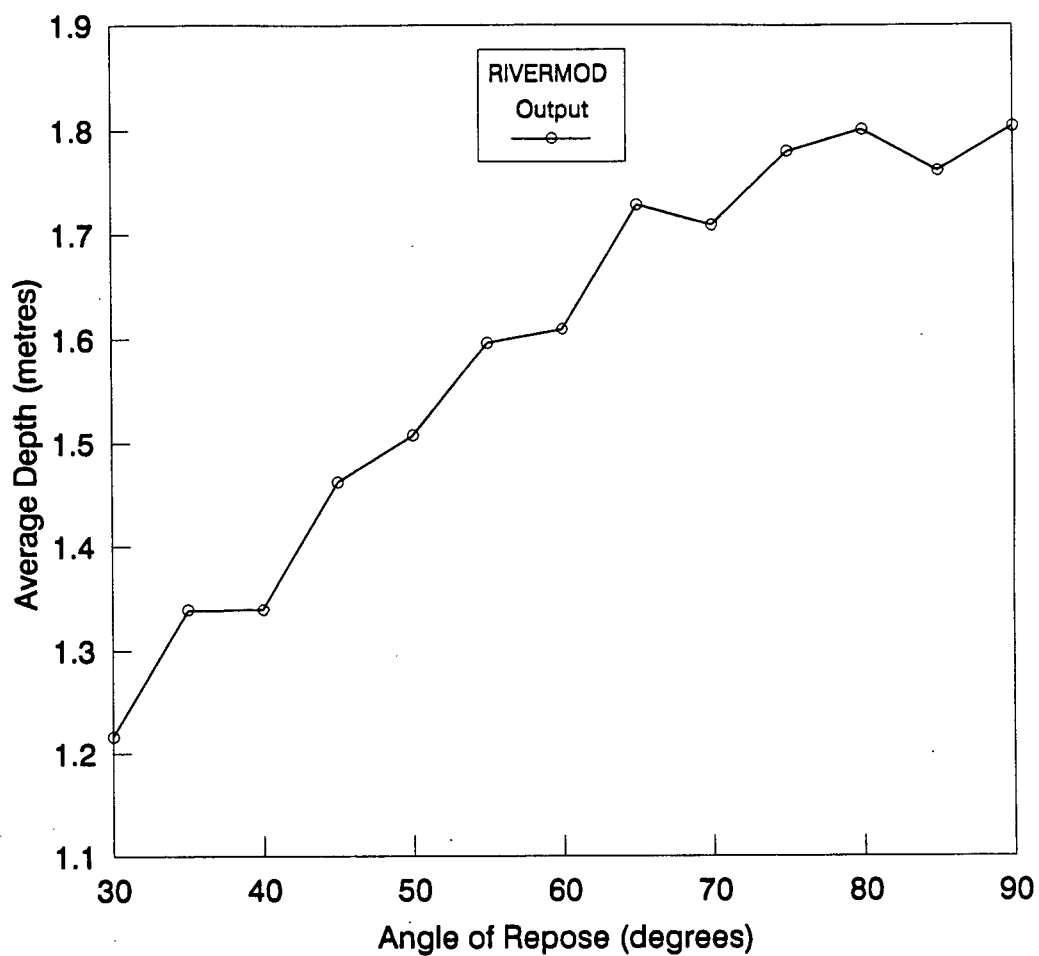


Figure 5.17: Effect of the Angle of Repose of the Bank Sediment on the Channel Average Depth. $Q = 100 \text{ m}^3/\text{sec}$, $d_{50} = 0.025 \text{ m}$, $D_{50} = 0.075 \text{ m}$, $D_{50_{bank}} = 0.075$, $G_b = 9.2 \text{ kg/sec}$.

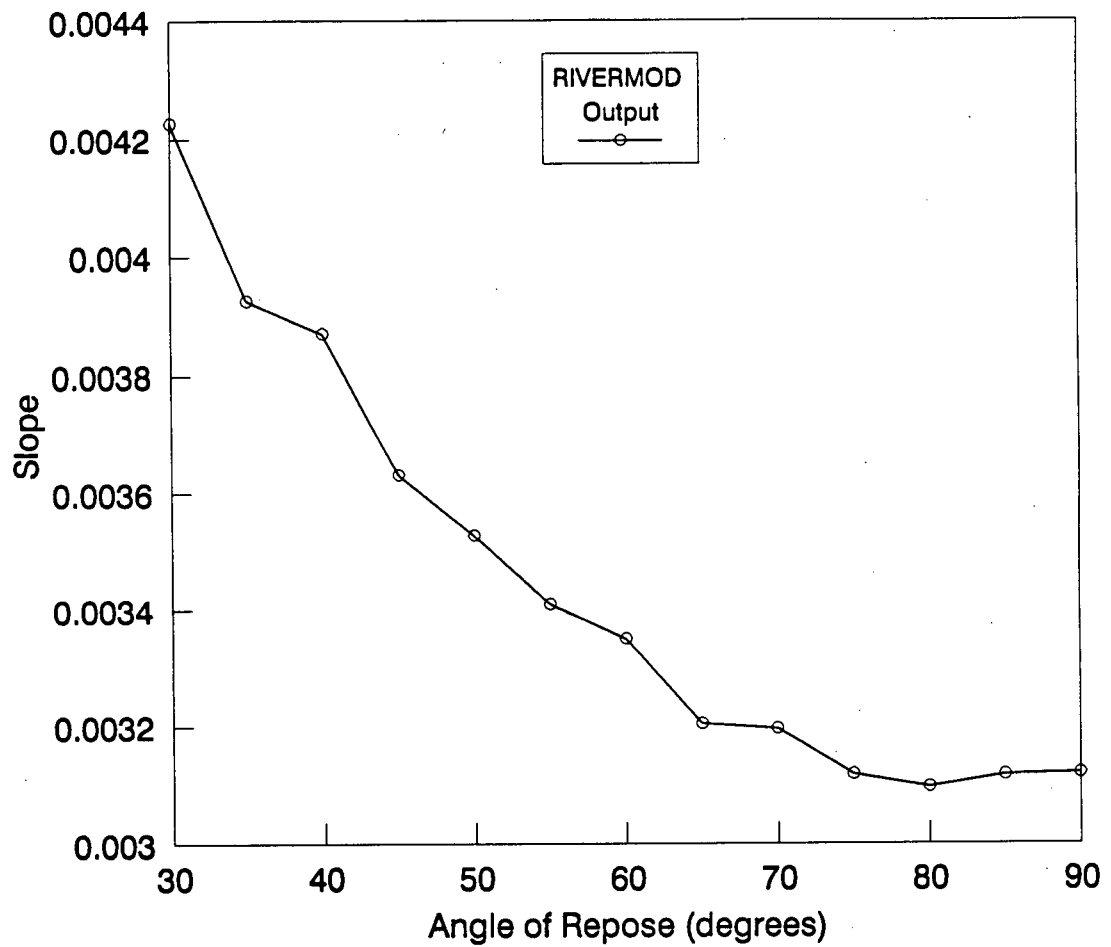


Figure 5.18: Effect of the Angle of Repose of the Bank Sediment on the Channel Slope.
 $Q = 100 \text{ m}^3/\text{sec}$, $d_{50} = 0.025 \text{ m}$, $D_{50} = 0.075 \text{ m}$, $D_{50_{bank}} = 0.075$, $G_b = 9.2 \text{ kg/sec}$.

vegetation has a strong influence on the channel width. The denser bank vegetation can be interpreted as an increase in ϕ' and thus a narrower (and deeper) channel would be expected.

An illustration of the effect of altering ϕ' is the now generally discontinued practice of stream-side logging. It has been shown that logging of the riparian zone may cause instability of the channel which can include increased channel width and tendency to a braided morphology (eg Roberts and Church, 1986).

Mechanical disturbance of the bank, together with removal by decay of the binding root masses, will result in a decrease in ϕ' . Thus the streambanks will no longer be able to withstand the shear stress imposed. The channel would be expected to adjust by increasing the channel width, and decreasing the channel bank angle and the channel slope. This instability would be exasperated in the short-term by the additional sediment produced by the erosion of the streambanks.

5.4.3 Discharge

The effect of varied Q_{bank} on the channel geometry is shown in Figures 5.19 to 5.21. The effect of increasing discharge is for the channel to increase W and Y , and to decrease S .

The qualitative equation of Lane (1955, see Equation 2.1) indicates that if the discharge is increased while the discharge and sediment size are held constant, the channel will adjust by decreasing S .

The qualitative model of Schumm (1969, see Equation 2.2) indicates that a channel subjected to an increase in the dominant discharge, while all other independent variables are held constant, will adjust its geometry by increasing its W , Y , sinuosity, Z , and meander wavelength, while decreasing S .

In engineering time ($< 100 - 200$ years) a channel may adjust its slope only by adjusting the channel sinuosity, Z . An increase in the sinuosity results a decrease in

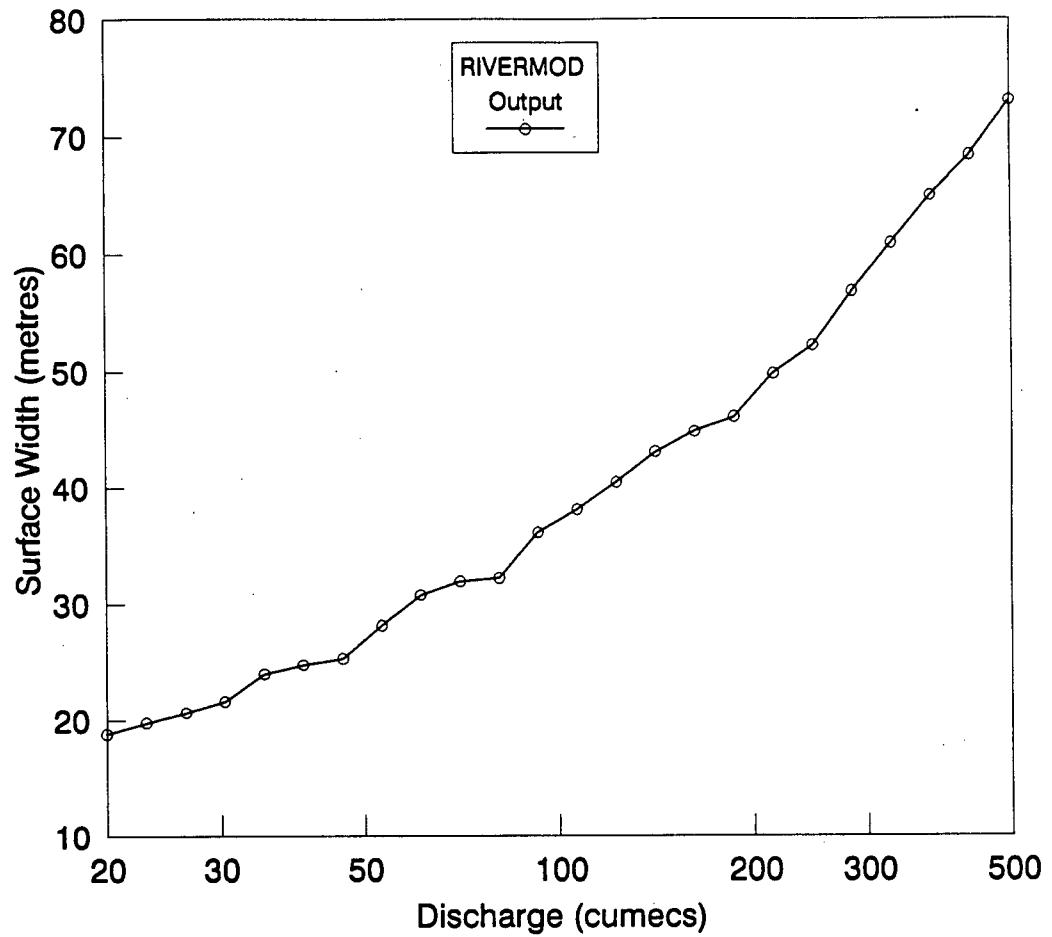


Figure 5.19: Effect of Discharge on the Channel Surface Width. $d_{50} = 0.025$ m, $D_{50} = 0.075$ m, $D_{50_{bank}} = 0.075$, $\phi = 40^\circ$, $G_b = 9.2$ kg/sec.

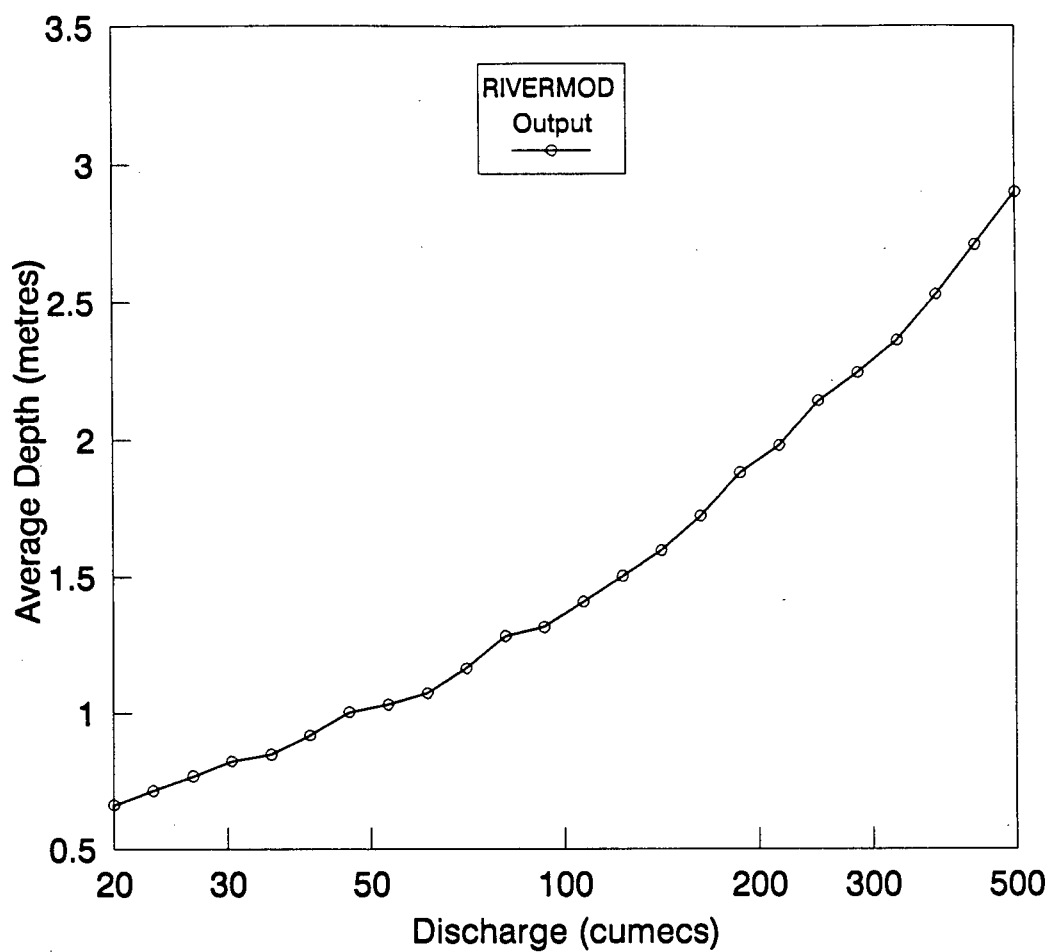


Figure 5.20: Effect of Discharge on the Average Channel Depth. $d_{50} = 0.025$ m, $D_{50} = 0.075$ m, $D_{50_{bank}} = 0.075$, $\phi = 40^\circ$, $G_b = 9.2$ kg/sec.

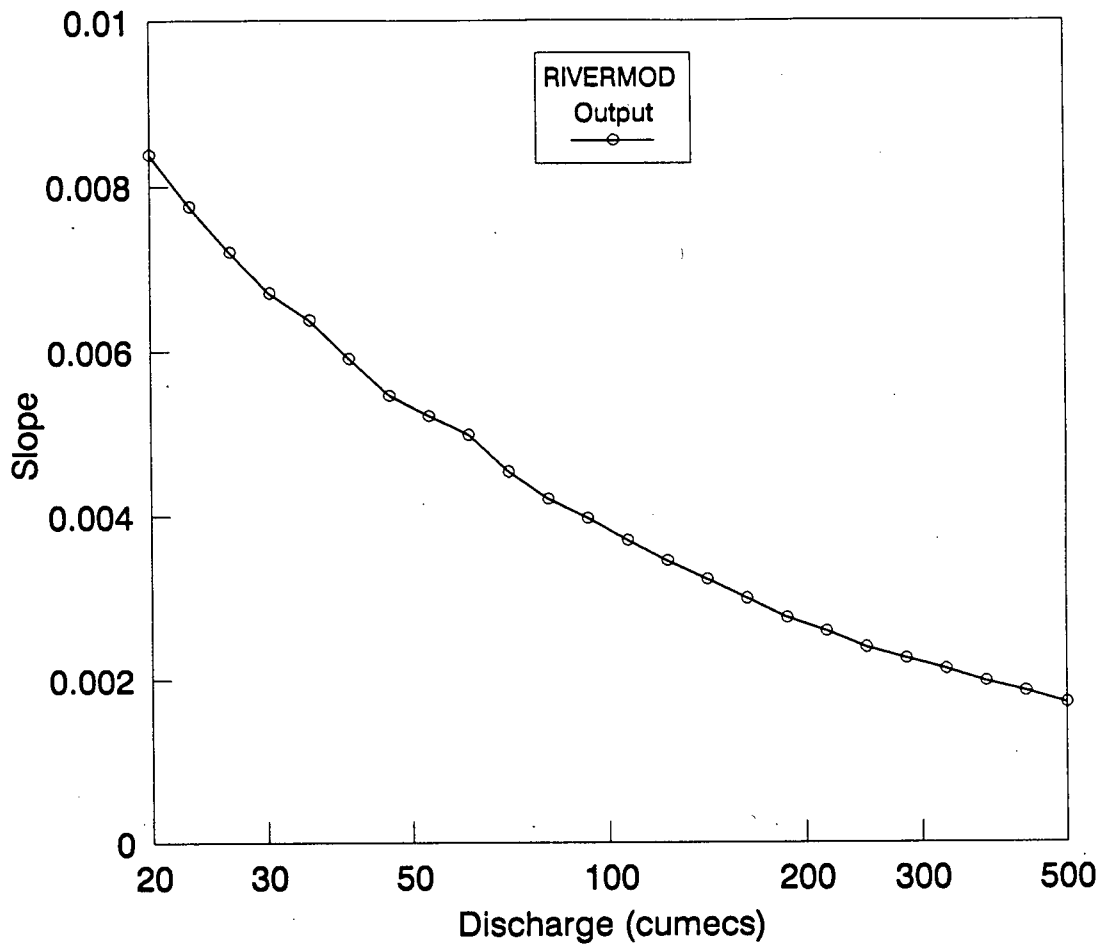


Figure 5.21: Effect of Discharge on the Channel Slope. $d_{50} = 0.025$ m, $D_{50} = 0.075$ m, $D_{50_{bank}} = 0.075$, $\phi = 40^\circ$, $G_b = 9.2$ kg/sec.

the channel slope. By altering the sinuosity a channel can quickly adjust its gradient. Adjustment of the channel through aggradation or degradation requires the deposition or erosion of large volumes of sediment and can only be considered significant over geologic time periods.

The predictions made by RIVERMOD for the adjustments of a channel to a variation in the magnitude of the dominant discharge agree with the qualitative observations indicated by Equations 2.1 and 2.2. The influence of discharge on the channel geometry is discussed further in Section 5.5.

5.4.4 Sediment Load

The effect of varied G_b on the channel geometry is shown in Figures 5.22 to 5.24. The effect of increasing sediment load is for the channel to increase W and S , and to decrease Y .

The qualitative equation of Lane (1955a, see Equation 2.1) indicates that if the sediment load is increased while the discharge and sediment size are held constant, the channel will adjust by increasing the channel slope.

The qualitative model of Schumm (1969, see Equation 2.3) indicates that a channel subjected to an increase in the sediment load, while all other independent variables are held constant, will adjust its geometry by increasing its W , L , and Z , while decreasing the Y and Z .

The predictions by RIVERMOD for a channel being subjected to a varied sediment load agree with the qualitative observations indicated by Equations 2.1 and 2.3.

A perusal of the data from Hey and Thorne (1986) indicates that single-thread gravel rivers typically have bankfull sediment transport rates in the order of 1 - 10 kg/sec as calculated by the equations of Parker *et al* (1982). The influence on the channel geometry of a ten-fold increase in the sediment load is to increase the width only very slightly from

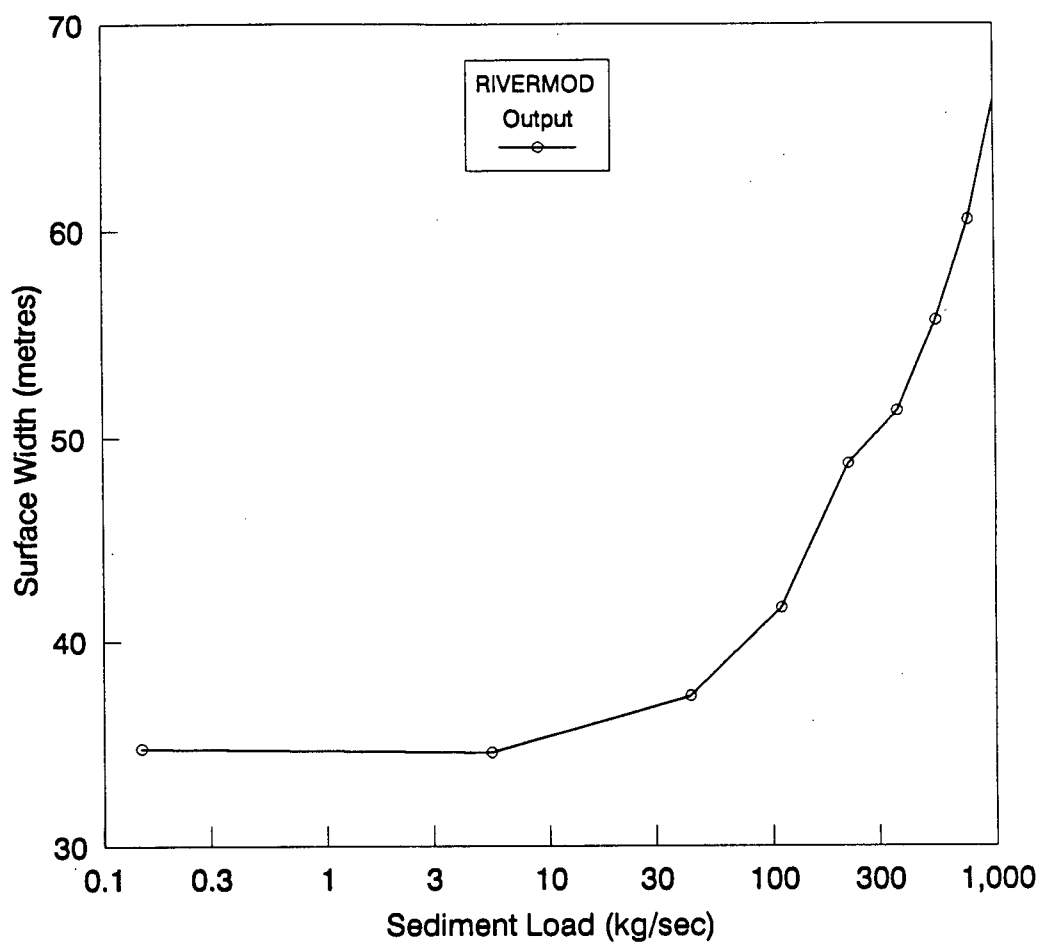


Figure 5.22: Effect of Sediment Load on the Channel Surface Width. $Q = 100 \text{ m}^3/\text{sec}$, $d_{50} = 0.025 \text{ m}$, $D_{50} = 0.075 \text{ m}$, $D_{50_{bank}} = 0.075$, $\phi = 40^\circ$.

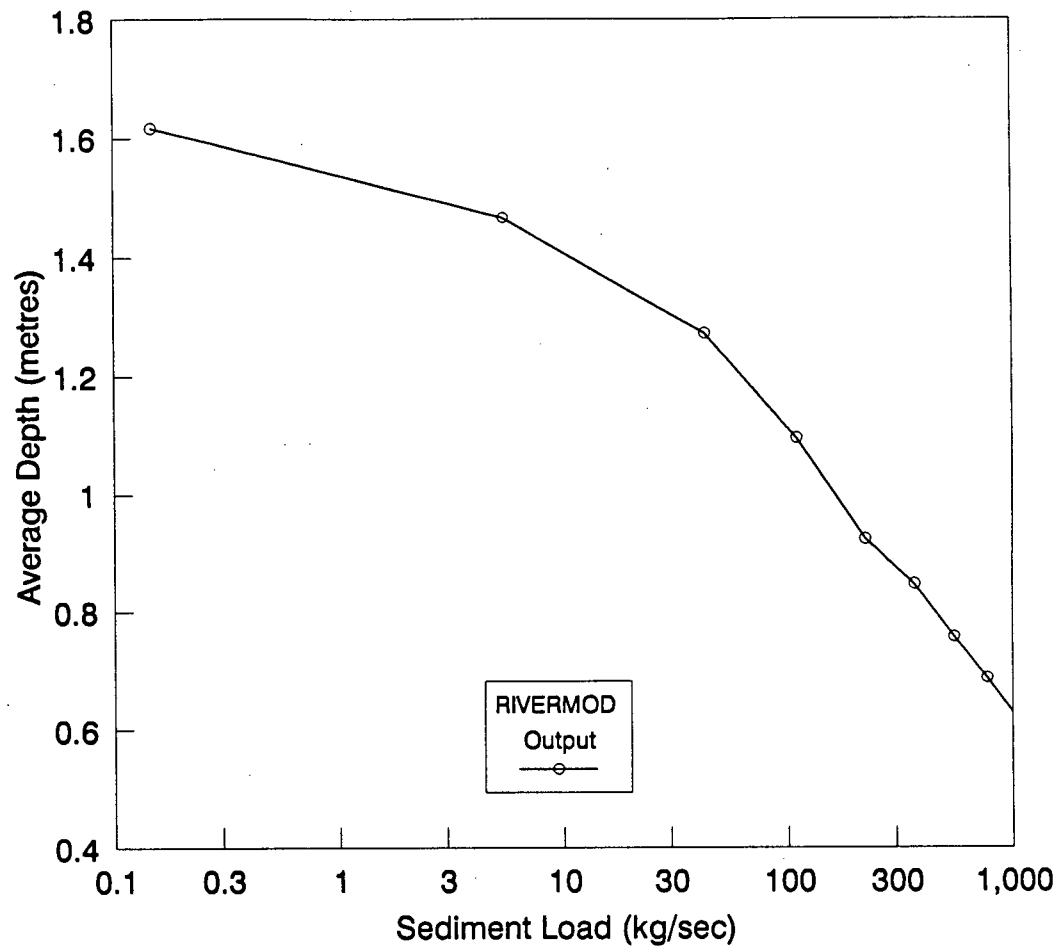


Figure 5.23: Effect of Sediment Load on the Average Channel Depth. $Q = 100 \text{ m}^3/\text{sec}$, $d_{50} = 0.025 \text{ m}$, $D_{50} = 0.075 \text{ m}$, $D_{50_{bank}} = 0.075$, $\phi = 40^\circ$.

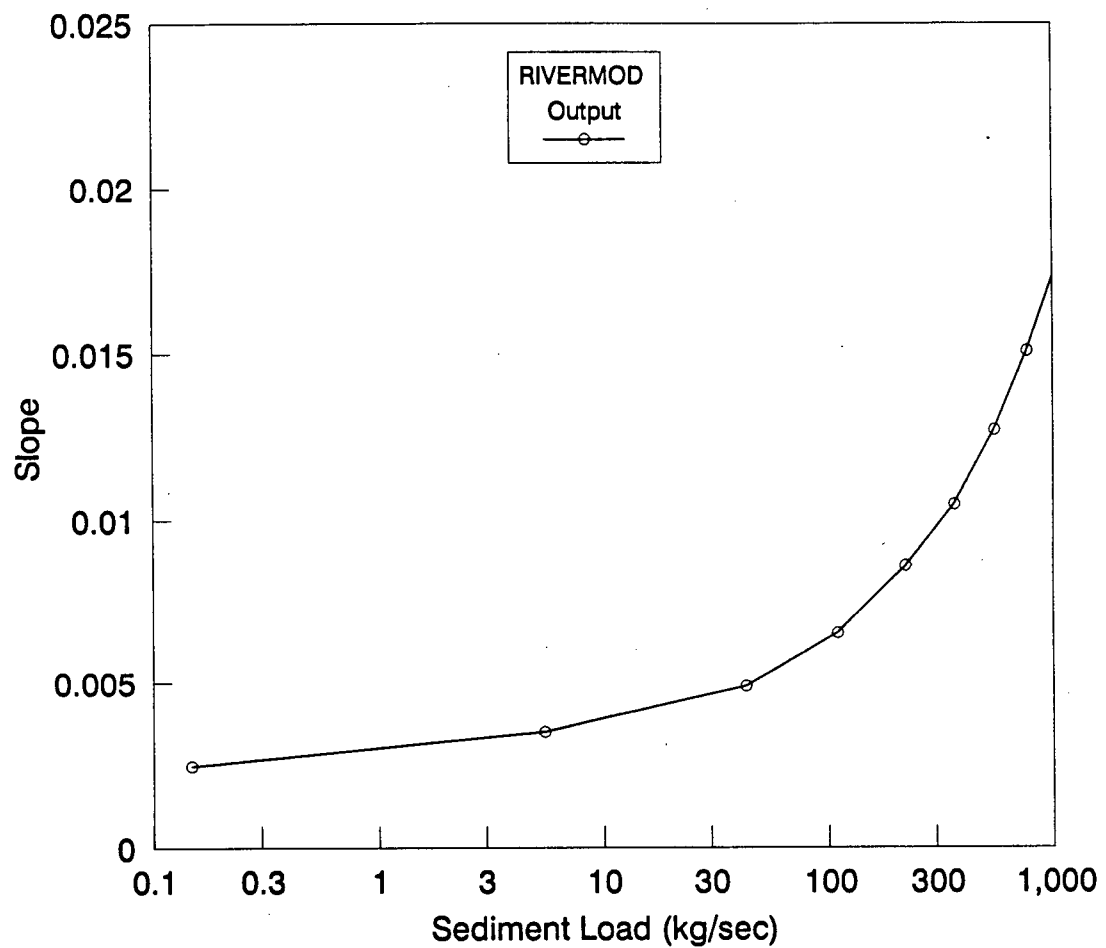


Figure 5.24: Effect of Sediment Load on the Channel Slope. $Q = 100 \text{ m}^3/\text{sec}$, $d_{50} = 0.025 \text{ m}$, $D_{50} = 0.075 \text{ m}$, $D_{50_{bank}} = 0.075$, $\phi = 40^\circ$.

approximately 35 to 36 metres, to decrease the average depth by 7% from 1.53 to 1.42 metres, and to increase the slope by 60% from 0.0025 to 0.004.

The effect on the channel geometry in this example is manifested principally as an increase in the channel slope. Large changes in the cross-sectional geometry occur only for steeper rivers with large sediment loads, in this case in excess of about 100 kg/sec. This is, according to Chang (1980), an observable feature of natural rivers.

The channel response modelled by RIVERMOD assumes that all the dependent variables are free to adjust to the imposed variables. Many rivers would not be able to increase their slopes by 60% to accommodate an increase in the sediment load. For example a river with a sinuosity of 1.2 could, in engineering time, increase its slope a maximum of only 20%. The maximum slope attainable without massive aggradation of the valley floor corresponds to a straight channel with a sinuosity of 1. An increase in the sediment load which required an increase in the channel slope in excess of 20% to maintain equilibrium could not be accommodated by such a channel. Channel aggradation and instability would be expected.

RIVERMOD is not able to predict the channel geometry of a channel once this critical sediment load, which corresponds to the sediment transport capacity of the steepest possible channel, is exceeded.

5.5 COMPARISON WITH REGIME EQUATIONS

An artificial data set was generated using random number generators. The discharge ranged between 10 - 500 m³/sec, D_{50} between .01 - .1 m, and the channel slope from 1 - 5 times the threshold slope as given by Equation 4.8. The data appears in Appendix F.

This data was input into RIVERMOD and a regression analysis performed on the

output channel geometry. The equations derived for width, W , and depth, Y , are:

$$W = 5.6 Q^{0.43} \quad (5.5)$$

$$Y = 0.33 Q^{0.38} \quad (5.6)$$

The general empirical regime equations derived from British gravel-bed river data by Hey and Thorne (1986, See Section 2.3) for thin bank vegetation are:

$$W = 4.33 Q^{0.50} \quad (5.7)$$

$$Y = 0.33 Q^{0.35} \quad (5.8)$$

The exponent in Equation 5.5 is less than that obtained by Hey and Thorne, and outside of the range 0.45 - 0.55 which is usually observed. The reason for the low exponent is not apparent at this point.

The exponent in equation 5.6 is larger than was found by the Hey and Thorne study, although falls within the range 0.33 - 0.41 which is usually observed.

5.6 CONCLUSIONS

Preliminary verification of RIVERMOD by predicting the geometry of existing rivers, despite the absence of key data necessary for the bank stability analysis, indicates the assumptions used in the development of RIVERMOD are generally valid.

The modelled channel widths and depths compare favourable with the widths and depths predicted by regime equations which were derived from the data set used in the verification.

RIVERMOD was very successful in predicting the channel slope. This success is due to the way in which the sediment load and sediment transport equations are used.

Bedload transport rates are available for only a few select rivers. Therefore it is generally necessary to calculate the sediment load of a river using a sediment transport

equation. The PKM equations were used to determine the sediment transport capacity from the observed channel geometry. This figure was then input into RIVERMOD in order to model the observed channel geometry.

RIVERMOD is designed as a model of river response. The response of the channel to altered flows or sediment supply is modelled relative to the original, undisturbed channel.

The sediment transport rate calculated for the observed channel is only a reference value. As was shown in this chapter the channel slope, which is highly dependent on the sediment transport capacity, can be predicted very successfully even though the grain size of the transported bedload is unknown.

Despite attempts by Hey and Thorne (1986, see section 2.3.3), the sediment load has not yet been successfully incorporated into a regime slope equation. This is because in a regression analysis the sediment load is regarded as an absolute value, and not as a relative index of sediment transport capacity as is used in RIVERMOD.

The adjustments of a channel to variations in the inputs and the bank strength agree with qualitative observations of river response. This agreement with the qualitative observations strengthens the confidence in the validity of RIVERMOD to model such changes.

The residual error analyses indicate that a systematic error is inherent in RIVERMOD whereby the residual errors increase with increasing $\tau_{D_{50}}^*$. This may account for the slight underestimation of the discharge exponent in Equation 5.5.

Chapter 6

CONCLUSIONS

6.1 SUMMARY

This thesis has presented the development of RIVERMOD, a physically-based model of river channel development and river response. RIVERMOD determines the stable, single-thread, equilibrium channel which will develop for a given set of independent input variables, principally the bankfull discharge and sediment load, sediment size, and the nature of the bank sediments. The dependent channel geometry variables, width, depth, slope, bank angle, and channel roughness, are free to dynamically adjust to the inputs.

The widely used qualitative and regime models, while indicating the general direction of river adjustments, are not able to deal with river response at a quantitative level. The existing analytical models such as those of Chang (1979, 1980), and White *et al* (1982), while promising, do not predict channel geometry to the accuracy required for engineering applications (Thorne *et al*, 1988).

The models of Chang and White are quite similar in structure and are based on the iterative solution of equations for continuity, flow resistance, and sediment transport, together with a fourth closure hypothesis. Chang uses the hypothesis of minimum stream power, and White *et al* the hypothesis of maximum transport capacity. Both hypotheses are generally equivalent.

A similar approach was developed for RIVERMOD. Additional refinements were included, principally the distribution of the boundary shear stress, together with an analysis of the bank stability. The previous models did not adequately account for bank stability. The bank stability analysis used in this version of RIVERMOD is the USBR method (Lane 1955b) which applies only to non-cohesive alluvial banks. The boundary shear stress distribution is determined from empirical formulae derived from experimental data by Flinham and Carling (1988).

For each iteration the flow resistance, water and sediment discharge capacity, boundary shear stress distribution, and the bank stability is calculated.

It was initially thought that the addition of the equations for the boundary shear stress distribution and bank stability would allow an explicit solution to be obtained for the channel geometry. However with each additional equation an additional unknown variable was also introduced. A further closure hypothesis was necessary. The hypothesis of maximum sediment transport potential (MSTP) was presented. The MSTP is a variation of the maximum transport capacity hypothesis of White *et al* (1982) and is roughly equivalent to the minimum stream power hypotheses of Chang (1979, 1980) and Yang (1976).

Solution of the governing equations, together with the MSTP hypothesis, permit a unique stable channel geometry to be determined for given inputs of discharge, sediment load, and bank sediment properties. RIVERMOD models the channel geometry as a function of the bankfull discharge and sediment transport capacity which are calculated from the initial, undisturbed channel geometry. The effective bankfull discharge, Q'_{bank} , is calculated from the channel geometry. This is used in preference to the actual bankfull discharge. This allows RIVERMOD to be used on ungauged rivers and eliminates the errors which result from non-grain roughness elements which are a source of significant errors in the models of Chang and White *et al*.

An attempt is made to account for the adjustment of the bed roughness elements. Previous models have assumed that the median pavement grainsize, D_{50} , (or whichever fraction is used to calculate the boundary roughness) remains constant during channel adjustment. This is known to be incorrect. A channel has the ability to adjust the grainsize distribution of the pavement layer, and hence to adjust the flow resistance. The dimensionless bed shear stress calculated from the median pavement grain diameter, $\tau_{D_{50}}^*$, is assumed to remain constant throughout channel adjustments. This permits D_{50} to dynamically adjust together with the other dependent variables.

Preliminary verification of RIVERMOD supports the theory presented. RIVERMOD was able to model the geometry of selected gravel rivers quite well despite the absence of data pertaining to the bank sediments. The ability of RIVERMOD to model the width and depth of these channels was close to the results obtained from empirical regime equations which were derived from the data tested. RIVERMOD was able to model the cross-sectional area and channel slope with considerably greater accuracy than the regime equations.

An analysis of the residual errors indicates a systematic variation in the residual errors from RIVERMOD when plotted as a function of the dimensionless bed shear stress, $\tau_{D_{50}}^*$. The reason for this variation is not clear, however it may be related to the assumption that the median bank grain diameter, $D_{50_{bank}}$, is equal to D_{50} .

The river channel responses predicted by RIVERMOD agree well with the qualitative models presented in Chapter 2. Increasing the dominant discharge will result in the channel adjusting by increasing its width and depth, and by decreasing its gradient. Increasing the sediment load will result in an increase in the channel width and slope, and a decrease in the depth.

A sensitivity analysis of the bank sediment properties indicates that the morphology of a river can be strongly influenced by the properties of the channel banks alone. It is

possible for a stable single-thread channel to develop an unstable braided morphology by varying only the angle of repose of the bank sediment.

In summary:

1. RIVERMOD in its current form is applicable only to single thread gravel-bed rivers. The model can be modified to include sand-bed rivers through the choice of suitable flow resistance and sediment transport equations.
2. RIVERMOD iteratively solves equations which describe the movement of water and sediment through a channel, namely flow resistance and continuity, while calculating the boundary shear stress distribution and analysing the bank stability.
3. RIVERMOD is designed to calculate the geometry of the stable channel which is required to convey the imposed water and sediment load. This geometry may not be attainable due to additional constraints such as valley slope and width.
4. RIVERMOD is not able to predict the timing of the river channel adjustments.
5. RIVERMOD cannot be applied to braided rivers as the model assumes that an equilibrium condition will develop.

The theory can be extended to the design of stable channels where the value of one of the dependent variables (usually the channel slope) is known.

6.2 APPLICATION TO THE CARMANAH VALLEY

The initial reason for developing RIVERMOD was to study the possible effects of increased sediment load in the Carmanah Valley. The following comments indicate the tentative conclusions that can be drawn and the nature of the channel changes that may occur.

The modelling in Section 5.4 indicates that an increase in the sediment load will result in an increase in the channel width, and slope, and a decrease in the channel depth. There is a tendency towards a braided channel morphology.

A critical sediment load exists below which the channel can develop an equilibrium configuration, and retain a single-thread morphology. Above this critical load, which requires that the channel slope exceed the constraining valley slope, the channel cannot transport the additional sediment and disequilibrium will result. The disequilibrium will be manifested by channel aggradation, widening, increased overbank flooding, and the development of a braided morphology.

Severe impact to the riparian spruce habitat can be expected if this critical sediment load is exceeded.

It is not possible at this stage to comment further on the magnitude of the possible channel adjustments without actually collecting the required field data and inputting it into RIVERMOD.

The field data required includes longitudinal and cross-sectional channel surveys, and the pavement, subpavement, and bank sediment size distributions. With this field data Q'_{bank} , G_b , $\tau_{D_{50}}^*$ and ϕ' can be calculated, as well as providing the d_{50} , D_{50} , and $D_{50_{bank}}$.

RIVERMOD must be used in conjunction with sediment budget estimates for a proposed land-use strategy.

6.3 FUTURE WORK

Although initially designed to model the impact of logging on Carmanah Creek, RIVERMOD can potential be applied to a variety of land-use and climatic changes which alter the magnitude of the bankfull discharge and sediment load. These changes include the effects of urbanization, flow regulation, flow diversions, deforestation, and changes in the

catchment precipitation.

RIVERMOD in its current form can be applied only to gravel rivers whose beds become mobile at some stage less than bankfull. The model does not contain an algorithm which determines the development of an immobile armour layer, and hence cannot at present be used to predict the channel degradation which would occur for example downstream of a dam closure.

RIVERMOD is currently at an early stage of development. Future areas of research and model development include:

1. Examination of the development of the pavement layer. How is it related to the subpavement grainsize? How does it vary with the sediment transport rate?
2. Incorporation of a bed armour algorithm to model channel degradation.
3. Increasing the sophistication of the bank stability analysis to include cohesive sediments and the effect of the bank vegetation.
4. Examination of the significance of the bankfull discharge. Is the bankfull discharge a dependent variable? Can a channel adjust its bankfull discharge to accommodate for example an increase in the sediment load?
5. Endeavouring to replace the requirement for an extremal hypothesis with a physically-based process.

In addition RIVERMOD should undergo rigorous testing and verification by modelling the channel changes which have been documented in a variety of case studies.

REFERENCES

- ASCE, 1963: Task force on friction factors in open channels. *Proc. Am. Soc. Civil Engrs.*, Vol. 98, HY 2, pp. 97.
- Andrews, E.D., 1983: Entrainment of gravel from naturally sorted riverbed material. *Geol. Soc. Am. Bull.* Vol. 94, pp. 1225 - 1231.
- Andrews, E.D., 1984: Bed material entrainment and the hydraulic geometry of gravel-bed rivers in Colorado. *Geol. Soc. Am. Bull.* Vol. 95, pp. 371 - 378.
- Bagnold, R.A., 1966: An approach to sediment transport from general physics. *U.S.G.S. Prof. Paper* I-442.
- Bagnold, R.A., 1977: Bedload transport by natural rivers. *Water Res. Res.*, Vol. 13, No. 2, pp. 303 - 312.
- Bagnold, R.A., 1980: An empirical correlation of bedload transport rate in flumes and natural rivers. *Proc. Roy. Soc., London, England, Ser. A.*, Vol. 372, pp. 452 - 473.
- Barishnikov, N.B., 1967: Sediment transport in river channels with flood plains. *Pub. I.A.H.S.*, Vol. 75, pp. 404 - 413.

- Beshta, R.L., 1978: Long term patterns of sediment production following road construction and logging in the Oregon Coast Range. *Water Res. Res.*, Vol. 14, No. 6, pp. 1011 - 1016.
- Bettess, R., White, W.R., Reeve, C.E., 1988: On the Width of Regime Channels. In *International Conference on River Regime*, W.P. White (Ed.). John Wiley and Sons. pp. 149 - 162.
- Bray, D.I., 1982 a: Flow resistance in gravel-bed rivers. In *Gravel-Bed Rivers*, Hey, R.D., Bathurst, J.C., and Thorne, C.R., (Eds.). John Wiley and Sons. pp. 109 - 137.
- Bray, D.I., 1982 b: Regime equations for gravel-bed rivers. In *Gravel-Bed Rivers*, Hey, R.D., Bathurst, J.C., and Thorne, C.R., (Eds.). John Wiley and Sons. pp. 517 - 552.
- Brown, C.B., 1950: Sediment transportation. In *Engineering Hydraulics*, H. Rouse (Ed.). John Wiley and Sons, Chapt. 12.
- Chang, H.H., 1979. Minimum stream power and river channel patterns. *J. Hydrol. (Amsterdam)*, Vol. 41, pp. 303 - 327.
- Chang, H.H., 1980. Geometry of gravel streams. *J. Hydr. Div. ASCE*, Vol. 106, HY 9, pp. 1443 - 1456.
- Chow, V.T., 1959: *Open Channel Hydraulics*. McGraw - Hill Co., New York.

Davies, T.R.H. and Sutherland, A.J., 1980: Resistance to flow past deformable boundaries. *Earth Surf. Proc.*, Vol. 5, pp. 175 - 179.

Einstein, H.A., 1942: Formulas for the transportation of bed load. *Trans. Am. Soc. Civil Engrs.*, Vol.107, pp. 561 - 597.

Fenton, J.D., and Abbott, J.E., 1977: Initial movement of grains on a stream bed: The effect of relative protrusion. *Proc. Roy. Soc., London, England, Ser. A.*, Vol. 352, pp. 523 - 537.

Flintham, T.P., and Carling, P.A., 1988: The prediction of mean bed and wall boundary shear in uniform and compositely roughened channels. In *International Conference on River Regime*, W.P. White (Ed.). John Wiley and Sons. pp. 267 - 287.

Gilbert, G.K., 1914: The transportation of debris by running water. *U.S.G.S. Prof. Paper* 86.

Grant, G.E., 1988: The RAPID technique: A new method for evaluating downstream effects of forest practices on riparian zones. *USDA For. Serv. Pac. Nor. West Res. Stn. Gen. Tech. Rept.*, PNW-GTR-230.

Grant, G.E., Crozier, M.J., Swanson, F.J., 1984: An approach to evaluating the off-site effects of timber harvest activities on channel morphology. In *Symposium on the effect of forest land use on erosion and slope stability*, Honolulu, Hawaii, May 1984.

Harr, R.D., 1986: Effects of clearcutting on rain-on-snow runoff in western Oregon: a

new look at old studies. *Water Res. Res.*, Vol. 22, No. 7, pp. 1095 - 1100.

Harr, R.D., Harper, J.T., and Hseih, H., 1974: Changes in storm hydrographs after road building and clearcutting in the Oregon Coast Range. *Water Res. Res.*, Vol. 11, No. 3, pp. 436 - 444.

Henderson, F.M., 1966: *Open Channel Flow*. Macmillan Pub. Co., New York. 522 p.

Hetherington, E.D., 1982: A first look at logging effects on the hydrological regime of the Carnation Creek experimental watershed. In *Carnation Creek Workshop*, G. Hartman (Ed.). Pacific Biological Station, Nanaimo, B.C., pp. 45 - 63.

Hetherington, E.D., 1984: Hydrology and logging in the Carmanah Creek watershed - what have we learned?. In *Applying 15 years of Carnation Creek results*, T.W. Chamberlin (Ed.). Pacific Biological Station, Nanaimo, B.C., pp. 11 - 15.

Hey, R.D., 1979: Flow resistance in gravel-bed rivers. *J. Hydr. Div. ASCE*, Vol. 105, HY 4, pp. 356 - 379.

Hey, R.D., and Thorne, C.R., 1986: Stable channels with mobile gravel beds. *J. Hydr. Div. ASCE*, Vol. 112, HY 8, pp. 671 - 689.

Kalinske, A.A., 1947: Movement of sediment as bed load in rivers. *Trans. Am. Geoph. Union*, Vol. 28, No. 4, pp. 615 - 620.

Kellerhalls, R., 1967: Stable channels with paved gravel beds. *J. Waterways and Harbours Div. ASCE*, Vol. 93, WW 1, pp. 63 - 83.

Keulegan, G.H., 1938: Laws of turbulent flow in open channels. *J. Res. Nat. Bur. Stand.*, Vol. 21, RP 1151, pp. 707 - 741.

Knight, D.W., 1981: Boundary shear in smooth and rough channels. *J. Hydr. Div. ASCE*, Vol. 107, HY 7, pp. 839 - 851.

Knight, D.W., Demetriou, J.D., Hamed, M.E., 1984: Boundary shear in smooth rectangular channels. *J. Hydr. Div. ASCE*, Vol. 110, HY 4, pp. 405 - 422.

Lacey, G., 1930: Stable channels in alluvium. *Proc. I.C.E.*, Vol. 229, pp. 259 - 292.

Lane, E.W., 1955 a: The importance of fluvial morphology in hydraulic engineering. *Proc. Am. Soc. Civil Engrs.*, Vol. 81, pp. 1 - 17.

Lane, E.W., 1955 b: The design of stable channels. *Trans. ASCE*, Vol. 120, pp. 1234 - 1279.

Leighly, J.B., 1932: Toward a theory of morphological significance of turbulence in the flow of water in streams. *Pub. in Geology*, Univ. of Calif. Berkley, Calif. Vol. 6, pp. 1 - 22.

Leopold, L.B., and Maddock, T., 1953: The hydraulic geometry of stream channels and some physiographic implications. *U.S.G.S. Prof. Paper* 252.

- Leopold, L.B., Wolman, M.G., and Miller, J.P., 1964: *Fluvial Processes in Geomorphology*. W.H.Freeman and Co., San Francisco.
- Limineros, J.T., 1970: Determination of the Manning coefficient for measured bed roughness in natural channels. *U.S.G.S. Water Supply Paper* 1898-B, Washington, D.C.
- Mackin, J.H., 1948: Concept of a graded river. *Bull. Geol. Soc. Am.*, Vol. 59, pp. 462 - 512.
- Megahan, W.F., 1972: The effects of logging roads on erosion and sediment deposition from steep terrain. *J. For.*, Vol. 70.
- Neill, C.R., 1968: A re-examination of the beginning of movement of coarse granular bed materials. *Hydr. Res. Stn. Rept.*, No. INT 68, 37 p.
- Nixon, M., 1959: A study of the bankfull discharges of rivers in England and Wales. Pap. No. 6322, *Proc. Inst. Civil Eng.*, Vol. 12, pp. 157 - 174.
- Osman, A.M. and Thorne, C.R., 1988: Riverbank Stability Analysis I: Theory. *J. Hydr. Div. ASCE*, Vol. 114, HY 2, pp. 134 - 150.
- Parker, G., Klingeman, P.C., and McLean, D.G., 1982: Bedload and size distribution in paved gravel streams. *J. Hydr. Div. ASCE*, Vol. 108, HY 4, pp. 544 - 571.
- Pickup, G., 1976: Adjustment of stream-channel shape to hydrologic regime. *J. Hydrol.*,

Vol. 30, pp. 365 - 373.

Roberts, R.G., and Church, M., 1986: The sediment budget in severely disturbed watersheds, Queen Charlotte Ranges, British Columbia. *Can. J. Forest Res.*, Vol. 16, No. 5, pp. 1092 - 1106.

Schuum, S.A., 1969: River metamorphosis. *J. Hydr. Div. ASCE*, Vol. 95, pp. 255 - 273.

Simons, D.B., and Albertson, M.L., 1963: Uniform water conveyance channels in alluvial material. *Trans. ASCE*, Vol. 128, Pt. 1, No. 3399, pp. 65 - 167.

Smith, C.D., 1989: Some aspects of flood plain flow in a valley with a meandering channel. *Proc. of the XXIII Congress I.A.H.R.*, Ottawa, Canada. pp. 355 - 362.

Swanston, D.N., and Swanson, F.J., 1976: Timber harvesting, mass erosion, and steep-land forest geomorphology in the Pacific northwest. In *Geomorphology and Engineering*, D.R. Coates (Ed.) Dowden, Hutchinson and Ross, Inc. Stroudsburg, Pa. pp. 199 - 221.

Thorne, C.R., 1988: Influence of bank stability on the regime geometry of natural channels. In *International Conference on River Regime*, W.P. White (Ed.). John Wiley and Sons. pp. 135 - 147.

Thorne, C.R. and Osman, A.M., 1988: Riverbank Stability Analysis II: Applications. *J. Hydr. Div. ASCE*, Vol. 114, HY 2, pp. 151 - 172.

Thorne, C.R., Hey, R.D., and Chang, H.H., 1988: Prediction of hydraulic geometry of

gravel-bed streams using the minimum stream power approach. In *International Conference on River Regime*, W.P. White (Ed.). John Wiley and Sons. pp. 29 - 40.

White, W.R., Bettess, R., Paris, E., 1982: An analytical approach to river regime. *J. Hydr. Div. ASCE*, Vol. 108, HY 10, pp. 1179 - 1193.

Williams, G.P., 1978: Bank-full discharge of rivers. *Water Res. Res.*, Vol. 14, pp. 1141 - 1154.

Wolman, M.G., 1955: The natural channel of Brandywine Creek. *U.S.G.S. Prof. Paper* 271.

Wolman, M.G., and Leopold, L.B., 1957: River floodplains: Some observations on their formation. *U.S.G.S. Prof. Paper* 282-C.

Wolman, M.G., and Brush, L.M., 1961: Factors controlling the size and shape of stream channels in coarse non-cohesive sands. *U.S.G.S. Prof. Paper* 282-G.

Yang, C.T., 1976: Minimum unit stream power and fluvial hydraulics. *J. Hydr. Div. ASCE*, Vol. 102, HY 7, pp. 919 - 934.

Yang, C.T. and Song, C.C.S., 1979: Theory of minimum rate of energy dissipation. *J. Hydr. Div. ASCE*, Vol. 105, HY 7, pp. 796 - 784.

Zimmerman, R.G., Goodlett, J.C., and Coner, G.H., 1967: The influence of vegetation on the channel form of small streams. *Pub. I.A.H.S.*, Vol. 75, pp. 255 - 275.

Appendix A

DATA FROM WOLMAN AND BRUSH (1961)

Table A.1 contains the experimental data of Wolman and Brush (1961) for the mobile channels in 0.67 mm sand. The data is presented in S.I. units.

Run Number	Q (cumecs)	Q' (cumecs)	Slope	Width (metres)	Depth (metres)	Gb (kg/sec)
2.00	0.00031	0.00018	0.0041	0.128	0.009	6.20000E-05
3.00	0.00057	0.00034	0.0039	0.204	0.010	0.00021
4.00	0.00108	0.00070	0.0039	0.284	0.013	0.00104
5.00	0.00057	0.00029	0.0038	0.177	0.010	0.00022
7.00	0.00054	0.00045	0.0064	0.214	0.010	0.00262
8.00	0.00113	0.00068	0.0068	0.378	0.009	0.00349
10.00	0.00071	0.00071	0.0071	0.247	0.012	0.00150
14.00	0.00062	0.00038	0.0035	0.204	0.011	0.00014
15.00	0.00096	0.00099	0.0042	0.265	0.016	0.00044
16.00	0.00116	0.00094	0.0023	0.247	0.020	9.50000E-05
17.00	0.00178	0.00100	0.0025	0.345	0.016	0.00034
19.00	0.00091	0.00063	0.0028	0.220	0.015	0.00018
22.10	0.00139	0.00102	0.0018	0.253	0.021	9.50000E-05
22.20	0.00110	0.00075	0.0021	0.241	0.017	7.80000E-05
23.00	0.00110	0.00069	0.0019	0.232	0.018	3.80000E-05
23.10	0.00139	0.00097	0.0017	0.271	0.020	8.00000E-05
24.00	0.00139	0.00084	0.0018	0.232	0.020	0.00082
27.00	0.00068	0.00046	0.0028	0.195	0.014	0.00080
28.00	0.00025	0.00024	0.0038	0.146	0.010	0.00160
28.11	0.00082	0.00035	0.0029	0.177	0.012	0.00160
28.12	0.00062	0.00039	0.0032	0.189	0.012	0.00160
28.13	0.00062	0.00043	0.0035	0.201	0.012	0.00160
29.00	0.00062	0.00037	0.0038	0.192	0.011	0.00162
31.00	0.00034	0.00023	0.0049	0.153	0.009	0.00086
34.00	0.00195	0.00102	0.0019	0.363	0.017	0.00020
40.00	0.00082	0.00075	0.0033	0.244	0.015	0.00025

Table A.1: Experimental Data of Wolman and Brush (1961) Used in this Thesis.

Appendix B

RIFFLE DATA FROM HEY (1979)

The riffle data from Hey (1979) presented below was used to derive the flow resistance equations in Section 3.3.

Reach Number*	Q (cumecs)	R (metres)	D84 (metres)	R/D84	Slope	f
1	0.995	0.243	0.250	0.97	0.00300	0.750
2	5.730	0.323	0.078	4.14	0.00666	0.178
3	84.900	1.379	0.080	17.24	0.00300	0.075
4	6.960	0.368	0.065	5.66	0.00401	0.153
5	15.300	0.613	0.065	9.43	0.00233	0.092
6	1.190	0.141	0.200	0.70	0.03100	0.928
7	13.100	0.447	0.095	4.71	0.00750	0.159
8	28.300	0.514	0.095	5.41	0.00753	0.114
9	12.500	0.465	0.046	10.11	0.00095	0.107
10	23.900	0.666	0.046	14.48	0.00090	0.089
11	12.100	0.434	0.069	6.29	0.00631	0.125
12	2.660	0.146	0.050	2.92	0.00610	0.209
13	17.400	0.460	0.050	9.20	0.00310	0.101
14	2.660	0.245	0.100	2.45	0.00350	0.261
15	17.400	0.427	0.100	4.27	0.00680	0.170
16	189.820	2.225	0.160	13.91	0.00250	0.088
17	141.783	1.910	0.114	16.75	0.00281	0.079

* See Hey (1979) for original Reach Numbers

Table B.1: Riffle Data from Hey (1979)

Appendix C

DERIVATION OF EQUATION 3.12

The derivation of Equation 3.13 is presented below.

The stream power per unit bed area in mass units, ω , is defined by Bagnold (1966) as:

$$\omega = \rho q S \quad (C.1)$$

where q is the discharge per unit width.

The Darcy - Weisbach Equation (Equation 4.3) can be rewritten as:

$$v = \sqrt{\frac{8}{f}} \sqrt{g R S} \quad (C.2)$$

Recall Equation 4.1:

$$\frac{1}{\sqrt{f}} = 2.03 \log \left(\frac{3.2 \tau^*}{S} \right)$$

Substituting Equations 4.1, C.2, and the values $\rho = 1000 \text{ kg/m}^3$, and $g = 9.81 \text{ m/sec}^2$ into Equation C.1, while assuming $q = v R$ yields:

$$\omega = 18000 (R S)^{1.5} \log \left(\frac{3.20 \tau^*}{S} \right) \quad (C.3)$$

Recall Equation 3.11 rewritten here for any size fraction:

$$\tau^* = \frac{R S}{1.65 D}$$

Substituting $R S = 1.65 \tau^* D$ into Equation C.3 yields:

$$\omega = 38200 \tau^{* 1.5} D^{1.5} \log \left(\frac{3.20 \tau^*}{S} \right) \quad (C.4)$$

which is presented as Equation 3.12 in Chapter 3.

Appendix D

DERIVATION OF EQUATION 4.7

The derivation of Equation 4.7, the slope at which the bed pavement layer will become mobile, is presented in this appendix. The derivation is based upon the approach of Lane (1955 b) for the type B channel, but applies here to a wide channel.

Consider Equation 3.11:

$$\tau_{D_{50}}^* = \frac{R S}{1.65 D_{50}}$$

Assuming from the work of Neill (1967) that the pavement becomes mobile when $\tau_{D_{50}}^* = 0.03$. Equation D can be rewritten as:

$$D_{50} = 20 R S \quad (D.1)$$

which expresses the median pavement grain diameter at the threshold of movement in terms of the channel geometry.

The Strickler equation relating the Manning coefficient n and D_{50} given in Henderson (1966, p 98; converted here to S.I. units) is:

$$n = 0.042 D_{50}^{0.17} \quad (D.2)$$

Substituting Equation D.1 into D.2 yields:

$$n = 0.07 (R S)^{0.17} \quad (D.3)$$

Equation D.3 substituted into the Manning equation for the mean stream velocity, and multiplied by the channel cross - sectional area (assumed here to be equal to $W * R$

for a wide channel) yields:

$$Q = 14 W R^{0.67} S^{0.33} \quad (\text{D.4})$$

The channel width, W , can be expressed as a function of Q using a regime equation. The equation of Hey and Thorne (1986) for Vegetation Type IV is used (see Section 2.3):

$$W = 2.34 Q^{0.5} \quad (\text{D.5})$$

The equation for thick bank vegetation was selected as this equation applies to the narrowest and deepest channels. The resulting threshold slope equation should represent the minimum possible slope for bed mobility.

Substituting Equation D.5 and $R = D_{50} (20 S)$ from Equation D.1 into Equation D.4 to eliminate W and R upon rearranging yields:

$$S = 0.36 D_{50}^{1.28} Q^{-0.43} \quad (\text{D.6})$$

which represents the maximum slope at which a channel with Type IV bank vegetation would become mobile. Channels with weaker bank vegetation, and hence wider and shallower, would become mobile at steeper slopes. Thus Equation D.6 represents the minimum slope possible for gravel rivers.

Appendix E

HYDRAULIC GEOMETRY OF SELECTED GRAVEL RIVERS

The following table contains the gravel-bed river data used to test RIVERMOD in this thesis. The rivers were selected from the data sets of Hey and Thorne (1986) and Andrews (1984) on the basis of reported *thin* bank vegetation.

Observed Data

River Number *	Q' (cumecs)	Width (metres)	Depth (metres)	Slope	Area (sq. metres)	D50 (metres)	d50 (metres)
1.01	4.78	10.40	0.479	0.00230	4.9816	0.023	0.0050
1.03	57.77	47.20	0.972	0.00140	45.8784	0.024	0.0080
1.06	12.41	11.90	0.731	0.00460	8.6989	0.061	0.0190
1.07	2.96	7.25	0.338	0.01100	2.4505	0.052	0.0190
1.15	44.22	34.00	0.844	0.00580	28.6960	0.098	0.0150
1.16	42.93	26.00	0.911	0.00670	23.6860	0.091	0.0360
1.17	7.08	11.60	0.518	0.00460	8.0088	0.046	0.0140
1.18	37.47	24.90	0.878	0.00580	21.8622	0.079	0.0140
1.19	115.02	36.60	1.450	0.00370	53.0700	0.064	0.0240
1.20	147.18	53.30	1.630	0.00180	86.8790	0.058	0.0170
1.21	74.72	24.40	1.620	0.00200	39.5280	0.045	0.0220
1.22	227.95	83.80	1.850	0.00088	155.0300	0.034	0.0067
1.24	113.62	36.60	1.650	0.00240	60.3900	0.070	0.0250
2.20	33.60	21.10	0.960	0.00340	20.2560	0.034	0.0110
2.23	8.30	13.70	0.500	0.00610	6.8500	0.048	0.0160
2.30	8.30	15.60	0.510	0.00520	7.9560	0.055	0.0180
2.34	8.80	12.30	0.500	0.01080	6.1500	0.068	0.0220
2.36	18.20	14.10	0.870	0.00550	12.2670	0.074	0.0250
2.38	319.20	57.80	2.690	0.00140	155.4820	0.056	0.0190
2.39	625.70	76.50	3.210	0.00160	245.5650	0.050	0.0170
2.44	121.60	41.70	1.280	0.00660	53.3760	0.091	0.0300
2.46	53.30	32.20	1.340	0.00110	43.1480	0.036	0.0120
2.47	55.40	28.00	1.050	0.00570	29.4000	0.064	0.0210
2.53	286.90	77.10	2.050	0.00160	158.0550	0.060	0.0200
2.60	16.20	17.50	0.650	0.00350	11.3750	0.020	0.0070

* 1. Denotes Andrews (1984) Data

2. Denotes Hey and Thorne (1986) Data

Table E.1: Observed Hydraulic Geometry of Selected Gravel Rivers From Andrews (1984) and Hey and Thorne (1986)

Calculated Data

River Number *	Width (metres)	Depth (metres)	Slope	Area (sq. metres)	Gb (kg/sec)	f ^{-1/2}
1.01	10.57	0.486	0.00217	5.14	0.218	3.31
1.03	31.52	1.362	0.00104	42.92	0.155	4.11
1.06	14.32	0.653	0.00481	9.35	0.046	2.73
1.07	7.77	0.327	0.01083	2.54	0.237	2.25
1.15	24.51	1.083	0.00499	26.54	71.815	2.61
1.16	24.40	0.973	0.00617	23.74	0.433	2.69
1.17	11.80	0.524	0.00435	6.18	0.033	2.77
1.18	23.38	0.936	0.00544	21.88	67.527	2.76
1.19	39.90	1.386	0.00370	55.32	11.676	3.34
1.20	44.94	1.896	0.00155	85.20	0.455	3.66
1.21	33.13	1.289	0.00249	42.70	0.021	3.55
1.22	55.08	2.601	0.00069	143.27	12.159	4.33
1.24	36.09	1.707	0.00225	61.61	0.080	3.43
2.20	25.97	0.791	0.00376	20.54	14.308	3.44
2.23	12.36	0.522	0.00577	6.45	0.359	2.70
2.30	12.12	0.577	0.00469	6.99	0.010	2.64
2.34	13.44	0.452	0.01129	6.07	8.148	2.33
2.36	16.84	0.711	0.00605	11.97	0.267	2.67
2.38	61.19	2.522	0.00142	154.32	2.296	3.99
2.39	99.00	2.567	0.00180	254.14	113.460	4.15
2.44	44.67	1.198	0.00675	53.52	115.598	2.90
2.46	28.76	1.393	0.00127	40.06	0.009	3.64
2.47	30.62	0.923	0.00615	28.25	44.822	2.98
2.53	58.43	2.523	0.00134	147.43	0.457	3.86
2.60	22.49	0.513	0.00402	11.55	10.364	3.53

* 1. Denotes Andrews (1984) Data

2. Denotes Hey and Thorne (1988) Data

Table E.2: Hydraulic Geometry of Selected Gravel Rivers Modelled by RIVERMOD.

Appendix F

DERIVATION OF EQUATION 3.32

The derivation of Equation 3.32 is presented.

The total dimensionless bedload, W^* , is defined by Parker *et al* as:

$$W^* = \frac{q_s^*}{\tau^{* 3/2}} \quad (\text{F.1})$$

q_s^* is the dimensionless Einstein bedload parameter = $q_s / (D \sqrt{(S_s - 1) g D})$; q_s is the volumetric bedload per unit bed width; and τ^* is the dimensionless bed shear stress.

By expanding q_s^* and simplifying, Equation F.1 becomes:

$$W^* = \frac{q_s (S_s - 1) g}{v^{* 3}} \quad (\text{F.2})$$

where v^* is the shear velocity = $\sqrt{g R S}$.

The Darcy-Weisbach Equation can be written:

$$v = \sqrt{\frac{8}{f}} v^* \quad (\text{F.3})$$

Substituting Equation F.3 into F.2 and cancelling g from top and bottom yields:

$$W^* = \sqrt{\frac{8}{f}} \frac{q_s (S_s - 1)}{v R S} \quad (\text{F.4})$$

Multiplying top and bottom of Equation F.4 by ρ gives:

$$W^* = \sqrt{\frac{8}{f}} \frac{q_s (S_s - 1) \rho}{\omega} \quad (\text{F.5})$$

in which ω is the stream power per unit bed area in mass units which for a wide channel is approximately equal to $\rho v R S$.

Equation F.5 can be rewritten as:

$$W^* = \sqrt{\frac{8}{f}} \frac{i_b}{\omega} \quad (\text{F.6})$$

where i_b is the bedload transport rate by immersed weight per unit bed width.

Note that the fraction i_b/ω is the bedload transport efficiency defined by Bagnold (1966).

Appendix G

ARTIFICIAL DATA SET

The artificial data set used to develop Equations 5.5 and 5.6 is tabled below. The data was produced using random number generators. The discharge and median grain size were randomly selected between 10 - 500 m³/sec and 0.01 - 0.1 metres respectively. The channel slope was varied randomly from 1 - 5 times the threshold slope given by Equation 4.10. This variation in the channel slope represents the effects of randomly imposed sediment load.

Run Number	Q (cumecs)	Gb (kg/sec)	D50 (metres)	Width (metres)	Depth (metres)	Slope
1	41.8	301.450	0.087	35.2	0.58	0.01758
2	18.5	0.016	0.056	19.5	0.81	0.00336
3	235.4	0.019	0.029	59.1	2.79	0.00051
4	92.2	3.200	0.029	39.5	1.46	0.00141
5	210.9	35.687	0.050	57.1	1.78	0.00231
6	35.3	0.015	0.045	24.8	1.14	0.00196
7	33.9	0.011	0.031	23.9	1.12	0.00138
8	105.8	0.338	0.029	40.6	1.72	0.00102
9	36.4	2.191	0.038	25.4	0.94	0.00283
10	133.3	0.024	0.022	46.1	2.14	0.00054
11	35.1	0.003	0.012	29.4	1.36	0.00043
12	80.9	22.412	0.052	36.2	1.19	0.00357
13	37.1	19.171	0.077	24.8	0.83	0.00722
14	104.5	94.577	0.085	39.9	1.19	0.00649
15	95.3	0.030	0.054	37.6	1.77	0.00150
16	38.5	16.779	0.072	24.8	0.86	0.00646
17	131.0	0.030	0.036	44.9	2.19	0.00083
18	139.1	0.069	0.085	43.8	1.93	0.00215
19	101.7	122.618	0.081	41.2	1.11	0.00696
20	55.6	103.502	0.088	35.3	0.79	0.01024
21	45.8	0.033	0.073	25.7	1.26	0.00289
22	105.6	18.209	0.076	36.5	1.42	0.00403
23	41.4	0.014	0.040	26.1	1.33	0.00150
24	39.1	0.008	0.029	26.3	1.28	0.00111
25	12.3	0.002	0.014	17.4	0.77	0.00088

Table G.1: Artificial Data Set Used to Develop Equations 5.5 and 5.6. Channels 1 - 25

Run Number	Q (cumecs)	Gb (kg/sec)	D50 (metres)	Width (metres)	Depth (metres)	Slope
26	49.7	0.021	0.045	28.9	1.36	0.00164
27	58.9	0.042	0.081	28.3	1.42	0.00282
28	75.1	0.016	0.027	35.0	1.79	0.00078
29	205.7	0.424	0.063	48.6	2.23	0.00159
30	89.4	0.061	0.089	35.6	1.64	0.00267
31	41.2	0.005	0.015	29.8	1.46	0.00051
32	101.6	119.298	0.058	45.0	1.06	0.00570
33	61.0	21.324	0.088	29.1	1.07	0.00627
34	243.4	129.875	0.061	63.3	1.65	0.00359
35	84.1	21.869	0.037	39.3	1.19	0.00271
36	36.1	0.015	0.030	24.8	1.14	0.00135
37	46.5	2.844	0.071	27.1	1.00	0.00464
38	263.9	0.010	0.015	65.5	3.24	0.00023
39	34.7	0.161	0.094	21.7	0.99	0.00511
40	42.9	0.051	0.052	25.4	1.14	0.00238
41	42.5	0.005	0.014	30.2	1.47	0.00049
42	57.9	0.012	0.026	32.2	1.59	0.00082
43	100.0	0.042	0.065	36.5	1.68	0.00190
44	104.0	203.280	0.077	45.8	1.01	0.00802
45	15.3	0.007	0.034	16.9	0.90	0.00189
46	37.5	0.035	0.013	27.7	1.23	0.00063
47	75.7	0.012	0.032	34.1	1.67	0.00095
48	69.7	50.940	0.079	34.5	1.00	0.00666
49	219.5	2.501	0.087	50.5	2.06	0.00258
50	42.1	341.719	0.098	35.1	0.58	0.01957

$d50 = D50/3$

$D50 \text{ (Bank)} = D50$

Table G.2: Artificial Data Set Used to Develop Equations 5.5 and 5.6. Channels 25- 50

Appendix H

RIVERMOD PROGRAM

The RIVERMOD computer program coded in QuickBasic is presented below.

'RIVERMOD IS DESIGNED TO CALCULATE THE EQUILIBRIUM GEOMETRY OF
'GRAVEL-BED RIVERS WITH MOBILE BEDS.

```

DECLARE SUB MSTP ()
DECLARE SUB seddischpkm ()
DECLARE SUB discharge ()
DECLARE SUB shearstress ()
DECLARE SUB stablechannel ()
DECLARE SUB varwidth ()
DECLARE SUB varslope ()

'DECLARE VARIABLES
'wmin!=minimum trial bed width           wmax!=maximum trial bed width
'winc!=trial bed width increment          wtrial!=trial bed width
'slope!=input slope                      qbank!=input bankfull discharge
'qcont!=trial discharge from continuity   stabilitytest$=test for stability
'd50sub!=subsurface median grain diam.    d50bed!=pavement median grain diam.
'd50bank!=bank median grain diameter      qsed!=input sediment load
'roughness=calculated flow resistance     threshstress!=threshold bank
'bankangle!=bank angle                   anglerepose!=angle of repose
'decangle!=bank angle decrement           kfactor!=k factor
'depthinc!=depth increment
'depth!=trial depth                      hydraulicradius!=trial hyd. rad.
'surfwidth!=surface width                percentfs!=percentage of shear
'bankperimeter!=bank perimeter           force acting on banks
'bankshear!=average bank shear stress     bedshear!=average bed shear stress
'maxhydraulicradius=hydraulic radius of max hydraulic radius geometry
'maxaveragedepth!=average depth of max hydraulic radius section
'maxdepth!=maximum depth of the max hydraulic radius section
'maxsurfwidth!=surface width of the max hydraulic radius geometry
'maxseddischarge!=sediment discharge of the max hydraulic radius geometry
'subsurfaceshields!=dimensionless shear stress acting on d50
'pavementshields!=dimensionless shear stress acting on pavement
'tempdepthinc!=temporary depth increment
'subsurfaceshields!=dimensionless shear stress acting on the subpavement d50
'slopemin!=threshold slope               'slopeinc!=slopeincrement
'widthbedshear=sediment transport capacity index "M"
'stabilitytest$=stability condition
'slopecond$=slope condition

COMMON SHARED wmin!, wmax!, winc!, wtrial!, qbank!
COMMON SHARED stabilitytest$, d50sub!, roughness!, threshstress!
COMMON SHARED bankangle!, anglerepose!, depth!, slope!, depthinc!
COMMON SHARED hydraulicradius!, surfwidth!, percentfs!, bankshear!, bedshear!
COMMON SHARED maxhydraulicradius!, maxbankangle!, maxseddischarge!, runnum%
COMMON SHARED maxsurfwidth!, bankperimeter!, d50bed!, qcont!, kfactor!
COMMON SHARED decangle!, vege%, maxaveragedepth!, maxdepth!, subsurfaceshields!
COMMON SHARED pavementshields!, tempdepthinc!, tempdecangle!
COMMON SHARED maxbedperimeter!, maxbankperimeter!, phi50!, dimensionlessbedload!
COMMON SHARED sedimentloadpkm!, maxsedimentloadpkm!, maximmobilesurfwidth!
COMMON SHARED maximmobileaveragedepth!, widthbedshear!, maxwidthbedshear!
COMMON SHARED qmax!, qsed!, slopeinc!, slopemin!, d50bank!, slopecond$, D50mod!
COMMON SHARED tempwinc!, seddischarge!, maxbedshear!, maxbankshear!

INPUT "Bankfull Discharge (cumecs) ", qbank!
INPUT "Median Subpavement Grain Diameter (m) ", d50sub!
INPUT "Median Pavement Grain Diameter (m) ", d50bed!
INPUT "Median Bank Grain Diameter (m) ", d50bank!
INPUT "Dimensionless Bed Shear Stress ", pavementshields!
INPUT "Angle of Repose of Bank Sediment (degrees) ", anglerepose!

```

```

INPUT "Sediment Load (kg/sec) ", qsed!
PRINT
  depthinc! = .5
  winc! = 10
  wmax! = 500
  slopemin! = .36 * d50bed! ^ 1.28 * qbank! ^ -.43
  slopeinc! = slopemin! / 5
  slope! = slopemin!
  decangle! = 5
  maxseddischarge! = 0
  threshstress! = 908 * d50bank! 'Dimensionless shearstress = 0.056 for banks
  slopecond$ = "tooshallow"

  DO WHILE slopecond$ <> "justright"
    widthbedshear! = 0
    maxbedshear! = 0
    maxwidthbedshear! = 0
    maxseddischarge! = 0
    wtrial! = winc!
    PRINT "Slope"; slope!
    PRINT
    CALL varwidth
    PRINT "Sediment Transport Capacity", maxseddischarge!
    PRINT
    PRINT
    CALL varslope

    IF slopecond$ = "tooshallow" THEN
      IF stabilitytest$ = "unstable" THEN
        EXIT DO
      END IF
    END IF

    IF slopeinc! < .000001 THEN
      BEEP
      PRINT "Convergence Problem" 'problem converging to qsed!
      PRINT
      EXIT DO
    END IF

  LOOP

  IF stabilitytest$ = "unstable" THEN
    PRINT "Unstable"
  ELSE
    PRINT
    PRINT "Channel Width", maxsurfwidth!
    PRINT "Channel Depth", maxaveragedepth!
    PRINT "Channel Slope"; slope!
    PRINT "Bank Angle"; maxbankangle!
  END IF
  PRINT
END

```

```

SUB discharge
  'sub increments depth until the channel capacity is sufficient
  'to convey the input bankfull discharge

  depth! = 0
  tempdepthinc! = depthinc!

  DO
    depth! = depth! + tempdepthinc!      'increment depth
    bankperimeter! = 2 * depth! / SIN(bankangle! * 2 * 3.141593 / 360)
    hydraulicradius! = (wtrial! * depth! + depth! ^ 2 / TAN(bankangle!
      * 2 * 3.141593 / 360)) / (wtrial! + bankperimeter!)
    'calc hydral rad
    roughness! = 2.5 * LOG(3.2 * pavementshields! / slope!) 'calc roughness
    qcont! = (wtrial! + bankperimeter!) * roughness! * hydraulicradius!
      * (9.81 * hydraulicradius! * slope!) ^ .5 'calc q
    IF qcont! > 1.01 * qbank! THEN      'decreases the depth increments
      depth! = depth! - tempdepthinc!
      tempdepthinc! = tempdepthinc! / 5 'as approach the design
      qcont! = 0.
    END IF
  LOOP UNTIL qcont! >= .99 * qbank!
END SUB

SUB MSTP
  'determines the MSTP configuration for an input slope

  widthbedshear! = wtrial! * bedshear! ^ 3 'calculates "M"
  IF widthbedshear! > maxwidthbedshear! THEN
    maxwidthbedshear! = widthbedshear!      'reset all maximized values
    maxbankshear! = bankshear!
    maxbedshear! = bedshear!
    maxbankangle! = bankangle!
    maxbedperimeter! = wtrial!
    maxsurfwidth! = surfwidth!
    maxaveragedepth! = depth! * (surfwidth! + wtrial!) / 2 / surfwidth
    qmax! = qcont!
    CALL seddischpkm
    maxseddischarge! = sedimentloadpkm!

  END IF
END SUB

SUB seddischpkm
  subsurfaceshields! = bedshear! / (1.65 * d50sub! * 9810)
  phi50! = subsurfaceshields! / .0876

  IF phi50! < .95 THEN
    dimensionlessbedload! = 0
  ELSEIF phi50! < 1.65 THEN
    dimensionlessbedload! = .0025 * EXP(14.2 * (phi50! - 1) - 9.28 * (phi50! - 1) ^ 2)
  ELSE
    dimensionlessbedload! = 11.2 * (1 - .822 / phi50!) ^ 4.5
  END IF
  sedimentloadpkm! = 1.9 * dimensionlessbedload! * (depth! * slope!) ^ 1.5 * 2650 * wtrial!
END SUB

```

```

SUB shearstress
  'uses the method of Flinham (1988) to calculate the boundary
  'shear stress distribution

  surfwidth! = wtrial! + 2 * depth! / TAN(bankangle! * 2 * 3.141593 / 360)
  'calc surface width

  percentfs! = 10 ^ (-1.4026 / 2.3 * LOG(wtrial! / bankperimeter! + 1.5) + 2.247)
  'calc % of shear force acting on the banks

  bankshear! = 9810 * depth! * slope! * .01 * percentfs! * ((surfwidth! + wtrial!) *
    SIN(bankangle! * 2 * 3.141593 / 360) / (4 * depth!))
  'calc bank shearstress

  bedshear! = 9810 * depth! * slope! * (1 - .01 * percentfs! * (surfwidth! /
    (2 * wtrial!) + .5))
  'calc bed shearstress
  IF bedshear! < 0 THEN bedshear! = 0

END SUB

SUB stablechannel
  'determines if the geometry is stable
  bankangle! = anglerepose! - decangle! 'set initial trial bank angle
  tempdecangle! = decangle!

  DO WHILE stabilitytest$ = "unstable"
    CALL discharge
    CALL shearstress
    kfactor! = (1 - SIN(bankangle! * 2 * 3.141593 / 360) ^ 2 / SIN(anglerepose! *
      2 * 3.141593 / 360) ^ 2) ^ .5
    'calc K factor by method of Lane (1955)
    IF bankshear! / kfactor! <= .99 * threshstress! THEN
      bankangle! = bankangle! + tempdecangle!
      tempdecangle! = tempdecangle! / 5
    ELSEIF bankshear! / kfactor! <= 1.01 * threshstress! THEN
      stabilitytest$ = "stable"
      CALL MSTP
    END IF
    bankangle! = bankangle! - tempdecangle! 'decrease bank angle
  IF tempdecangle! < .0002 THEN
    stabilitytest$ = "stable"
  EXIT DO
END IF
  IF bankangle! < 10 THEN EXIT DO 'sets minimum bank angle =10
  LOOP
END SUB

SUB varslope
  'varies the trial slope according to the slope condition

  IF maxseddischarge < .99 * qsed! THEN
    slope! = slope! + slopeinc!
    slopecond$ = "tooshallow"
  ELSEIF maxseddischarge! < 1.01 * qsed! THEN
    slopecond$ = "justright"
  ELSE
    slope! = slope! - .8 * slopeinc!
    slopeinc! = slopeinc! / 5
    slopecond$ = "toosteep"
  
```

```
        slopecond$ = "toosteepest"
    END IF
END SUB

SUB varwidth
    'varies the channel width until a maximum is attained
    tempwinc! = winc! 'create temporary variable

    DO WHILE wtrial! <= wmax!
        PRINT "Trial Bed Width", wtrial!
        stabilitytest$ = "unstable"
        CALL stablechannel
        IF widthbedshear! < maxwidthbedshear! THEN
            IF maxbedperimeter! < wtrial! THEN
                wtrial! = wtrial! - 1.8 * tempwinc!
                tempwinc! = tempwinc! / 5
            END IF
        END IF
        wtrial! = wtrial! + tempwinc!
        IF tempwinc! < .01 THEN EXIT DO
    LOOP
END SUB
```